This is to certify that the

dissertation entitled

THE STEADY-STATE GREEN'S FUNCTION METHOD AND ITS APPLICATIONS TO UNIMOLECULAR REACTIONS IN LIQUIDS. BOND-BREAKING ELECTRON TRANSFER REACTIONS

presented by

Olga Borisovna Jenkins

has been accepted towards fulfillment
of the requirements for

Ph.D. degree in Chemistry

Robert Cukier
Major professor

Date 11/2/95

THE STEADY-STATE GREEN'S FUNCTION METHOD AND ITS APPLICATIONS TO UNIMOLECULAR REACTIONS IN LIQUIDS. BOND-BREAKING ELECTRON TRANSFER REACTIONS

By

Olga Borisovna Jenkins

A DISSERTATION

Submitted to

Michigan State University

in partial fulfillment of the requirements

for the degree of

DOCTOR OF PHILOSOPHY

Department of Chemistry

1995

ABSTRACT

THE STEADY-STATE GREEN'S FUNCTION METHOD AND ITS APPLICATIONS TO UNIMOLECULAR REACTIONS IN LIQUIDS.
BOND-BREAKING ELECTRON TRANSFER REACTIONS

By

Olga Borisovna Jenkins

A new theory for evaluation of the dynamic effects in unimolecular reaction in liquids is presented. Unlike previous theories which require calculation of time-dependent population probabilities, our theory is based on *steady-state* differential or integral equations for evaluation of the reaction rate constants. New forms of the Green's functions convenient for evaluation of reaction rate constants, the steady-state Green's functions, were introduced and their physical meaning was established. Predicated upon these Green's functions the concept of mean first passage time (MFPT) was generalized from the "MFPT to a point" to the definition of the "effective MFPT", which was defined as an average time to reach a region on the reactive surface, rather than a point.

In the frameworks of the suggested steady-state Green's function theory, the *decoupling approximation* for solution of the integral equations was designed and the criterion of its applicability was formulated. We explicitly proved that for reactions on narrow sinks the dynamic effects can be separated from the rest of the reaction, and thus can be treated independently.

The steady-state Green's function theory as well as the effective MFPT concept were tested on one- and two-dimensional potential surface reactions. Special attention was addressed to high activation barrier reactions on narrow as well as wide reaction sinks. The rate constants for reactions on one- and two-dimensional harmonic oscillator and bistable potentials were evaluated for all barrier heights.

The *bond-breaking electron transfer reactions* (BBET) were considered as a special application of the presented theory. The effect of solvent and intramolecular dynamics on the rate of concerted as well as consecutive BBET reactions was investigated. The reaction took place on two-dimensional diabatic potential surfaces with one coordinate the solvent polarization and the other the breaking bond's displacement. We assumed that the polarization fluctuations are always overdamped and viewed two classical (overdamped and energy-diffusion) and one quantum mechanisms of dynamics along the bond-breaking coordinate. For the classical dynamics along the bond-breaking coordinate we found that the overall rate for both concerted and consecutive BBET can be considered as a combination of non-adiabatic rate constants (TST analogs) and various effective MFPT (purely responsible for the dynamic effects). A special method of analysis was developed for situations where one dynamics is fast/slow compared with the other.

For the quantum bond-breaking mechanism it was found that the original two-dimensional surfaces are reduced to one-dimensional diabatic potentials with multiple channels providing the decay into the products. In this picture the overall rate constant can *never* be separated into non-adiabatic and diffusional parts.

ACKNOWLEDGMENTS

It is my pleasure to thank Professor R. I. Cukier, my advisor, for his encouragement and help during my research work at Michigan State University.

I am grateful to Professor A. B. Doktorov who initially directed my research interests into the field of stochastic reaction theory. I also would like to express my gratitude Professors A. I. Burshtein, K. Hunt and A. A. Ovchinnikov for their interest in my work.

The Department of Chemistry at Michigan State University is also acknowledged for offering me its resources and support during the preparation of this dissertation.

TABLE OF CONTENTS

LIST OF FIGURES

INTRODUCTION

This work has two major goals. First, we present a new theory, the steady-state Green's function theory, based on steady-state differential and integral equations for description of irreversible unimolecular reactions. Apart from simplifications in evaluating reaction rate constants, this new approach also permits generalization of the mean first passage time (MFPT) concept, which is extensively used in understanding solvent dynamic effects in liquids. Second, the steady-state Green's function theory has been applied to some important classes of unimolecular reactions among which are electronic relaxation processes and electron transfer reactions. Special attention has been paid to bond-breaking electron transfer reactions which not only are quite common but also present a challenge from a theoretical point of view.

Unimolecular reactions are a prevalent phenomenon and play a central role in many chemical processes such as electron transfer reactions, electronic relaxation, and the breaking and forming of chemical bonds. Unimolecular reaction rate theory has a long and extended history, and a great number of methods and approaches have been developed in order to describe diffusion-influenced unimolecular reactions, see Ref.[1 - 25]. While some attempts have been made in order to progress in the reversible description of reactions, the irreversible formulation of the theory is widely used as a model for evaluation of reaction rates. The formulation implies that in order to obtain the chemical rates it is sufficient to consider the reaction decay from the initially populated reaction state. The reactants which escape from the initial state potential surface through some reaction region are considered to be withdrawn from the process.

Following Kramers [1] many studies of bond breaking or forming reactions use the model of a system moving along a ground-state adiabatic surface over a barrier. The

particles are subject to thermal damping, the objective being to escape irreversibly out of the reactant potential well. Thus, the reaction model may be characterized by a single potential surface (activated or otherwise) for which one defines an effective reaction region beyond which the reaction dynamics is no longer interesting as the reaction was assumed to be irreversible.

Although the general approach to the description of electron transfer (ET) reactions in solutions is based on the scheme of transitions between two adiabatic or diabatic surfaces, the irreversible mechanism displayed acceptable results. In this case orientational polarization of the solvent presents one potential energy surface for each of the reactant and product. Electronic coupling between the two surfaces provides the reaction region for the reactants to move onto the product state. The reverse reaction from the product to reactant surface is neglected for simplicity, which can be justified for activated reactions. Serious attention was paid to high activation barrier [26, 27] as well as low barrier [6, 7] reactions. Of course, there are many electron transfer reactions where bonds are broken or formed in a way which is connected to the electron transfer event [28, 29]. This type of process is referred to as bond-breaking electron transfer (BBET) [30] and is often associated with realm of organic chemistry. A theory of BBET is intrinsically more complicated then that for ET as it must involve at least two distinct reaction coordinates: one connected with the orientational polarization of the solvent and the other a bond-stretch coordinate along the direction of the chemical transformation. Nevertheless, despite the obvious multidimensional nature, the irreversible mechanism of reaction decay can also be applied here by analogy with the straightforward ET.

Another class of unimolecular reactions of interest consists of electronic relaxation processes involving large amplitude stochastic motion. In this case it is assumed that the stochastic motion of reactants on the excited-state potential surface leads to irreversible transitions to the ground state due to the coupling between the ground and excited state electronic surfaces. The reaction potential may or may not present a barrier to the motion

along the reaction coordinates leading to the decay of the initially formed excited state population. In this case the irreversible mechanism seems to be especially suitable, as the exothermicity of the reaction is extremely large. Theoretical investigations of the electronic relaxation processes were directed towards both high activated barrier and activationless reactions [12, 13, 17, 18, 20] dealing with these two types separately. In experimental observations cis/trans isomerization and photochemical transformations proceed through high activation barrier [31, 32], whereas photolysis of a large number of organic dye molecules and isomerization reactions exhibit activationless behavior [31].

As one can see, the variety of reactions falling under the irreversible scheme (accompanied by a great range of theoretical models) is enormous and it would be pointless here to describe them in detail. On the other hand, there are a few general features which are common for all these reactions. All of them are assumed to take place on a single reaction potential surface from which there exists some mechanism providing the population decay. This mechanism can often be represented by a reaction region, or sink. The other important feature for us is that the reactions under study are diffusion-influenced, so that the dynamical effects on the reaction rates are extremely important.

However, theoretical study of the reaction kinetics and rate constants is difficult, even for irreversible reactions, not to mention for reversible ones. It is impossible to list here all of the approaches developed to describe these reactions. Development of experimental techniques and theory dictate that the reaction models become more and more complicated. Widely used early one-dimensional potential surface models fail to describe the gradually increasing number of chemical reactions so that multidimensional potential surface models become more and more valuable [7, 19, 21, 33, 34] as is the case, for example, with BBET [30]. Therefore, theoretical studies of the reaction kinetics and the reaction rates face more and more complications. These complications arise partially due to the use of a well-accepted technique wherein all reaction rate constants are evaluated through the evolution of the total population remaining on the reaction surface. Thus, from

the theoretical point of view, the highest priority has been to evaluate the time-dependent population density of the decaying initial state. As a partial solution to the problem, numerical methods have become more and more popular [8, 16 - 19, 21, 30]. Despite the usefulness of numerical investigations in interpreting the experimental data, they do not provide clear parametric dependence of the reaction kinetics and reaction rate constants and hamper a clear comprehension of the real nature of the physical phenomena. Furthermore, they may be expensive and time-consuming to perform. This, for example, appeared to be the case with the modeling of one-dimensional evolution for the Fokker-Planck underdamped motion [17, 18]. Therefore, even a simple extension to motion along a multidimensional surface may be extremely difficult. Note that, in reality, analysis of the steady-state characteristics alone such as fluorescence yield or reaction rate constants is sufficient for the explanation of experimental data.

In other words, whether or not it is possible to avoid the solution of the well-known time-dependent equation for calculations of the steady-state characteristics in unimolecular reaction has become a significant question. It would dramatically simplify the evaluation of the reaction rates not only from the analytical, but also from the numerical perspective. Introduction of steady-state equations instead of the time-dependent ones would be extremely profitable for investigation of multidimensional problems.

In the first Part of the present work, we develop methods for the direct evaluation of the reaction rate constants, based on solution of appropriate steady-state (rather than the traditional time-dependent) equations. A profitable method for calculation of the reaction kinetics is also suggested. The concept of the mean first passage time is generalized, which permits evaluation of the mean time to reach a reaction region, rather than a point, on the reaction surface. Further in Part I we test our generalized system against the well-defined adiabatic and diabatic models for the reaction potentials. An effective one-dimensional bistable potential is considered for the case of adiabatic reactions. In the diabatic case the

reaction rates were evaluated for one- and two-dimensional harmonic oscillator surfaces accompanied by a special analysis for high activation barrier reactions.

Part II contains a detailed description of charge transfer processes which are accompanied by forming or breaking of chemical bonds (BBET reactions). BBET is considered to be a two-dimensional process following either a concerted or a consecutive mechanism. The main interest is focused on the dynamical influence of the ET as well as the bond breaking (BB) on the kinetics of such reactions. So, the theory describing this type of reaction is more sophisticated than the ordinary ET description as the latter one does not include any knowledge about dynamical influences from the other degrees of freedom but the electron-transfer driving coordinate. In contrast, as will be shown in Part II, the dynamics along the second, BB coordinate strongly influences the total kinetics. Two stochastic (overdamped and energy diffusion) and one quantum mechanism will be considered for transformations along the BB coordinate.

As will be shown, the nature of the reaction surfaces can provide a distinction between the concerted and consecutive pathways in BBET. Predicating on study of the early works in this field [29, 35] we will introduce an intermediate state which can easily span the two extreme reaction mechanisms. The more stable is the intermediate state, the more preferable could be the consecutive mechanism in comparison with the concerted one.

PART I. THE STEADY-STATE GREEN'S FUNCTION THEORY FOR UNIMOLECULAR IRREVERSIBLE REACTIONS IN LIQUIDS

CHAPTER I. THEORY, GENERAL OBSERVATION OF IRREVERSIBLE REACTIONS

The time evolution for the case of irreversible reactions can be modeled as the stochastic motion of solute particles on a one- or multi-dimensional potential surface with a position-dependent sink, which provides localized decay of the reaction population. In this case, the theoretical description of the reactions is based on the solution of the Fokker - Plank equation for the survival probability distribution function $P(\vec{x},\vec{v},t)$ at time t, with the reaction surface coordinate $\vec{x}$, and the instantaneous velocity of the Brownian particle $\vec{v}$ [15]:

$$\frac{\partial}{\partial t}P(\vec{x},\vec{v},t) = \hat{L}(\vec{x},\vec{v})P(\vec{x},\vec{v},t) - W(\vec{x})P(\vec{x},\vec{v},t) \qquad \text{(I.1.1)}$$

where $W(\vec{x}) = W_0 S(\vec{x})$ is a position-dependent sink (max $S(\vec{x})$ = 1) and $\hat{L}(\vec{x},\vec{v})$ is a functional operator describing the stochastic motion. In the case of underdamped motion the operator $\hat{L}(\vec{x},\vec{v})$ is given by the equation:

$$L(\vec{x},\vec{v}) = -(\vec{v},\vec{\nabla}_x) + \frac{1}{m}(\vec{\nabla}_x V(\vec{x}),\vec{\nabla}_v) + \frac{\zeta}{m}(\vec{\nabla}_v,(\vec{v} + \frac{k_B T}{m}\vec{\nabla}_v))$$

where $\vec{\nabla}_i,(i = \vec{x},\vec{v})$ is the gradient, (,) is the scalar product, $V(\vec{x})$ is the potential energy surface, m is the effective mass and ζ is the relevant friction coefficient.

In the case of overdamped motion Eq. (I.1.1) becomes the Smoluchowski equation, which is defined in the same way as Eq. (I.1.1), but for the survival probability distribution function $P(\vec{x},t) = \int P(\vec{x},\vec{v},t)d\vec{v}$. Thus, the stochastic motion operator along the reaction coordinate $\vec{x}$ is given as:

$$L(\vec{x}) = \vec{\nabla}_x D(\vec{\nabla}_x + \beta\vec{\nabla}_x V(\vec{x})) \equiv D\vec{\nabla}_x \varphi(\vec{x})\vec{\nabla}_x \frac{1}{\varphi(\vec{x})} \qquad \text{(I.1.2)}$$

where $\beta = 1/k_B T$ and D = $1/(\beta\gamma)$ is the space diffusion coefficient, which, in principle, can depend upon position $\vec{x}$, and $\varphi(\vec{x}) = Z_0^{-1}\exp(-\beta V(\vec{x}))$ is the Boltzmann distribution.

In the case of ET in Debye solvents, the diffusion coefficient D is given through the longitudinal polarization relaxation time τ_L by the formal identity $\gamma=\lambda\tau_L$ where λ is an elasticity constant for the harmonic potential $V(\vec{x}) = \lambda(\vec{x} - \vec{x}_0)^2 / 2$ [6].

The boundary conditions for Eq. (I.1.1) require that the kinematic flux at the boundary S of the reaction space under study (which may be, in particular, infinite) is zero, i. e.:

$$\hat{j}P|_{\vec{x}\in S} = 0$$

where $\hat{j}$ is the kinematic flux operator defined as $\hat{L}P = -div(\hat{j}P)$

Owing to this condition the following property holds:

$$\iint \hat{L}(\vec{x},\vec{v})P(\vec{x},\vec{v},t)d\vec{x}d\vec{v} = \iint_S \vec{\hat{j}}(\vec{x})P(\vec{x},\vec{v},t)d\vec{S}d\vec{v} = 0 \qquad \text{(I.1.3)}$$

This is the conservation law for the number of particles in the system (if the reaction does not take place).

The kinetics of the process, that is the total population remaining on the reaction potential surface at time t, is defined through the values $P(\vec{x},\vec{v},t)$ or $P(\vec{x},t)$ as:

$$P_*(t) = \iint P(\vec{x},\vec{v},t)d\vec{x}d\vec{v} \equiv \int P(\vec{x},t)d\vec{x} \qquad \text{(I.1.4)}$$

In the general case, it is assumed to obey the differential kinetic equation:

$$\frac{d}{dt}P_*(t) = -k(t)P_*(t) \qquad \text{(I.1.5)}$$

which is usual for first order reactions, but the rate "constant" depends upon time. Such equations are called "non-Markovian kinetic equations" [36]. When the rate "constant" k(t) reaches a constant value over a long time (see Fig. 1):

$$k = \lim_{t->\infty} k(t) = -\lim_{t->\infty} \frac{d}{dt}\ln\left(P_*(t)\right), \qquad \text{(I.1.6)}$$

Eq. (I.1.5) obtains the form of the mass action law. The constant in Eq. (I.1.6) is called the long time rate constant and is traditionally identified with the rate constant of the quasi-steady-state exponential decay. However, the existence of the above limit is a necessary, but not a sufficient condition for existence of exponential asymptotic behavior (e.g. the steady-state decay) at t-> ∞ [37, 38] (see also Chap. II of this Part). In addition, the

absence of the steady-state kinetics as t-> ∞ does not mean that it can not occur in a sufficiently wide intermediate time interval as discussed in Ref. [38].

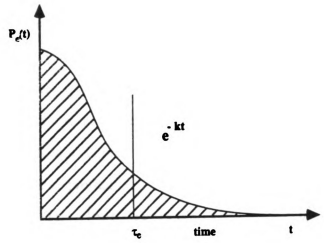

Figure 1. Schematic picture of reaction kinetics $P_e(t)$.

The other rate constant in unimolecular reactions is called the generalized probability and is defined as :

$$æ^{-1} = \int_0^\infty P_e(t)dt = \int_0^\infty t(-\frac{dP_e(t)}{dt})dt = \tau_{surv} \qquad (I.1.7)$$

This constant is the reciprocal of the mean survival time τ_{surv}. The mean survival time depends upon the motion along the reaction surface, the form of the reaction region (sink) and the intensity of the reaction, W_0. When the intensity of the reaction sink is infinitely strong, the mean survival time becomes the mean first passage time (MFPT), τ_p, i.e. $\tau_{surv} = \tau_p$ at $W_0 \to \infty$ [6, 8]. MFPT is the average time that a particle moving randomly starting from the domain outside the sink takes to leave the domain and appear in the reaction region for the first time. This time depends only upon the dynamics along the reaction surface and the form of the sink. Further, we pay special attention to the evaluation of the MFPT because in many cases it is the key to understanding of the whole decay

process. From a practical point of view it is important to distinguish between MFPT to a point and to a region on the reaction surface.

It is clear that the generalized probability depends strongly on the initial distribution on the reaction surface. Despite the fact that æ is an integral characteristic, it is very common to approximate the survival probability using this rate constant instead of the long time one: $P_e(t) = \exp(- æ\, t) = \exp(- t / \tau_{surv})$ [9, 13]. The legitimacy of this approximation will be discussed later.

The differential form of kinetic equation (I.1.5) is convenient for evaluation of the long time kinetic behavior. In order to calculate generalized probability (I.1.7), the integral-differential form is more profitable:

$$\frac{d}{dt}P_e(t) = -\int_0^t æ(t-\tau)P_e(\tau)d\tau \qquad \text{(I.1.8)}$$

This form is widely used in reaction theory based on the memory function formalism [39] or the projection operator technique [40] and in the case of non-Markovian encounter theory to describe reactions in diluted solutions [36].

Applying the Laplace transformation given as:

$$\tilde{f}(s) = \int_0^\infty f(t)\exp(-st)dt \qquad \text{(I.1.9)}$$

to convolution type equation (I.1.8), one can easily connect the Laplace transforms of the reaction kinetics and the integral kernel :

$$\tilde{P}_e(s) = \frac{1}{s + \tilde{æ}(s)} \qquad \text{(I.1.10)}$$

The integral kernel may also be used to evaluate the generalized probability $æ = \tilde{P}_e(0)^{-1} = \tilde{æ}(0)$

The main goals of Part I are to investigate the conditions of the quasi-steady-state regime and to develop methods for direct calculation of the long time rate constant k and the generalized probability æ *without* solution of time-dependent equation (I.1.1). The other aim was to generalize the way of calculating the MFPT, τ_p and obtain the method of evaluating the MFPT to a reaction region. This was achieved through the introduction of

the Green's functions independent of the reaction, which we call the steady-state Green's functions. The procedure for evaluating the MFPT from one point on the one-dimensional reaction surface to another is well-known and has been used by many authors (see Ref. [8] and the references therein for the review). However, we should strongly emphasize that the previous methods used for evaluating the MFPT can not be extended to the case wherein one is interested in MFPT from a certain distribution to a spatially-dependent reaction region (i.e., when the region is not a point on the reaction surface). Such reaction regions are very common for diabatic reactions [6, 13, 41, 42].

In Chapter II of the Part I we connect the rates of reversible reactions with the rates for irreversible processes. Thus, under a few assumptions evaluation of irreversible kinetics could be sufficient to define a more general reversible process. In Chapter III the link between different rate constants is established and both integral and differential steady-state methods for their evaluation are derived. The detailed analysis of the principal steady-state equations is given using the steady-state Green's functions in Chapter IV. Chapter V presents evaluations of the reaction kinetics for both pinhole and narrow reaction sinks. First, the MFPT to a point is introduced through the steady-state Green's functions. Then we generalize the concept of MFPT and give a definition for the effective MFPT which is the mean first passage time to a reaction region, not a point. To complete the steady-state Green's function formalism, the decoupling approximation as a method of solution of steady-state integral equations for narrow reaction regions is presented in Chapter VI. The strict conditions of applicability of the above approximation are also derived. Finally, in Chapter VII we apply the steady-state Green's function formalism to both adiabatic and diabatic reaction potentials and use the generalized definition for the MFPT to evaluate the reaction rates. We consider the bistable potential as the model for adiabatic reactions and the decay on one- and two-dimensional harmonic oscillators as examples of irreversible diabatic reactions.

CHAPTER II. REVERSIBLE REACTIONS

In the previous Chapter we considered irreversible reactions. Here we show how the reversible reaction rates are expressed through the irreversible ones at the present state of the theory of reversible reactions.

The reversible problem is usually formulated by introducing two states - initial and final - coupled to each other. Then it is considered that the initial state is populated at the starting moment of the reaction and the coupling to the final state leads to the transition between these two levels. Thus, the Liouvillian for the reversible problem incorporates the system of four equations for the density matrix $\hat{\rho}$ which describes the evolution of the population under the effect of stochastic motion:

$$\begin{aligned}
\frac{\partial}{\partial t}\rho_{11} &= L_{11}\rho_{11} - iV_{12}(\rho_{21} - \rho_{12}) \\
\frac{\partial}{\partial t}\rho_{22} &= L_{22}\rho_{22} + iV_{12}(\rho_{21} - \rho_{12}) \\
\frac{\partial}{\partial t}\rho_{12} &= L_{12}\rho_{12} - i(U_1 - U_2)\rho_{12} - iV_{12}(\rho_{22} - \rho_{11}) \\
\rho_{21} &= \rho_{12}{}^*
\end{aligned} \qquad \text{(I.2.1)}$$

where V_{12} is the coupling between the two states, L_{ii} is the motion operator along the U_i potential, and L_{12}=L_{21} describes the motion along the cross-surfaces $(U_1 + U_2)/2$.

Currently, the above system has been solved under the assumption that the length over which the two surfaces are coupled to each other is short compared with the size of the reaction space. This means that the crossing dynamics are very localized and the off-diagonal elements of the density matrix vary rapidly [43] and can be eliminated to yield two closed equations for the diagonal elements of the density matrix [23, 42, 44].

The next assumption traditionally made concerns the form of the reaction kinetics. The forward k_{12} and back k_{21} rate constants are defined from the population equations:

$$\tau_p^{21}\frac{d}{dt}\begin{bmatrix} N_1 \\ N_2 \end{bmatrix} = -\begin{bmatrix} k_{12} & -k_{21} \\ -k_{12} & k_{21} \end{bmatrix}\begin{bmatrix} N_1 \\ N_2 \end{bmatrix} \qquad \text{(I.2.2)}$$

where $N_i = \int d\bar{x}\rho_{ii}$ are the populations of the initial (i=1) and final (i=2) states, and $N_1+N_2=1$.

Form (I.1.12) implies that the reaction kinetics obey the exponential law, and the reaction rate constants k_{12} and k_{21} are, in fact, assumed to be the long-time rate constants for the decay from the initial and final states respectively. Whereas assumption (I.2.2) is quite acceptable for high barrier reactions, it is much more difficult to justify for lower barrier crossings.

Nevertheless, these two assumptions produce the answer which allows for the forward and backward reactions (initial to final state and vice versa). The rate constant for the forward reaction can be written in the form:

$$k_{12} = \frac{K_r^{12}}{1 + K_r^{12}\tau_p^{12} + K_r^{21}\tau_p^{21}} \qquad \text{(I.2.3)}$$

The reverse rate is obtained by interchanging the indexes 1 and 2. Here K_r^{ij} are the non-adiabatic rate constants (see Part I, Ch. V) for forward and back reactions and τ_p^{ij} are the mean first passage times to the crossing region from the initial state well (τ_p^{12}) and from the final state one (τ_p^{21}).

The important point made by Eq. (I.2.3) is the fact that it is not necessary to solve even the system of the two closed equations for ρ_{11} and ρ_{22} in order to evaluate k_{12} and k_{21}. Each of the reaction rates K_r^{ij} and τ_p^{ij} can be evaluated from appropriate irreversible problems. K_r^{12} and τ_p^{12} (K_r^{21} and τ_p^{21}) can be evaluated from the solution of Eq. (I.1.1) for the irreversible motion along the initial (final) state potential U_1 (U_2) with the reaction sink $W(\bar{x})$ located at the crossing region with the intensity W_0 proportional to the strength of the coupling, V_{12}.

Thus, the above mentioned arguments extend the application of the irreversible approach to evaluation of the chemical rates onto the reversible processes. So, the rest of the present work will be devoted exclusively to the irreversible reactions.

CHAPTER III. REACTION RATE CONSTANTS AND THE CONNECTION BEWEEN THEM

It is easy to see that the reaction kinetics given by Eqs. (I.1.5) and (I.1.8) are equivalent for description of irreversible reactions. However, whereas there is a complicated integral connection between k(t) in Eq. (I.1.5) and the integral kernel $\tilde{æ}(s)$ of Eq (I.1.8), it is easy to connect the long time constant k in Eq. (I.1.6) with $\tilde{æ}(s)$. Actually, if the exponential asymptotic of the kinetics exists, the following equation may readily be obtained using Eq. (I.1.10) and the main property of the Laplace transform [45]:

$$\lim_{t->\infty} P_e(t)\exp(kt) = \lim_{s->0} s\tilde{P}_e(s-k) = \lim_{s->0} \frac{s}{s-k+\tilde{æ}(s-k)} = const$$

So, we have:

$$\lim_{s->0} \frac{\tilde{æ}(s-k)-k}{s} = const, \qquad or \qquad \lim_{s->0} \tilde{æ}(s-k) = k$$

Thus, the desired long time rate constant is a positive root of the equation :

$$\tilde{æ}(-k) = k. \tag{I.3.1}$$

Analyzing the behavior of Eq. (I.1.10) on a complex plane of s, one can easily deduce that the point s = -k is the extremely right isolated singular point, moreover, it is a simple pole. This means that this root corresponds to the first order zero of the function s + $\tilde{æ}(s)$.

If the properties of the root differ from the above mentioned ones, for example, if it corresponds to an essentially singular point of Eq. (I.3.1) on the complex plane, the exponential asymptotic ~exp*(-kt)* is just an intermediate part of the time scale of the reaction kinetics. This case, in principle, may occur if Eq. (I.3.1) does not have a positive root.

Apart from this, it is not difficult to prove that if exponential decay with rate constant k occurs at all times, then $\tilde{æ}(s)=\tilde{æ}(0)=æ= k$. So, the integral-differential form of Eq. (I.1.8) permits us to reduce the calculation of the steady-state characteristics to the investigation of the integral kernel $\tilde{æ}(s)$ only.

1. The reaction rate "constant"

To formulate a steady-state differential equation for the long-time rate constant k let us introduce the modified population probability [45]:

$$n(\vec{x},\vec{v},t)=\frac{P(\vec{x},\vec{v},t)}{P_e(t)}\,, \qquad \iint n(\vec{x},\vec{v},t)d\vec{x}d\vec{v}=1 \tag{I.3.2}$$

which satisfies the equation:

$$\frac{\partial}{\partial t}n(\vec{x},\vec{v},t)-k(t)n(\vec{x},\vec{v},t)=\hat{L}(\vec{x},\vec{v})n(\vec{x},\vec{v},t)-W(\vec{x})n(\vec{x},\vec{v},t)$$

Taking into account property (I.1.3), the rate "constant" in Eq. (I.1.5) may be defined through this new function as

$$k(t)=\iint W(\vec{x})n(\vec{x},\vec{v},t)d\vec{x}d\vec{v}$$

This expression is a complete analog of the definition of the reaction rate constants in bimolecular reaction theory [38, 46].

The advantage of using $n(\vec{x},\vec{v},t)$ appears at the limit as t->∞. If the long time rate constant exists, this limit can be carried out directly in Eq. (I.3.2) $n(\vec{x},\vec{v})=\lim_{t->\infty} n(\vec{x},\vec{v},t)$ and we can write down the differential equation for the long-time rate constant k

$$-\hat{L}(\vec{x},\vec{v})n(\vec{x},\vec{v})+W(\vec{x})n(\vec{x},\vec{v})=kn(\vec{x},\vec{v}) \tag{I.3.3}$$

supported by the requirement

$$\iint n(\vec{x},\vec{v})d\vec{x}d\vec{v}=1. \tag{I.3.4}$$

The boundary conditions for this differential equation are the same as those for Eq. (I.1.1).

However, it should be mentioned that even if Eq. (I.3.3) looks like an ordinary eigenvalue equation, its solution for the definition of k and $n(\vec{x},\vec{v})$ does not require utilization of a property such as completeness of the set of eigenfunctions. This requirement is substituted by the normalization condition for $n(\vec{x},\vec{v})$, which significantly simplifies the problem. Moreover, as will be discussed below, Eq. (I.3.3) exhibits a simple connection with the function which determines the integral kernel of Eq. (I.1.8).

2. The integral kernel of the kinetic equation

In this Section we define the integral kernel of Eq. (I.1.8) and present the steady-state differential equation for the generalized probability æ. Due to the convolution nature in equation (I.1.8), for convenience we generated Laplace transforms (I.1.9) for all values relevant to the discussion. As a result, we obtained from Eq. (I.1.1) the following:

$$\hat{L}(\vec{x},\vec{v})\tilde{P}(\vec{x},\vec{v},s) - W(\vec{x})\tilde{P}(\vec{x},\vec{v},s) = s\tilde{P}(\vec{x},\vec{v},s) - f(\vec{x},\vec{v}) \qquad \text{(I.3.5)}$$

where $f(\vec{x},\vec{v})$ is the normalized initial-distribution function.

Let us introduce

$$\xi(\vec{x},\vec{v},s) = \frac{\tilde{P}(\vec{x},\vec{v},s)}{\tilde{P}_{\bullet}(s)} = (s + \tilde{æ}(s))\tilde{P}(\vec{x},\vec{v},s) \qquad \text{(I.3.6)}$$

This function satisfies the normalization property $\iint \xi(\vec{x},\vec{v},s)d\vec{x}d\vec{v} = 1$ and will be called here the modified population Laplace transform (note that it is not the Laplace transform of the modified population probability $n(\vec{x},\vec{v},t)$, but a completely *different function*). Now the Laplace transform of the integral kernel is

$$\tilde{æ}(s) = \iint W(\vec{x})\xi(\vec{x},\vec{v},s)d\vec{x}d\vec{v}. \qquad \text{(I.3.7)}$$

According to definition (I.3.6), Eq. (I.3.5) yields:

$$\hat{L}(\vec{x},\vec{v})\xi(\vec{x},\vec{v},s) - W(\vec{x})\xi(\vec{x},\vec{v},s) = s\xi(\vec{x},\vec{v},s) - (s + \tilde{æ}(s))f(\vec{x},\vec{v}) \qquad \text{(I.3.8)}$$

Even though Eqs. (I.3.5) and (I.3.8) look very similar, a few words should be said about their differences. First, according to Eqs. (I.1.10) and (I.3.1), the Laplace transform of the kinetics $\tilde{P}_{\bullet}(s)$ diverges at s->-k, therefore $\tilde{P}(\vec{x},\vec{v},s)$ has the same feature. So, it is impossible to take the limit s->-k correctly in Eq. (I.3.5). On the other hand, at s-> -k Eq. (I.3.8) generates Eq. (I.3.3) for the calculation of the long-time rate constant k. Moreover, the transition from Eq. (I.3.8) to Eq. (I.3.3) at s-> -k clearly demonstrates the physically obvious fact that the long-time rate constant, k, does not depend on the initial distribution

$f(\vec{x},\vec{v})$. The connection between values $n(\vec{x},\vec{v})$ and $\xi(\vec{x},\vec{v},s)$ is given as $n(\vec{x},\vec{v}) = \xi(\vec{x},\vec{v},-k)$

The singularity of $\tilde{P}_e(s)$ and $\tilde{P}(\vec{x},\vec{v},s)$ may appear even in the limit s->0, which would cause difficulties for the calculation of the time averaged rate constant æ=$\tilde{æ}$(0). Actually, the following steady-state equation, drawn from Eq. (I.3.5) for $\tilde{P}(\vec{x},\vec{v}) = \tilde{P}(\vec{x},\vec{v},0)$ is completely legitimate:

$$\hat{L}(\vec{x},\vec{v})\tilde{P}(\vec{x},\vec{v}) - W(\vec{x})\tilde{P}(\vec{x},\vec{v}) = -f(\vec{x},\vec{v}), \qquad \text{(I.3.9)}$$

but it is not directly applicable to the calculation of $\tilde{P}_e(0)$ = 1/æ in the strong non-adiabatic case when W_0 -> 0 and the rate is controlled exclusively by weak non-adiabatic transitions between the reactants and products, i.e. by perturbations near the transition point. In this case one has æ -> 0 and, hence, $\tilde{P}_e(0)$ diverges [6].

On the contrary, the transition $\xi(\vec{x},\vec{v}) = \xi(\vec{x},\vec{v},0)$ is perfectly legitimate and Eq. (I.3.8) results in the following steady-state equation for æ

$$\hat{L}(\vec{x},\vec{v})\xi(\vec{x},\vec{v}) - W(\vec{x})\xi(\vec{x},\vec{v}) = -æ f(\vec{x},\vec{v}), \qquad \text{(I.3.10)}$$

which should be completed with normalization condition

$$\iint \xi(\vec{x},\vec{v})d\vec{x}d\vec{v} = 1. \qquad \text{(I.3.11)}$$

Now, perturbation series based on $\xi(\vec{x},\vec{v})$ can be easily constructed for æ at W_0 -> 0 using a iterative procedure. In the zero-order perturbation theory for W_0 (W_0 = 0; æ=æ$^{(0)}$=0) from Eq. (I.3.10) one can obtain $\xi^{(0)}(\vec{x},\vec{v}) = \varphi(\vec{x},\vec{v})$. Taking into account the definition of the generalized probability æ:

$$æ = \iint W(\vec{x})\xi(\vec{x},\vec{v})d\vec{x}d\vec{v}, \qquad \text{(I.3.12)}$$

the first order approximation gives:

$$æ^{(1)} = æ_r = K_r = \iint W(\vec{x})\varphi(\vec{x},\vec{v})d\vec{x}d\vec{v}, \qquad \text{(I.3.13)}$$

where K_r is the non-adiabatic rate constant.

Taking into account definition (I.3.13), it is convenient to represent the sink rate in the form

$$W(\vec{x}) = K_r \psi_0(\vec{x}) \qquad \text{(I.3.14)}$$

where $\psi_0(\vec{x})$= $W_0 S(\vec{x})/K_r$ is the function normalized with the weight $\varphi(\vec{x}) \equiv \int \varphi(\vec{x},\vec{v})d\vec{v}$ and $\int \varphi(\vec{x})\psi_0(\vec{x})d\vec{x} = 1$. Now the function $\psi_0(\vec{x})$ defines the true geometric form of the reaction zone.

It should be mentioned that the legitimacy of the limit s -> 0 taken directly in differential equation (I.3.5) (and even more so, the transition to the field of negative values of s->-k on the complex plane in Eq. (I.3.8)) is not obvious.

To substantiate that these transitions are correct, we now consider the integral form of Eqs. (I.3.5) and (I.3.8) using the steady-state Green's function formalism.

CHAPTER IV. INTEGRAL FORM OF THE PRINCIPAL EQUATIONS AND THE STEADY-STATE GREEN'S FUNCTION METHOD

1. The Green's function representation

The Green's function $G(\vec{x},\vec{v},\vec{x}',\vec{v}',s)$ for the operator $\hat{L}(\vec{x},\vec{v})$ satisfies the equation

$$\hat{L}(\vec{x},\vec{v})G(\vec{x},\vec{v},\vec{x}',\vec{v}';s) - sG(\vec{x},\vec{v},\vec{x}',\vec{v}';s) = -\delta(\vec{x}-\vec{x}')\delta(\vec{v}-\vec{v}') \qquad \text{(I.4.1)}$$

where $\delta(\vec{x})$ is the Dirac delta-function. This Green's function describes only the stochastic motion along the surface, not the reaction, and has the same reflecting boundary conditions at the edges of the reaction space as those for Eq. (I.3.5). Function G is the Laplace transform of the conditional probability density function $\rho(\vec{x},\vec{v},\vec{x}',\vec{v}';t)$ which corresponds to the conditional probability of realization of values $\vec{x}$ and $\vec{v}$ at time t if they had values $\vec{x}'$ and $\vec{v}'$ at t=0. The Green's function satisfies the steady-state and normalization conditions:

$$\iint G(\vec{x},\vec{v},\vec{x}',\vec{v}';s)\varphi(\vec{x}',\vec{v}')d\vec{x}'d\vec{v}' = \frac{1}{s}\varphi(\vec{x},\vec{v}) \qquad \int G(\vec{x},\vec{v},\vec{x}',\vec{v}';s)d\vec{x}d\vec{v} = \frac{1}{s} \qquad \text{(I.4.2)}$$

where $\varphi(\vec{x},\vec{v}) = \lim_{t->\infty}\rho(\vec{x},\vec{v},\vec{x}',\vec{v}';t) = \lim_{s->0} sG(\vec{x},\vec{v},\vec{x}',\vec{v}';s)$ is the Boltzmann distribution. Moreover, it can be easily proved that:

$$\hat{L}(\vec{x},\vec{v})\varphi(\vec{x},\vec{v}) = 0 \qquad G(\vec{x},\vec{v},\vec{x}',\vec{v}';s) \sim \frac{1}{s}\varphi(\vec{x},\vec{v}) \quad \text{at s -> 0.} \qquad \text{(I.4.3)}$$

Note, that the steady-state condition in Eq. (I.4.2) is only the consequence of the detailed balance principle $G(\vec{x},\vec{v},\vec{x}',\vec{v}';s)\varphi(\vec{x}',\vec{v}') = G(\vec{x}',\vec{v}',\vec{x},\vec{v};s)\varphi(\vec{x},\vec{v})$

The Green's function $G(\vec{x},\vec{v},\vec{x}',\vec{v}';s)$ is the kernel of the integral operator $\hat{G}(s) = (s - \hat{L})^{-1}$. Thus, considering the second members in both the right and left parts of Eq. (I.3.5) as the non-homogeneous part of this equation, one can obtain the integral equation

$$\tilde{P}(\vec{x},\vec{v},s) = \iint G(\vec{x},\vec{v},\vec{x}',\vec{v}';s)f(\vec{x}',\vec{v}')d\vec{x}'d\vec{v}' - \iint G(\vec{x},\vec{v},\vec{x}',\vec{v}';s)W(\vec{x}')\tilde{P}(\vec{x}',\vec{v}',s)d\vec{x}'d\vec{v}' \qquad \text{(I.4.4)}$$

By analogy, the integral equation for $\xi(\vec{x},\vec{v},s)$ is:

$$\xi(\vec{x},\vec{v},s) = (s+\tilde{æ}(s))\iint G(\vec{x},\vec{v},\vec{x}',\vec{v}';s)f(\vec{x}',\vec{v}')d\vec{x}'d\vec{v}' -$$
$$-\iint G(\vec{x},\vec{v},\vec{x}',\vec{v}';s)W(\vec{x}')\xi(\vec{x}',\vec{v}',s)d\vec{x}'d\vec{v}'. \qquad \text{(I.4.5)}$$

However, according to the second equation in (I.4.3), the Green's function $G(\vec{x},\vec{v},\vec{x}',\vec{v}';s)$ has a singularity at s ->0 and this limit is prohibited in Eq. (I.4.1). This means that the direct transition from the time-dependent Green's function to a steady-state one is impossible. Thus, we are obliged to question the limit s -> 0 in Eqs. (I.3.5) and (I.3.8) which was taken in order to obtain steady-state equations (I.3.9) and (I.3.10), as far as the latter two equations cannot be represented in the integral form through the Green's function G at s = 0.

2. The steady-state Green's functions

First of all, we are going to prove that the limit transition s -> 0 is legitimate in Eqs. (I.3.5) and (I.3.8) and explain the apparent contradiction. For this purpose let us introduce the modified Green's function $\overline{G}(\vec{x},\vec{v},\vec{x}',\vec{v}';s)$ as in [14]:

$$\overline{G}(\vec{x},\vec{v},\vec{x}',\vec{v}';s) = G(\vec{x},\vec{v},\vec{x}',\vec{v}';s) - \frac{\varphi(\vec{x},\vec{v})}{s}, \qquad \text{(I.4.6)}$$

where the subtracted part is, in fact, the limit of the ordinary Green's function, $G(\vec{x},\vec{v},\vec{x}',\vec{v}';s)$ at s->0. According to Eq. (I.4.1), the above function satisfies the following equation:

$$\hat{L}(\vec{x},\vec{v})\overline{G}(\vec{x},\vec{v},\vec{x}',\vec{v}';s) - s\overline{G}(\vec{x},\vec{v},\vec{x}',\vec{v}';s) = -\delta(\vec{x}-\vec{x}')\delta(\vec{v}-\vec{v}') + \varphi(\vec{x},\vec{v}). \qquad \text{(I.4.7)}$$

This equation has the same reflecting boundary conditions as the original differential equation. The modified Green's function has the following properties:

$$\iint \overline{G}(\vec{x},\vec{v},\vec{x}',\vec{v}';s)\varphi(\vec{x}',\vec{v}')d\vec{x}'d\vec{v}' = 0 \qquad \iint \overline{G}(\vec{x},\vec{v},\vec{x}',\vec{v}';s)d\vec{x}d\vec{v} = 0. \qquad \text{(I.4.8)}$$

Contrary to the initial Green's function, the modified function $\overline{G}(\vec{x},\vec{v},\vec{x}',\vec{v}';s)$ allows the limit transition s ->0. Moreover, if the long-time rate constant k exists, the modified Green's function guarantees the transition to the field of the negative values of s (s -> -k).

At s=0, this function turns into a steady-state Green's function $\overline{G}(\vec{x},\vec{v},\vec{x}',\vec{v}')$, $\overline{G}(\vec{x},\vec{v},\vec{x}',\vec{v}') = \overline{G}(\vec{x},\vec{v},\vec{x}',\vec{v}',s=0)$. $\overline{G}(\vec{x},\vec{v},\vec{x}',\vec{v}')$ has the same properties as the ones given by Eq. (I.4.8).

Integral equation (I.4.5) can be rewritten in the steady-state form:

$$\xi(\vec{x},\vec{v}) = \varphi(\vec{x},\vec{v}) + æ\iint \overline{G}(\vec{x},\vec{v},\vec{x}',\vec{v}')f(\vec{x}',\vec{v}')d\vec{x}'d\vec{v}' - \iint \overline{G}(\vec{x},\vec{v},\vec{x}',\vec{v}')W(\vec{x}')\xi(\vec{x}',\vec{v}')d\vec{x}'d\vec{v}'. \qquad (I.4.9)$$

When the initial distribution f is Boltzmann, the second member on the right hand side is zero and the integral equation obtains its simplest form.

As one can see, the introduction of the new Green's function, $\overline{G}(\vec{x},\vec{v},\vec{x}',\vec{v}',s)$ allows us to manipulate the integral equations (Eqs. (I.4.4) and (I.4.5)) in a way which is the most profitable for us. By doing this we achieved two things. First of all, we proved that the steady-state differential equations for $P(\vec{x},\vec{v})$ and $\xi(\vec{x},\vec{v})$, Eqs. (I.3.5) and (I.3.8), are completely legitimate. Thus, the fact that the limit transition s->0 is prohibited in integral equations (I.4.4) and (I.4.5) does not affect the differential equations. Second, we formulated the correct steady-state integral equations. Therefore, now we have two alternative types of approaches - differential and integral - for evaluation of the desired rate constants.

For all cases with non-statistical initial distribution, it is convenient to introduce another modified Green's function which also permits the limit transition s ->0

$$\tilde{G}(\vec{x},\vec{v},\vec{x}',\vec{v}';s) = G(\vec{x},\vec{v},\vec{x}',\vec{v}';s) - \iint G(\vec{x},\vec{v},\vec{x}',\vec{v}';s)f(\vec{x}',\vec{v}')d\vec{x}'d\vec{v}' \equiv \overline{G}(\vec{x},\vec{v},\vec{x}',\vec{v}';s) - \iint \overline{G}(\vec{x},\vec{v},\vec{x}',\vec{v}';s)f(\vec{x}',\vec{v}')d\vec{x}'d\vec{v}'. \qquad (I.4.10.a)$$

It satisfies the differential equation:

$$\hat{L}(\vec{x},\vec{v})\tilde{G}(\vec{x},\vec{v},\vec{x}',\vec{v}';s) - s\tilde{G}(\vec{x},\vec{v},\vec{x}',\vec{v}';s) = -\delta(\vec{x}-\vec{x}')\delta(\vec{v}-\vec{v}') + f(\vec{x},\vec{v}) \qquad (I.4.10.b)$$

and has the following properties

$$\iint \tilde{G}(\vec{x},\vec{v},\vec{x}',\vec{v}';s)f(\vec{x}',\vec{v}')d\vec{x}'d\vec{v}' = 0 \qquad \iint \tilde{G}(\vec{x},\vec{v},\vec{x}',\vec{v}';s)d\vec{x}d\vec{v} = 0. \qquad (I.4.11)$$

It is obvious that $\overline{G}$ is only a particular case of the general modified Green's function $\tilde{G}$ for $f(\vec{x},\vec{v})=\varphi(\vec{x},\vec{v})$.

The equation for evaluation of the steady-state Green's function $\tilde{G}(\vec{x},\vec{v},\vec{x}',\vec{v}') = \tilde{G}(\vec{x},\vec{v},\vec{x}',\vec{v}',0)$ is

$$\hat{L}(\vec{x},\vec{v})\tilde{G}(\vec{x},\vec{v},\vec{x}',\vec{v}') = -\delta(\vec{x}-\vec{x}')\delta(\vec{v}-\vec{v}') + f(\vec{x},\vec{v}). \qquad \text{(I.4.12)}$$

The important point here is that the property $\iint \hat{L}(\vec{x},\vec{v})\tilde{G}(\vec{x},\vec{v},\vec{x}',\vec{v}')d\vec{x}d\vec{v} = 0$ is only a consequence of Eq. (I.4.12). So, the previous reflecting boundary conditions can not be used as the boundary conditions for Eq. (I.4.12). Instead of them, Eq. (I.4.12) should be completed with the additional requirement

$$\iint \tilde{G}(\vec{x},\vec{v},\vec{x}',\vec{v}')d\vec{x}d\vec{v} = 0. \qquad \text{(I.4.12a)}$$

The integral equation for the steady-state modified population probability can be obtained from integral equation (I.4.5) with account of definition (I.4.10.a).

$$\xi(\vec{x},\vec{v}) = \varphi(\vec{x},\vec{v}) - \iint \tilde{G}(\vec{x},\vec{v},\vec{x}',\vec{v}')W(\vec{x})\xi(\vec{x}',\vec{v}')d\vec{x}'d\vec{v}'. \qquad \text{(I.4.13)}$$

To sum up, evaluation of the generalized probability æ can be based either on differential (I.3.10) or integral (I.4.13) steady-state equations for $\xi(\vec{x},\vec{v})$. The differential method requires use of normalization conditions (I.3.11) whereas the integral one combines Eq. (I.4.13) with the definition for the survival probability in Eq. (I.3.12).

At the end of this Chapter we would like to mention the existence of one more problem which is discussed in Appendix A. It concerns the pseudostationary Green's function $G_0(\vec{x},\vec{v},\vec{x}',\vec{v}')$ which is the direct Green's function for the solution of differential equation (I.3.10).

CHAPTER V. REACTIONS ON THE PINHOLE AND NARROW SINKS

For reactions on one-dimensional potential surfaces a quite narrow reaction sink can usually be approximated by an infinitely narrow, or pinhole, sink. This presumption significantly simplifies calculations of the reaction rates in ET and electronic relaxation processes [6, 12, 13, 14]. The only problem with this simplification lies in drawing up the appropriate criteria for its application. In Ref. [6] the authors suggested that the pinhole formalism can be applied when the width of the reaction sink is much smaller then the width of the Boltzmann distribution on the reaction surface. This case was called the "narrow reaction window" limit and the sink was taken as a point on the reaction surface. The criterion of validity of this approximation will be considered in Chapter VI. In this Chapter we are going simply to assume that it is satisfied with a note that the criterion formulated in Ref. [6] is *not* sufficient for the pinhole reaction to take place.

1. Reactions on the pinhole sink

For the decay on a pinhole sink we can present the reaction sink in the form $W(x) = K_r \psi_0(x) = \frac{K_r}{\varphi(x_p)} \delta(x - x_p) \equiv K_0 \delta(x - x_p)$ where $K_r = K_0 \varphi(x_p)$ is the nonadiabatic rate constant defined in Eq. (I.3.13) and $\varphi(x)$ is the Boltzmann distribution. From Eq. (I.4.9) and definitions (I.3.7) and (I.4.10.a) we can easily find the integral kernel:

$$\tilde{æ}(s) = \frac{K_r(1 + s\int \overline{G}(x_p, x; s) f(x) dx / \varphi(x_p))}{1 + K_r \tilde{G}(x_p, x_p; s) / \varphi(x_p)}. \qquad \text{(I.5.1)}$$

According to Eqs. (I.5.1) and (I.4.10.a), the long-time rate constant k may be obtained from Eq. (I.3.1) in the form:

$$\frac{1}{k} = \frac{1}{K_r} + \frac{\overline{G}(x_p, x_p; -k)}{\varphi(x_p)}. \qquad \text{(I.5.2)}$$

As one can see, the long time rate constant does not depend on the initial distribution f(x) and depends only on the Green's function $\overline{G}$ corresponding to the Boltzmann initial distribution. The long-time rate constant k can be obtained through the analytical expansion of the function $G(x_p, x_p, s)$ to the region of negative real values of s as

$$G(x_p, x_p, -k) = -\frac{\varphi(x_p)}{K_r} \equiv -\frac{1}{K_0}. \qquad \text{(I.5.3)}$$

According to Eq. (I.5.1), the reciprocal value of æ=$\tilde{æ}$(0) for the δ-functional sink is always given as a sum of the reciprocal nonadiabatic rate constant and MFPT, τ_p. MFPT in this case is the average time for particles to reach the absorbing point x_p having started from the initial distribution f(x):

$$\frac{1}{æ} = \frac{1}{K_r} + \frac{1}{æ_d} \equiv \frac{1}{K_r} + \tau_p. \qquad \text{(I.5.4)}$$

As one can clearly see, only the generalized probability is calculated through MFPT, and not k as sometimes is implied.

The formalism outlined in Eqs. (I.5.1)-(I.5.4) is straightforward to extend to multidimensional processes if one is interested only in the average time to reach a point on the reaction surface. Such a problem appears, for example, in multidimensional adiabatic reactions with high activation barriers [8]. In this case the MFPT is evaluated as the average time to reach the saddle point having started from some distribution deep inside the reactant well. However, if the reaction region is considered to be different for a multidimensional process, then the "narrow reaction window" limit is not so easy to define. We come back to its definition for multidimensional reactions in Sec. 2 of this Chapter and Part II.

For one-dimensional surface reactions τ_p can be defined through the Green's functions in Appendix A:

$$\tau_p = \frac{1}{æ_d} = \frac{\tilde{G}(x_p, x_p)}{\varphi(x_p)} = \int_{-\infty}^{x_p} \frac{dy}{D(y)\varphi(y)} \int_{-\infty}^{y} \varphi(z)dz \int_{-\infty}^{y} f(z)dz + \int_{x_p}^{\infty} \frac{dy}{D(y)\varphi(y)} \int_{y}^{\infty} \varphi(z)dz \int_{y}^{\infty} f(z)dz .$$

(I.5.5)

Thus, we have established the physical meaning of the function $\tilde{G}(x_p, x_p)$, which determines the MFPT to the point x_p at the given initial distribution f(x).

Taking as an example the initial distribution $f(x)=\delta(x-x_0)$, we can express the time at which a particle having started at some point x_0, first reaches the point x_p:

$$\tau_p(x_0) = \frac{\overline{G}(x_p, x_p) - \overline{G}(x_p, x_0)}{\varphi(x_p)} = \begin{cases} \int_{x_0}^{x_p} \frac{dy}{D(y)\varphi(y)} \int_{-\infty}^{y} \varphi(z)dz & \text{where } x_0 \le x_p \\ \int_{x_p}^{x_0} \frac{dy}{D(y)\varphi(y)} \int_{y}^{\infty} \varphi(z)dz & \text{where } x_0 \ge x_p \end{cases} \qquad \text{(I.5.6)}$$

The integral form for the case $x_0 > x_p$ was obtained by Szabo et. al. [9] by considering reactions on a black absorbing boundary located at x_p. The approach presented in [9] was developed for Green's functions which described an infinitely fast reaction at the boundary x_p (the Smoluchowski boundary condition for the reaction described by the sink function is $W(x) = K_0\Theta(x-x_p)$ where Θ is a step-function and $K_0 \to \infty$). The above Green's functions shouldn't be confused with the ones which are used in the present work. The steady-state Green's functions do not include any knowledge about the reaction region, they are defined solely for the reaction potential with the reflecting boundary conditions at the edges of the reaction space which makes them universal for any reaction region on the given reaction surface.

Taking into account the above expression for $\tau_p(x_0)$ and Eq. (I.5.5), the MFPT for the pinhole sink located at x_p can be represented as:

$$\tau_p = \int \tau_p(x_0) f(x_0) dx_0 \qquad \text{(I.5.7)}$$

where the integration is carried out over all reaction space, which is intuitively sensible.

2. Reactions on the narrow sink

If we assume that the reaction takes place in a multidimensional space on a narrow reaction region which is given by the function $\psi_0(\vec{x})$ in Eq. (I.3.14), then the integral kernel in Eq. (I.5.1) can be represented in the general form:

$$\tilde{æ}(s) = \frac{K_r(1 - s\Delta g(s))}{1 + K_r g(s)}$$

where

$$\Delta g(s) = -\iint \psi_0(\vec{x})\overline{G}(\vec{x},\vec{x}';s)f(\vec{x}')d\vec{x}d\vec{x}'.$$

For s=0, Δg gives the time difference between MFPT to reach the zone $\psi_0(\vec{x})$ having started from an arbitrary initial distribution $f(\vec{x})$ and the one for the Boltzmann initial distribution $\varphi(\vec{x})$:

$$\Delta\tau_p = \Delta g(0) = -\iint \psi_0(\vec{x})\overline{G}(\vec{x},\vec{x}')f(\vec{x}')d\vec{x}d\vec{x}' \qquad \text{(I.5.8)}$$

By analogy we can introduce:

$$g(s) = \iint \psi_0(\vec{x})\overline{G}(\vec{x},\vec{x}';s)\psi_0(\vec{x}')f(\vec{x}')d\vec{x}d\vec{x}'$$

For s=0 this time is the average time for particles to reach the *reaction zone* (not a point) on multidimensional reaction surface for a first time:

$$\tau_p = \iint \psi_0(\vec{x})\tilde{G}(\vec{x},\vec{x}')\psi_0(\vec{x}')\varphi(\vec{x}')d\vec{x}d\vec{x}'. \qquad \text{(I.5.9)}$$

This MFPT is vitally different from all previous average times. We will call it the effective MFPT. Introduction of the effective MFPT is absolutely necessary for reactions on multidimensional potential surfaces even if the reaction sink ψ_0 is infinitely narrow (a line on the multidimensional surface). The effective MFPT can not be evaluated using the Smoluchowskii boundary conditions as was done in Refs. [8, 9] As far as the reaction region has to be narrow, for the one-dimensional case Eq. (I.5.9) gives only a correction to the MFPT to a point. This correction should include the effective width of the reaction region and is important only for diabatic potential surfaces, because the traditional adiabatic

approach does not require reactive particles to reach a region, but a point. However, the above definition is extremely important for both adiabatic and diabatic multidimensional reactions. For irreversible reactions on diabatic surfaces the reaction region is formed by the area near the line of intersection of the initial and final diabatic surfaces. The reaction decay occurs through the whole region and the MFPT to a point cannot be of any interest. For high activation barrier adiabatic reactions on multidimensional surfaces the reaction rate still can be evaluated through the MFPT to a point, as was mentioned before (in this case it is the MFPT to the saddle point) [8]. However, for less than extremely high activation barriers, the particles escape from the metastable state along many trajectories, which may or may not go through the saddle point. Therefore, again, evaluation of the MFPT to a region is necessary.

For the narrow zone we can also generalize the expression for the long-time rate constant k,

$$-\frac{1}{K_r} = \iint \psi_0(\vec{x}) G(\vec{x}, \vec{x}'; -k) \psi_0(\vec{x}') \varphi(\vec{x}') d\vec{x} d\vec{x}' .$$

Now we intend to demonstrate that the condition for the applicability of the decoupling approximation (suggested in [6] for one-dimensional reactions) is not sufficient. The condition required small values of the reaction sink width δ compared with the width Δ of the Boltzmann distribution.

Let us consider a decay process on a one-dimensional potential surface V(x) when the sink located at some point x_p has the width $\delta << x_p$ and the reaction occurs over a high activation barrier. That means the requirement $\beta V(x_p) >> 1$ is satisfied, which is equivalent to the condition $\Delta << x_p$. However, the relationship between Δ and δ is not bounded. Using Eq. (A14) and asymptotic estimate (A10) from Appendix A, one can obtain the form of the modified Green's function $\tilde{G}(x, x')$ when x and x' are located inside the reaction sink ($\beta V(x_p) >> 1$):

$$\tilde{G}(x,x') = \begin{cases} \dfrac{\varphi(x)}{D\beta V'(x_p)\varphi(x')} & x \geq x' \\ \dfrac{1}{D\beta V'(x_p)} & x \leq x' \end{cases} \qquad \text{(I.5.10)}$$

For this case, Eq. (I.4.13) may be represented as:

$$\xi(x) = \varphi(x) - \frac{\varphi(x)}{D\beta V'(x_p)} \int_{-\infty}^{x} \frac{W(x')}{\varphi(x')} \xi(x')dx' - \frac{1}{D\beta V'(x_p)} \int_{x}^{\infty} W(x')\xi(x')dx'. \qquad \text{(I.5.11)}$$

Despite the required restrictions for Green's function (I.5.10) on the location of x, the solution of Eq. (I.5.11) is meaningful for the whole reaction space, $-\infty<x<\infty$. However it should be taken into account that the above solution coincides with the correct one only inside the reaction region. Application of this solution is legitimate because according to Eq. (I.3.12) the generalized probability æ is defined by the part of the solution which is located only in the reaction region.

Let us accept the condition which was suggested in [6] as the criterion for the "narrow-reaction window" case:

$$\delta << \Delta. \qquad \text{(I.5.12)}$$

Now, in order to be consistent with results (I.5.10) and (I.5.11) we should use the following representation of the Boltzmann distribution:

$$\varphi(x) \approx \frac{1}{Z_0} \exp[-(\beta V(x_p) + \beta V'(x_p)(x - x_p))]. \qquad \text{(I.5.13)}$$

This representation helps us to produce the new differential equation:

$$\xi''(x) + \beta V'(x_p)\xi'(x) - \frac{1}{D} W(x)\xi(x) = 0, \qquad \text{(I.5.14)}$$

with the boundary conditions which follow from Eqs. (I.3.12) and (I.5.11):

$$\xi(x) - \varphi(x) \underset{x->-\infty}{->} -\frac{æ}{D\beta V'(x_p)}, \qquad \xi'(x) - \varphi'(x) \underset{x->-\infty}{->} 0.$$

The equation thus generated obviously does not correspond to the case of a "narrow reaction window" limit, as far as its solution depends on the form of W(x). Specifically, we suppose for simplicity that the sink has the form of a plateau

$$W(x) = \begin{cases} K_0 / \delta & x_p - \delta/2 \le x \le x_p + \delta/2 \\ 0 & x < x_p - \delta/2, x > x_p + \delta/2 \end{cases}$$

Then the nonadiabatic rate constant K_r can be defined through Eq. (I.3.13) as:

$$K_r = \frac{2K_0}{\delta\beta V'(x_p)Z_0} sh(\beta V'(x_p)\delta/2)\exp(-\beta V(x_p)). \qquad (I.5.15)$$

Moreover, Eq. (I.5.14) rewritten for the intervals $-\infty<x<x_p - \delta/2$ and $x_p - \delta/2 \le x \le x_p - \delta/2$ generates a differential equation with constant coefficients. Its solutions can be obtained easily and the expression for the generalized probability at $\delta << \Delta << x_p$ is:

$$æ = \frac{\frac{2K_0}{\delta\Xi Z_0}\exp(-\beta V(x_p) + \alpha\delta/2) th(\delta\Xi/2)}{1 + \frac{\alpha^2 + \Xi^2}{2\Xi\alpha} th(\delta\Xi/2)} \qquad (I.5.16)$$

where

$$\alpha = \beta V'(x_p), \quad \Xi = \sqrt{\alpha^2 + 4K_0 / D\delta}.$$

Note that the nonadiabatic and diffusion constants K_r and $æ_d$ cannot be separated in this expression for æ. At $K_0 \to \infty$, as expected, Eq. (I.5.16) may be transformed to the pure diffusion rate constant

$$\frac{1}{æ} \approx \frac{1}{æ_d} \equiv \tau_p \approx \frac{Z_0}{D\alpha}\exp(\beta V(x_p - \delta/2)) \qquad (I.5.17)$$

which corresponds to the reaction with infinite intensity at the point $x_p - \delta/2$.

The result of the "narrow reaction window" limit, Eq. (I.5.4) may be obtained from Eq. (I.5.16) with the additional condition:

$$\delta << \frac{1}{\alpha} = \frac{1}{\beta V'(x_p)} \sim \Delta\frac{\Delta}{x_p} << \Delta \qquad (I.5.18)$$

which is more rigid than the original one in Eq. (I.5.12). Restriction (I.5.18) exists for any form of the reaction sink W(x). When condition (I.5.18) is satisfied, one can neglect the second member of the exponent in Eq. (I.5.13).

In the case when criterion (I.5.18) is reversed:

$$\frac{1}{\beta V'(x_p)} = \frac{1}{\alpha} << \delta << \Delta \qquad (I.5.19)$$

one can obtain the expression for the generalized probability from Eq. (I.5.16):

$$æ \approx \frac{4K_r}{(1+\sqrt{1+4K_r/æ_d})^2} \qquad (I.5.20)$$

where $æ_d$ is the diffusion generalized probability (I.5.17) and the nonadiabatic rate constant may be represented in the form:

$$K_r = \frac{K_0}{\delta\beta V'(x_p)Z_0}\exp(-\beta V(x_p - \delta/2)) \qquad (I.5.21)$$

which follows from Eq. (I.5.15) under the condition (I.5.19). Therefore, let us emphasize the fact that although the width of the reaction zone is much smaller than the width of the Boltzmann distribution, the last result does not correspond to the "narrow reaction window" limit and strongly depends on the form of the reaction sink. Moreover, the generalized probability still cannot be represented as the sum of two reciprocals $1/K_r$ and $1/æ_d$ which is a direct sign that the "narrow reaction window" case is not applicable to the situation.

One more significant note should be made. For any "narrow", but extensive reaction sink, a powerful limitation on the diffusion rate is required for the validity of the "narrow-reaction window" approximation. Roughly speaking, when the reaction sink is essentially localized in space, but has weak long tails (sharp Gaussian or exponential forms of W(x) may be given as examples) one can see that when the motion along the reaction surface becomes somewhat slow, the portion of reactants enduring the reaction decay on those tails becomes more and more significant. In this case no "narrow-reaction window" picture can be involved in description of the reaction kinetics, even though the condition $\delta << \Delta$ can still be satisfied.

CHAPTER VI. THE DECOUPLING APPROXIMATION

The "decoupling approximation" is a procedure for solving the integral equation for the probability distribution function (like Eqs. (I.4.4) or (I.4.13)) in order to obtain the reaction rate constants. The decoupling procedure breaks the connection between the integral kernel in the integral equation (the Green's function) and the probability distribution function [6]. This allows us to separate the motion along the reaction surface from the reaction itself.

One of the first applications of the decoupling approximation to solution of diffusion-type motion equation for unimolecular reactions was made by Sumi and Marcus [6]. They called the case when the approximation is applicable the "narrow reaction window" limit. Some attempts to estimate the range of applicability of this approximation were also made by Nadler and Marcus [7] and by Sumi himself [47].

Since this method is a very powerful tool for solution of integral equations, the precise conditions of its applicability are very important. The empirical condition is quite simple - we can break the connection between the motion and the reaction only if the reaction decay occurs in a narrow region compared with the whole reaction space. In other words, if the effective width of the reaction sink $W(\vec{x})$, σ is much smaller then the width of the Boltzmann distribution, Δ , then the narrow window limit takes place. If this is the case, then the reaction disturbs the population inside the potential well only in a small, insignificant area. This statement seems to be very reasonable. However, as was shown in the previous Chapter, this requirement is not sufficient for the "narrow reaction window" limit to take place even in a simple one-dimensional case. The problem appears to be more complicated if one tries to generalize the definition of the "narrow reaction window" for a multidimensional reaction. Is the same geometrical criterion still applicable in this case? How do the different ratios between the relaxation times along different coordinates in the

system affect the limit? What happens if the relaxation along one of the coordinates is very fast? These and many other questions must be asked when trying to apply the "narrow reaction window" limit for multidimensional processes.

Taking all of the above arguments into consideration, our aim here is to introduce the applicability conditions for the decoupling approximation using the kinematic approach developed for bimolecular reactions [46, 48] and to discuss some important physical characteristics which can be evaluated using this method.

In order to evaluate the reaction rate constants we can use the integral equation for the modified population probability, $\xi(\vec{x},s)$ (Eq. (I.4.9)) which in the case of the Boltzmann distribution is as follows:

$$\xi(\vec{x},s) = \varphi(\vec{x}) - \iint \overline{G}(\vec{x},\vec{x}',s)W(\vec{x}')\xi(\vec{x}',s)d\vec{x}'. \qquad \text{(I.6.1)}$$

The above integral equation has to be accompanied by the definition of the integral kernel $\tilde{æ}(s) = \int W(\vec{x}')\xi(\vec{x}',s)d\vec{x}'$. The limit transition s->0 is legitimate in the above equations (and the following equations as well).

Let us introduce the new function $\xi^+(\vec{x},s)$:

$$\xi(\vec{x},s) = \xi^+(\vec{x},s)\varphi(\vec{x}). \qquad \text{(I.6.2)}$$

The modified Green's functions satisfies the following equilibrium property:

$$\overline{G}(\vec{x},\vec{x}',s)\varphi(\vec{x}') = \overline{G}(\vec{x}',\vec{x},s)\varphi(\vec{x}). \qquad \text{(I.6.3)}$$

Taking the last two equations into account we can rewrite Eq. (I.6.1) as:

$$\xi^+(\vec{x},s) = 1 - \int \overline{G}(\vec{x}',\vec{x},s)W(\vec{x}')\xi(\vec{x}',s)d\vec{x}' \qquad \text{(I.6.4)}$$

with the new definition of the integral kernel:

$$\tilde{æ}(s) = \int W(\vec{x})\xi^+(\vec{x},s)\varphi(\vec{x})d\vec{x}. \qquad \text{(I.6.5)}$$

Let us construct a new function which is simply some normalized "zone" encircled by the reaction sink $W(\vec{x})$:

$$\psi(\vec{x},s) = \frac{W(\vec{x})\xi^+(\vec{x},s)}{\langle W(\vec{x})|\xi^+(\vec{x},s)\rangle} \qquad \text{(I.6.6)}$$

where $\langle W|\xi^{+}\rangle$ denotes the average $\int d\vec{x}W(\vec{x})\xi^{+}(\vec{x},s)\varphi(\vec{x})$. Using this function and definition (I.6.5) we can present Eq. (I.6.4) in the following form:

$$\frac{\psi(\vec{x},s)}{W(\vec{x})}+\int d\vec{x}'\overline{G}(\vec{x}',\vec{x},s)\psi(\vec{x}',s)=\frac{1}{\tilde{æ}(s)}. \tag{I.6.7}$$

We can introduce the symmetric integral operator:

$$H(\vec{x}',\vec{x},s)=\frac{\delta(\vec{x}-\vec{x}')}{W(\vec{x})}+\overline{G}(\vec{x}',\vec{x},s) \tag{I.6.8}$$

which allows us to rewrite Eq. (I.6.7) in a convenient form of average:

$$\langle\psi(\vec{x},s)|H(\vec{x}',\vec{x},s)|\psi(\vec{x}',s)\rangle=\frac{1}{\tilde{æ}(s)}. \tag{I.6.9}$$

From the form of Hamiltonian (I.6.8) and the above equation it follows immediately that the integral kernel $\tilde{æ}(s)$ can be separated into two parts:

$$\frac{1}{\tilde{æ}(s)}=\frac{1}{\tilde{æ}_r(s)}+\frac{1}{\tilde{æ}_d(s)} \tag{I.6.10}$$

where $\frac{1}{\tilde{æ}_r(s)}=\left\langle\psi(\vec{x},s)\left|\frac{\psi(\vec{x},s)}{W(\vec{x})}\right.\right\rangle$, $\frac{1}{\tilde{æ}_d(s)}=\left\langle\psi(\vec{x},s)\left|\hat{\overline{G}}(\vec{x}',\vec{x},s)\psi(\vec{x}',s)\right.\right\rangle$,

and $\hat{\overline{G}}(\vec{x}',\vec{x},s)$ (or shorter $\hat{\overline{G}}(s)$) denotes an integral operator. Function $\psi(\vec{x},s)$ itself is the solution of the following equation:

$$\psi(\vec{x},s)=\psi_0(\vec{x})\left\{1+K_r\left(\left\langle\psi_0\left|\hat{\overline{G}}(s)\psi\right.\right\rangle-\hat{\overline{G}}(s)\psi(\vec{x}',s)\right)\right\} \tag{I.6.11}$$

where $K_r=\langle W(\vec{x})\rangle=\int d\vec{x}W(\vec{x})\varphi(\vec{x})$ is a nonadiabatic rate constant and

$$\psi_0(\vec{x})=\frac{W(\vec{x})}{\langle W(\vec{x})\rangle}=\frac{W(\vec{x})}{K_r} \tag{I.6.12}$$

is the original "zone" function $\psi(\vec{x},s)$ in a zero-order approximation, i.e. when $\xi^{+}(\vec{x},s)=1$.

The decoupling approximation uses the above zero-order "zone" function $\psi_0(\vec{x}')$ instead of the real function $\psi(\vec{x},s)$ in order to evaluate an approximate value for the integral kernel $\tilde{æ}(s)$ in Eq. (I.6.9). In other words, from Eq. (I.6.10) we obtain

$$\frac{1}{\tilde{æ}(s)} \approx \frac{1}{\tilde{æ}^0(s)} = \frac{1}{K_r} + \frac{1}{\tilde{æ}_d^0(s)} \tag{I.6.13}$$

where the diffusion part of the integral kernel is

$$\frac{1}{\tilde{æ}_d^0(s)} = \tau_p(s) = \left\langle \psi_0 \middle| \hat{\overline{G}}(s)\psi_0 \right\rangle = \frac{1}{K_r^2}\iint d\vec{x}, d\vec{x}'\varphi(\vec{x})W(\vec{x})\overline{G}(\vec{x}',\vec{x},s)W(\vec{x}') \tag{I.6.14}$$

and $\tau_p(s)$ is some "time" which depends only upon the motion on the reaction surface. The exact physical meaning of this value exists for the steady-state value $\tau_p = \lim_{s->0}(\tau_p(s))$. τ_p is the MFPT to the reaction region $W(\vec{x})$which was given in Eq. (I.5.8). Limit s->0 turns the integral kernel in Eq. (I.6.13) into the generalized probability æ:

$$\frac{1}{æ^0} = \frac{1}{K_r} + \frac{1}{æ_d^0} = \frac{1}{K_r} + \tau_p. \tag{I.6.15}$$

Here τ_p is the effective MFPT, i. e. an average time for particles started (in our case from a Boltzmann distribution) to reach the reaction region $W(\vec{x})$ given in Eq. (I.5.9). If the reaction occurs at one point (a pinhole sink) $W(\vec{x}) = K_0\delta(\vec{x} - \vec{x}_0)$, then the effective MFPT becomes the MFPT to the point, $\vec{x}_0$ and Eq. (I.5.8) produces Eq. (I.5.5).

Using the decoupling approximation formalism we can introduce another important time which depends on the motion along the potential surface. This is the average time inside the "zone" $\psi_0(\vec{x})$ if the motion started at some point $\vec{x}$:

$$\tau_0(\vec{x}) = \hat{\overline{G}}\psi_0(\vec{x}) = \int d\vec{y}\overline{G}(\vec{y},\vec{x})\psi_0(\vec{y}). \tag{I.6.16}$$

Then the effective MFPT in Eq. (I.5.9) can be rewritten in the form of an average:

$$\tau_p = \left\langle \psi_0(\vec{x}) \middle| \tau_0(\vec{x}) \right\rangle = \overline{\tau_0}. \tag{I.6.17}$$

Now, coming back to the formalism itself, we can easily construct the first-order approximation of the "zone" function (I.6.11) predicated on Eqs. (I.6.12) and (I.6.13):

$$\psi_1(\vec{x},s) = \psi_0(\vec{x})\left\{1 + \frac{K_r}{\tilde{æ}_d^0(s)} - K_r\hat{\overline{G}}(s)\psi_0(\vec{x})\right\}. \qquad \text{(I.6.18)}$$

This function can be rearranged into a more familiar form using definition (I.6.6) of the "zone", definition (I.6.2) and property (I.6.3):

$$\xi(\vec{x},s) = \varphi(\vec{x}) - \frac{1}{K_r}\int d\vec{x}\overline{G}(\vec{x}',\vec{x},s)\varphi(\vec{x}')\bullet\int d\vec{x}W(\vec{x})\xi(\vec{x},s). \qquad \text{(I.6.19)}$$

This is the original integral equation, Eq. (I.6.1), after the decoupling approximation has been used in order to separate the kernel $\overline{G}(\vec{x}',\vec{x},s)$ from the solution $\xi(\vec{x},s)$. Function (I.6.18) used in Eqs. (I.6.9) and (I.6.10) easily gives us the first-order correction $\tilde{æ}^1(s)$ to the integral kernel , then the second-order approximation to the "zone" and so on.

Thus, the decoupling formalism enables us to build infinite series for the integral kernel and the survival probability æ. If the decoupling approximation (see Eqs. (I.6.13)-(I.6.15)) works well, these series should converge quickly. In other words, for the zero-order generalized probability, Eq. (I.6.1), to be a good approximation to the real æ, the first-order correction should be small. It was proved precisely in Refs. [46, 48] that for the decoupling approximation to hold, the dispersion of the effective MFPT should be much smaller than its square value:

$$d_0 << \tau_p^2. \qquad \text{(I.6.20)}$$

The dispersion is evaluated through the time of being inside the reaction region, Eq. (I.6.16):

$$d_0 = \overline{\tau_0^2} - \overline{\tau_0}^2 = \left\langle \psi_0(\vec{x}) \middle| \tau_0^2(\vec{x}) \right\rangle - \left\langle \psi_0(\vec{x}) \middle| \tau_0(\vec{x}) \right\rangle^2. \qquad \text{(I.6.21)}$$

Eq. (I.6.20), accompanied by definition (I.6.21) for dispersion, is the desirable condition for the decoupling approximation to be applicable to the solution of integral equations of type (I.6.1).

Thus, in this Chapter we presented the decoupling method for the solution of the integral form of reaction equations for irreversible unimolecular reactions. It should be mentioned that the above presentation of the decoupling approximation given through the kinematic approach is much clearer, simpler and more complete than the one given in [6]. The key stone of this simplicity and completeness is the steady-state Green's function which allowed us to represent all of the differential and integral equations in the specific form analogous to the steady-state one in bimolecular reaction theory. It appears that this form is the most advantageous for evaluation of reaction rates. The decoupled integral equation for $\xi(\vec{x},s)$ is given in Eq. (I.6.19). A similar expression can be obtained for the ordinary population probability, but calculations would be somewhat cumbersome. More than that, the decoupling procedure enabled us to generalize the MFPT concept and evaluate the effective MFPT, Eq. (I.5.9). Another physically meaningful value obtained by means of the decoupling formalism is the average time for particles to spend inside the reaction zone if started from some point on the reaction surface, Eq. (I.6.16). It was this time which provided us with the criterion of applicability of the decoupling approximation, Eq. (I.6.20). As one can see, this criterion is much broader than the simple requirement $\sigma<<\Delta$ and may include not only the geometrical form of the reaction region, but the type of reaction motion as well.

CHAPTER VII APPLICATIONS OF THE STEADY-STATE GREEN'S FUNCTION METHOD

1. The bistable potential

In this Section we consider application of our method to adiabatic, but still one-dimensional potential surface reactions. The standard framework for discussion of chemical rates in this case is provided by the concept of transitions in the bistable potentials:

$$V(x) = \frac{\beta a^2}{16 E_A} x^4 - \frac{a}{2} x^2, \qquad \text{(I.7.1)}$$

where E_A is the height of the activation barrier, the frequency in the wells is $\omega_0^2 = 2a$ and the frequency on the top of the barrier is $\omega_b^2 = -a$, see also Fig. 2.

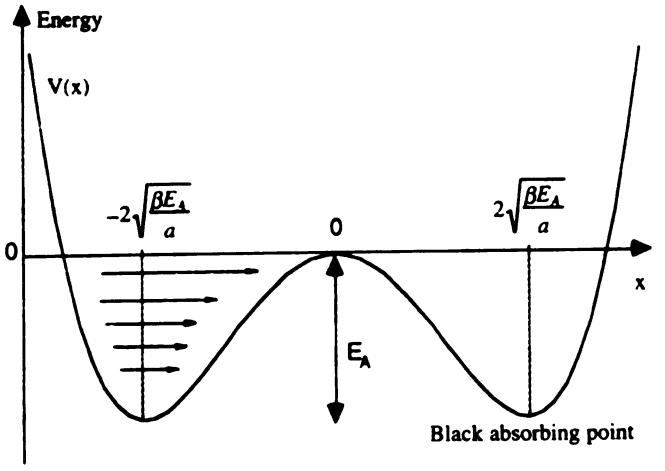

Figure 2. Profile of the bistable potential given by Eq. (I.7.1).

In the case of thermally activated reactions the Kramers' theory gives the reaction rate constants for all ranges of the friction coefficient γ [1, 2]. Traditionally this theory is applied to activated processes which exhibit an effective one-dimensional and Markovian character. However, these requirements are not always fulfilled, which gave impetus to the

development of a more sophisticated theory involving both the non-Markovian nature of the interaction between the reactants and solvent and the multidimensional nature of the unimolecular process.

Part of this theory calls for the necessity of considering a position-dependent friction along the reactive coordinate which, as was shown in [10] arises from the multidimensional nature of the chemical transformations.

For high friction the Kramers' reaction rate

$$k_{Kr} = \frac{\omega_0 \omega_b}{2\pi} \frac{1}{\gamma} \exp[-\beta E_A] \qquad \text{(I.7.2)}$$

was corrected by Compiany [11] to take into account the modulated, non-constant friction $\gamma_{eff}(x)$. The interested reader can find the details of these formulations in Refs. [10] and [11]. Here we just give the final outline and emphasize that the rates have been calculated only for very high activation barrier reactions. Our goal here is to demonstrate the application of the steady-state Green's function method to the solution of the problem for reactions with any barrier height.

The problem starts from the introduction of the second reactive mode, y coupled to the reaction coordinate x, so that the total reactive potential is

$$U(x,y) = V(x) + \frac{\omega_y^2 y^2}{2} + \alpha y \frac{x^2}{2},$$

where V(x) is given by Eq. (I.7.1) and α is the strength of the coupling between x and y. Each of these coordinates has its own friction (γ for x and ζ for y). Thus, by means of the adiabatic elimination procedure the y-dynamics is projected onto the x-dynamics [10, 11] which results in the one-dimensional overdamped equation of type (I.1.1) with the diffusion coefficient $D_{eff}(x) = (\beta\, \gamma_{eff}(x))^{-1}$, where $\gamma_{eff}(x) = (\gamma + \sigma x^2)$ and $\sigma = \alpha\, \zeta/(\omega_y{}^4 \gamma)$. So, the stochastic motion operator of the problem becomes

$$L(x) = \frac{d}{dx} \frac{1}{\beta \gamma_{eff}(x)} [\frac{d}{dx} + \beta \frac{dV(x)}{dx}]. \qquad \text{(I.7.3)}$$

Initially the reactive particles are distributed exclusively in the reactant (R) potential well, so the initial distributions is $f_0(x) = \sqrt{\omega_0^2 / \pi}\, \exp(-\omega_0^2 / 2(x + 2\sqrt{E_A / \beta a})^2)$.

The rate constant in this process is just the reciprocal of MFPT to the product (P) well, i.e. to the point $2\sqrt{E_A/\beta a}$ (no nonadiabatic constant, of course). From Eq. (I.5.6) we get

$$\frac{1}{k} = \tau_p = \int_{-\infty}^{2\sqrt{\beta E_A/a}} \beta\gamma_{eff}(y) e^{\beta V(y)} dy \int_{-\infty}^{y} e^{-\beta V(z)} dz \int_{-\infty}^{y} f(z)dz = \tau_p^0 + \tau_p^{corr}, \qquad \text{(I.7.4)}$$

where the total MFPT is the sum of the two separate times

$$\tau_p^0 = \beta\gamma \int_{-\infty}^{2\sqrt{\beta E_a/a}} e^{\beta V(y)} dy \int_{-\infty}^{y} e^{-\beta V(z)} dz \int_{-\infty}^{y} f(z)dz, \quad \tau_p^{corr} = \beta\gamma\sigma \int_{-\infty}^{2\sqrt{\beta E_a/a}} y^2 e^{\beta V(y)} dy \int_{-\infty}^{y} e^{-\beta V(z)} dz \int_{-\infty}^{y} f(z)dz$$

For the high activation barrier the answer is known [11]: $\tau_p{}^0=\tau_p{}^{Kr}$ and $\tau_p{}^{corr}=\sigma/a\ \tau_p{}^{Kr}$ so

$$\tau_p = \tau_p^{Kr}(1+\frac{\sigma}{a}), \qquad \text{(I.7.5)}$$

where $\tau_p{}^{Kr}=1/k_{Kr}$ and k_{Kr} is given in Eq. (I.7.2). Unfortunately, analytical integration of Eq. (I.7.4) is possible only in the high barrier case and produces the above result. However, this problem can be easily solved numerically and we can analyze the dependence of $\tau_p{}^0$ and $\tau_p{}^{corr}$ parameters of the bistable potential E_A and a. It is interesting that both of these times can be re-normalized to extract the dependence on a (or ω_0 and ω_b):

$$\tau_p^0 = \tau_p^{Kr} g(\beta E_A) = \frac{2\pi\gamma}{\omega_0\omega_b} g(\beta E_A) e^{\beta E_A} \qquad \text{(I.7.6a)}$$

$$\tau_p^{corr} = \frac{\sigma}{a}\tau_p^{Kr} g_{corr}(\beta E_A) = \frac{4\pi\alpha\zeta}{\omega_y^4\omega_0^2\omega_b^2} g_{corr}(\beta E_A) e^{\beta E_A}. \qquad \text{(I.7.6b)}$$

Functions $g(\beta E_A)$ and $g_{corr}(\beta E_A)$ tend to 1 when $\beta E_A \to \infty$. So, when the coupling α is small, $\tau_p{}^{corr}$ is a linear correction to the one-dimensional MFPT. When the coupling is moderate or strong, the contribution from the other (y) mode is dominant, therefore the dependence on ζ, not γ should be the point of interest. Fig. 3 depicts the form of the functions $g(\beta E_A)$ and $g_{corr}(\beta E_A)$.

In order to demonstrate the influence of the initial distribution on the rate constant, we took not only the Boltzmann distribution in the R well, but also the distribution $f_0'(x)=\delta(x+2\sqrt{E_A/\beta a})$. As one can see, the difference between the rate constants for $f_0(x)$

and $f_0'(x)$ is indistinguishable (never more then 10%). Thus we can conclude that from the experimental point of view the question of the influence of a non-statistical distribution on the rate in the case of bistable potential can be left aside. We found the following interpolation functions for $g(\varepsilon)$ and $g_{corr}(\varepsilon)$ which can be easily used for interpretation of the experimental data (the error of the interpolation is about 0.1%):

$$g(\varepsilon) = 1/(\Theta(2.75-\varepsilon)F(\varepsilon) + \Theta(\varepsilon-2.75)F_1(\varepsilon)) \qquad \text{(I.7.7a)}$$

$$g_{corr}(\varepsilon) = 1/(\Theta(4.56-\varepsilon)F^{corr}(\varepsilon) + \Theta(\varepsilon-4.56)F_1^{corr}(\varepsilon)), \qquad \text{(I.7.7b)}$$

where $\Theta(\varepsilon)$ is the step-function.

$$F(\varepsilon) = 34.8575 + 0.0481e^{-0.9684(\varepsilon-4.2298)} - 9.3574e^{-0.3228(\varepsilon-4.2298)} - \frac{0.0104}{\varepsilon^3} + \frac{0.0852}{\varepsilon^2} - \frac{0.014}{\varepsilon} -$$

$$9.7399\varepsilon + 1.1694\varepsilon^2 - 0.0582\varepsilon^3$$

$$F_1(\varepsilon) = 1. + \frac{2.7051}{\varepsilon^3} - \frac{1.5052}{\varepsilon^2} - \frac{0.2894}{\varepsilon}$$

$$F^{corr}(\varepsilon) = 0.1333 - 0.0043e^{-1.785(\varepsilon-1.7116)} - 0.0012e^{-0.595(\varepsilon-1.7116)} - \frac{0.007}{\varepsilon^3} + \frac{0.2246}{\varepsilon^2} + \frac{0.4713}{\varepsilon} +$$

$$0.0755\varepsilon + 0.0117\varepsilon^2 - 0.0016\varepsilon^3$$

$$F_1(\varepsilon) = 1. + \frac{17.589}{\varepsilon^3} - \frac{6.9351}{\varepsilon^2} - \frac{0.7658}{\varepsilon}.$$

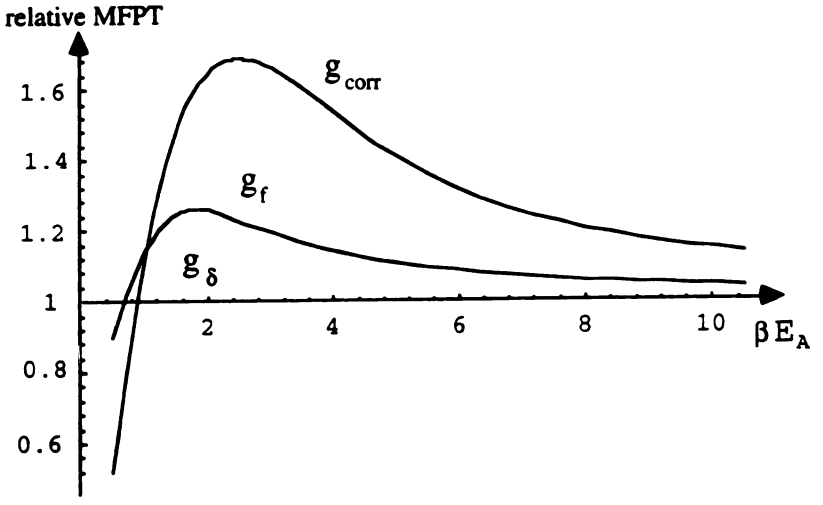

Figure 3. Dependence of the relative MFPT values $g(\beta E_A)$ and $g_{corr}(\beta E_A)$ in Eqs. (I.7.7a) and (I.7.7b). $g_f(\beta E_A)$ corresponds to the function $g(\beta E_A)$ calculated for the Boltzmann initial distribution inside the reactant well, f_0. $g_\delta(\beta E_A)$ is calculated for the δ-functional initial distribution $f_0'(x) = \delta(x + 2\sqrt{E_A/\beta a})$.

Thus, we can write down the rate constant for the bistable potential with a medium - to high activation barrier (βE_A>3) with the contribution from the position-dependent friction:

$$k = \frac{\omega_0 \omega_b}{2\pi\gamma_{eff}} \exp(-\beta E_A) \qquad \text{(I.7.8)}$$

where $\gamma_{eff} = \gamma(1 + \frac{0.341}{\beta E_A} + \frac{1.394}{(\beta E_A)^2} - \frac{1.777}{(\beta E_A)^3}) + \frac{2\alpha\zeta}{\omega_y^4 \omega_0 \omega_b}(1 + \frac{0.297}{\beta E_A} + \frac{14.185}{(\beta E_A)^2} - \frac{27.603}{(\beta E_A)^3})$.

As one can see, the corrections to the original Kramers' constant are significant for the barriers with E_A<20-30 K_BT.

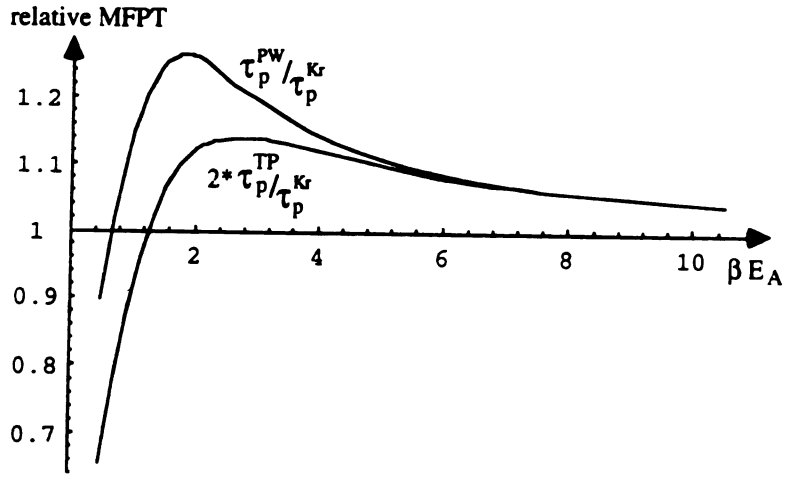

Figure 4. MFPT for the reactants to reach the product well τ_p^{PW} and MFPT for the reactant to reach the top of the barrier, τ_p^{TB} are shown as the ratios to the Kramers' MFPT.

Another interesting question arises from the reversibility of the transitions in the bistable potentials. As it is well-known [8], for irreversible high activation barrier reactions, MFPT for the reactants to reach the product well, τ_p^{PW} is twice as long as the MFPT for the reactants to reach the top of the activation barrier, τ_p^{TB}. The reason for this correlation is that the particles which have reached the top have probability 1/2 to fall back into the R well and probability 1/2 to escape to the products and never come back. Fig. 4

presents the situation for all barrier heights. One can see that τ_p^{PW} is not equal to $2*\tau_p^{TB}$ for moderate and low barriers, which is caused by the reversible reaction R -> P. Because τ_p^{PW} is the "average" time for particles to reach the product well, it includes the contribution from the particles which move back into reactant well after they have reached the P minimum and thus increase the average time τ_p^{PW}. So, even though each individual particle still has the probability (1/2,1/2) to go either to the right or to the left of the barrier, the reversibly moving particles shift the average probability to the left and on average the probability for particles on the top to return to the R well is higher then the probability to escape.

To sum up, the results of this Section extend the traditional Kramers' result for transitions in the bistable potential. In our case the analysis was carried out without drawing in the harmonic approximations on the top and in the bottom of the potential. The combination of times (9.6) gives the rate constant for reactions with any barrier height and includes the contribution from the position-dependent friction. The treatment doesn't assume that γ_{eff} undergoes small variations along the potential. The presence of the position-dependent friction in the reaction rate is related to the breakdown of the assumption of the existence of clear-cut reaction coordinates in some unimolecular reactions. As one can see from Eq. (I.7.8), strong coupling α to another mode (it can be the solvent or another vibration mode) might lead to significant corrections in the rate, or might even change the reaction picture completely and make in multidimensional. This method leads to the change of the power law friction dependence in the rate constant. For the purely one-dimensional case the dependence of the rate on friction behaves according to $1/\gamma$ (see Eq. (I.7.2)). If the coupling to another mode is present, this law changes to the $1/\gamma^p$ ($p<1$) dependence and the stronger the coupling, the closer p is to 0. This effect becomes more significant for lower barriers.

2. The harmonic oscillator potential

In this Section we consider diabatic two- and one-dimensional harmonic oscillator potentials as reaction surfaces. We assume that in both cases the irreversible reactions take place in narrow regions. Here we are going to demonstrate the application of the steady-state Green's function method to both pinhole and narrow sinks, see Chapters V and VI. We presumed the reaction motion to be overdamped.

2.1. One-dimensional harmonic oscillator $V(x)=x^2/2$

The reaction model we investigate here is considered for many classes of chemical reactions. Among the most important are the ETR and electronic relaxation processes. The demonstration of how this model has been used can be found in Refs. [6, 14, 26, 27] for the case of ETR and in works [12, 13, 17, 18, 20, 31, 49] for isomerization and photolysis. The simplest case is when it is assumed that the transitions take place on the pinhole sink $W(x)=K_0\,\delta(x-x_p)$ located at the point of intersection of the two diabatic harmonic oscillator potentials, with $x_p = \dfrac{\lambda_x + \Delta G_0}{\sqrt{2\lambda_x}}$ where λ_x is the reorganization energy for the x-coordinate and ΔG_0 is the exothermicity of the reaction. The generalized probability, as æ in Eq. (I.5.4) for the pinhole sink, is determined through the MFPT, which in the case of the Boltzmann initial distribution, $\varphi(x) = \sqrt{\beta / 2\pi}\exp(-\beta x^2 / 2)$ has the form :

$$\tau_p = \tau_x\left(\ln 2 + 2\sqrt{\pi}\int_0^{\sqrt{\beta V(x_p)}} erf(y)\exp(y^2)dy \right) \qquad \text{(I.7.9)}$$

where τ_x is the relaxation time along the potential (τ_x=1/(βD)), and erf(y) is the error function (for any other type of initial distribution see Appendix A or Eq. (I.5.5)).

In order to evaluate the long-time rate constant k we used the following Green's function (it was also calculated by Sebastian [50]):

$$G(x,x';s) = \sqrt{\frac{1}{2\pi\beta}}\frac{\Gamma(-\nu)}{D}\begin{cases}\exp(-\beta(x^2-x'^2)/4)D_\nu(\sqrt{\beta}x)D_\nu(-\sqrt{\beta}x') & x \ge x' \\ \exp(-\beta(x^2-x'^2)/4)D_\nu(-\sqrt{\beta}x)D_\nu(\sqrt{\beta}x') & x \le x'\end{cases}$$

(I.7.10)

where $\Gamma(z)$ is the Euler gamma function, $D_\nu(z)$ is the Parabolic cylinder function and $\nu = -s/(D\beta)$. Equation (I.5.3) for the definition of k through the analytic expansion of function (I.7.10) has the form :

$$\Gamma(-\nu_0)D_{\nu_0}(\sqrt{\beta}x_p)D_{\nu_0}(-\sqrt{\beta}x_p) = -\frac{1}{q} \qquad \text{(I.7.11)}$$

where $\nu_0 = k\ \tau_x$, $q = \frac{K_r}{d_0}$ and $d_0 = D\beta\exp(-\beta x_p^2/2)$, the parameter q is the relative sink intensity and d_0 represents the speed of diffusion along the potential. The lowest positive root of this equation gives the long-time rate constant k for any barrier height $V(x_p)$. For the barrierless reaction $x_p = 0$ and Eq. (I.7.11) can be significantly simplified:

$$-\Gamma(-\frac{p}{2})/\Gamma(\frac{1-p}{2}) = \frac{2}{\sqrt{\pi}q} \qquad \text{where} \quad p = \frac{k}{d_0}.$$

Fig. 5 presents the dependence of the reaction efficiencies æ/d_0 and k /d_0 as functions of the relative sink intensity q for the barrierless reaction (x_p=0), for $\sqrt{\beta}x_p = 1$, and for $\sqrt{\beta}x_p = 2$. For comparison we also calculated the approximate long-time rate constant k' in the form $1/k' = 1/K_r + 1/K_d$ where the diffusion constant, K_d was the root of Eq. (I.7.11)

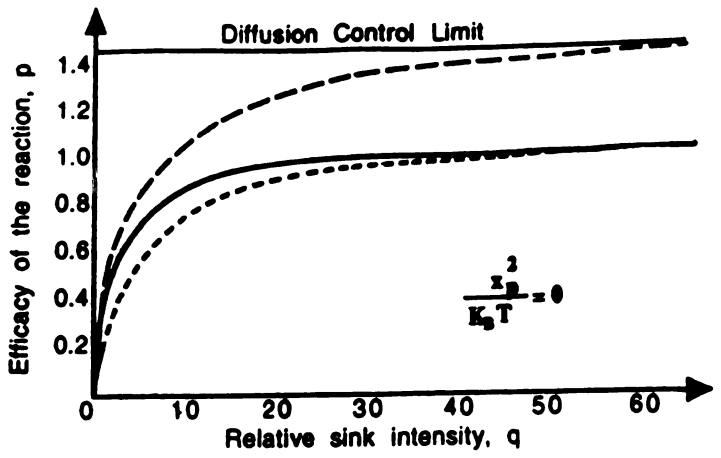

Fig. 5a

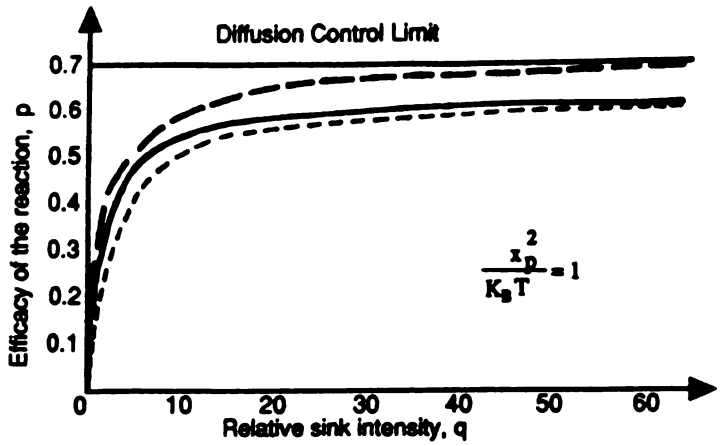

Fig. 5b

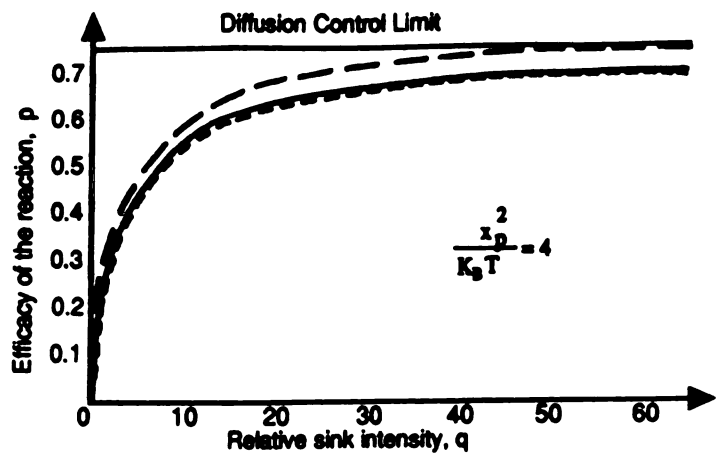

Fig. 5c

Figure 5. Dependence of the reaction rate constants æ, k and k' on the relative sink intensity $q=K_r/d_0$, where $d_0=\lambda^2 D/K_B T \exp(-\lambda x_p^2/(2K_B T))$ for the reaction on the δ-function sink located at three different barrier heights on the harmonic oscillation reaction surface $V(x)=(1/2)\lambda x^2$: a) $\lambda x_p^2/(K_B T) = 0$; b) $\lambda x_p^2/(K_B T) = 1$ and c) $\lambda x_p^2/(K_B T) = 2$. (— —): generalized probability $æ = \frac{æ_r æ_d}{æ_r + æ_d}$, where $æ_r=K_r$ and $æ_d=\tau_d$, is given as the dependence $p=æ/d_0$ on q; (———): long-time rate constant k which is the solution of Eq. (7.24) given as a function $p=k/d_0$ of q; (- - -): approximation of the real long-time rate constant k with the form $k'=K_r K_d/(K_r+K_d)$, $p=k'/d_0$.

at q->∞ (for barrierless reactions $K_d=d_0$). The dependence of the ratio $p' = k'/d_0$ on q is also given on Fig. 5. k' gives an upper estimate to the real long-time rate constant k and, obviously, the higher is the activation barrier, the better the approximation.

For large values of K_r (q › 1) æ is not a very good approximation to k for any finite barrier, i.e. $P_e(t) = \exp(-æt)$ works less effectively as the sink intensity increases. The biggest deviations occur, of course, at the diffusion control limit ($K_r >> K_d$, or q->∞) when the generalized probability is exactly the MFPT to x_p. Thus, Fig. 5 clearly demonstrates objections against calculations of k through the MFPT [9]. The ratio æ/k at $K_r/K_d>1$ is always more than unity. For barrierless reactions it has the maximum:

$$\lim_{q->\infty}\frac{æ}{k}=\frac{æ_d}{K_d}=\frac{q}{1+q\ln 2}\underset{q->\infty}{->}\frac{1}{\ln 2}.$$

This indicates that the non-exponential reaction decay is always present in such reactions. However, as one can expect, the gap between $æ_d$ and K_d definitely decreases as the barrier becomes high.

As the barrier goes up, the analysis of the reaction constants becomes easier. The MFPT becomes independent on the initial distribution as in Eq. (B3) :

$$\tau_p \approx \tau_x\sqrt{\frac{\pi}{\beta V(x_p)}}\left(1+\frac{1}{2\beta V(x_p)}\right)\exp(\beta V(x_p)) \qquad (I.7.12)$$

and $$\frac{1}{æ}=\frac{1}{k}=\frac{1}{K_r}+\tau_x\sqrt{\frac{2\pi}{\beta V(x_p)}}\exp\left(\beta x_p^2/2\right).$$

The relaxation time of the system may be calculated from Eq. (A17) in Appendix A (see also Appendix B) and is equal to:

$$\tau_e=\tau_x\left(\sqrt{\pi}\int_0^{\sqrt{\beta V(x_p)}}dy erfc(y)\cdot\exp y^2-\ln 2\right)\underset{\beta V(x_p)->\infty}{\sim}\tau_x\ln\sqrt{\beta V(x_p)\Gamma} \qquad (I.7.13)$$

where $D=1/\beta\tau_x$, $\Gamma=\exp C$ and C is the Euler constant. The relaxation time τ_e is absolutely correct for sufficiently large barriers, but it could serve as an estimate for lower barriers.

For example, in the case of activationless reaction MFPT to the point x_p=0 may be evaluated using the second equation in (I.5.6) when x_0>>1:

$$\tau_p = \tau_x \ln\left(2\sqrt{\beta V(x_0)\Gamma}\right), \qquad \beta V(x_0) = \beta x_0^2 / 2 >> 1. \qquad \text{(I.7.14)}$$

It is easy to see that both τ_e in Eq. (I.7.13) and τ_p in Eq. (I.7.14) for barrierless reactions are of the same order of magnitude as the relaxation time τ_x. So, the non exponential stage of the reaction decay is very deep and the exponential decay corresponds only to a small part of the kinetic curve.

Above, the chemical rates were evaluated for the reactions on the infinitely narrow, or pinhole sink. The situation when the sink is narrow but not a point has been considered in a number of works [6, 13, 30, 42]. The origin of the argument in favor of such a sink arises from the multidimensional nature of the reaction potential surfaces. While the coordinate x diffuses under the influence of the potential V(x), there could exists another reaction coordinate, q which is assumed to be equilibrated under very fast damping. For the electron transfer reactions the variable x is proportional to a certain component of the polarization vector which passes through the two minimum energy points associated with the reactants and products in the polarization coordinate space. The other coordinate, q is considered as the intramolecular vibration coordinate, which can be immediately generalized to include more coordinates. The vibration relaxation is usually much faster then the fluctuations in the polarization, so it is supposed that while the distribution of x on the reactant's surface may not to be an equilibrium one, that of q is. Thereby one can define a sink function W(x) which involves at each x a suitable averaging over the population in the q coordinate. If there is no q coordinate, W(x) is proportional to a delta function which is peaked at some value of x, x_p (the pinhole sink). Otherwise, the Gaussian sink function is obtained:

$$W(x) = K_0\sqrt{\frac{\beta\pi}{\lambda_q}}\exp\left(-\frac{\beta\lambda_x}{2\lambda_q}(x - x_p)^2\right), \quad x_p = \frac{\lambda_0 + \Delta G_0}{\sqrt{2\lambda_x}}, \qquad \text{(I.7.15)}$$

where λ_x and λ_q are the reorganization energies for the x and q coordinates respectively, $\lambda_0=\lambda_x+\lambda_q$. It is obvious that the sink in (I.7.15) can be considered to be narrow when $\sigma=\lambda_q/\lambda_x<<1$.

In order to evaluate the chemical rates for reactions on sink (I.7.15) the decoupling approximation described in Ch. VI has to be used. Thus, the generalized probability æ has the form given be Eq. (I.6.15): $1/æ = 1/K_r + \tau_p^{eff}$, where the nonadiabatic rate constant is

$$K_r = \int dx W(x)\varphi(x) = K_0\sqrt{\frac{\beta\pi}{\lambda_0}}\exp(-\beta E_A), \quad E_A = \frac{(\lambda_0+\Delta G_0)^2}{4\lambda_0} \tag{I.7.16}$$

and the effective MFPT, τ_p^{eff} has to be evaluated using Eq. (I.5.9):

$$\tau_p^{eff} = \iint \psi_0(x)\overline{G}(x,x')\psi_0(x')\varphi(x')dxdx', \quad \psi_0 = W(x)/K_r, \tag{I.7.17}$$

which is the average time for particles to reach the Gaussian region having started from some distribution. Below, we will calculate the effective MFPT for the Boltzmann initial distribution, so the steady-state Green's function in Eq. (I.7.17) satisfies Eq. (I.4.2) for f(x) = $\varphi(x)=\sqrt{\beta/2\pi}\exp(-\beta x^2/2)$. For the convenience of evaluating integral (I.7.17) let us introduce a new function:

$$g(x) = \int \overline{G}(x,x')\psi_0(x')\varphi(x')dx'. \tag{I.7.18}$$

Then the evaluation of the effective MFPT is reduced to one integration:

$$\tau_p^{eff} = \int \psi_0(x)g(x)dx.$$

Function g(x) satisfies the differential equation which can be easily obtained from Eq. (I.4.2)

$$L(x)g(x) = \varphi(x)\big(1-\psi_0(x)\big). \tag{I.7.19}$$

Instead of the boundary conditions for the above equation, one has to use the condition $\int dx g(x) = 0$ which comes from the properties of the steady-state Green's function, $\overline{G}(x,x')$.

For the overdamped stochastic operator for the harmonic oscillator reaction surface, $L(x) = \frac{1}{\beta\tau_x}\frac{d}{dx}\left(\frac{d}{dx}+\beta x\right)$, Eq. (I.7.19) can be solved using the Fourier transformation

method. The Fourier transforms $\tilde{f}(v)=\frac{1}{\sqrt{2\pi}}\int_{-\infty}^{\infty}f(x)e^{-ixv}$ of the differential operator and all the functions in (I.7.19) are easy to obtain. As a result, we can express the effective MFPT through the Fourier transform $\tilde{g}(v)$

$$\tau_p^{eff}=\tau_x\sqrt{\frac{\lambda_0}{2\pi\beta\lambda_x}}e^{\beta E_A}\int_{-\infty}^{\infty}dv\tilde{g}(v)\exp\left(-\frac{v^2\lambda_q}{2\beta\lambda_x}+ivx_p\right)$$

where

$$\tilde{g}(v)=e\exp\left(-\frac{v^2}{2\beta}\right)\int_0^1\frac{dy}{y}\left(\exp\left[\frac{v^2\lambda_x}{2\beta\lambda_0}y^2-iyv\frac{\lambda_x}{\lambda_0}x_p\right]-1\right). \qquad \text{(I.7.20)}$$

The final result for the effective MFPT in the case of the Boltzmann initial distribution is quite simple:

$$\tau_p^{eff}=\tau_x\int_0^1\frac{dy}{y}\left[\frac{e^{\left(\frac{2\beta E_A\varepsilon y}{1+\varepsilon y}\right)}}{\sqrt{1-\varepsilon^2y^2}}-1\right], \qquad E_A=\frac{\varepsilon x_p^2}{2}, \qquad \varepsilon=\frac{\lambda_x}{\lambda_0}=\frac{1}{1+\sigma}. \qquad \text{(I.7.21)}$$

It is straightforward to evaluate the above integral for activationless reactions, i.e. for E_A=0:

$$\tau_p^{eff}(E_A=0)=\tau_x\ln\frac{2}{1+\sqrt{1-\varepsilon^2}}=\tau_p(E_A=0)-\tau_x\ln(1+\sqrt{1-\varepsilon^2}). \qquad \text{(I.7.22)}$$

So, a narrow Gaussian sink with the width σ compared with the pinhole sink located at the bottom of the potential well, decreases the MFPT for the reaction by the factor ~ $\ln(1+\sqrt{2\sigma})$.

The integration in Eq. (I.7.21) can also be carried out for the case of high activation barrier. For the large parameter βEA>>1 the Laplace method can be applied, Ref. [51]. The effective MFPT of the first order for a high activation barrier reaction is

$$\tau_p^{eff}\approx\tau_x\frac{1+\varepsilon}{2\varepsilon}\frac{e^{\beta E_A}}{\sqrt{\beta E_A}}\left\{\Gamma(\frac{1}{2},\mu)+\frac{1-\varepsilon}{2\varepsilon\mu}(1-2\mu)\Gamma(\frac{3}{2},\mu)\right\}, \quad \mu=\frac{\beta E_A(1-\varepsilon)}{1+\varepsilon} \qquad \text{(I.7.23)}$$

where Γ(α,x) is the incomplete Gamma function. The above equation for a pinhole reaction (ε=1) transforms into Eq. (I.7.12). If we assume that the parameter μ is small (we will talk about the validity of this assumption concerning the "narrow reaction window" limit below), Eq. (I.7.23) can be given in its simplest form:

$$\tau_p^{eff} \sim \tau_p - \tau_x e^{\beta E_A}\left(2\sqrt{\frac{2E_A\sigma}{2+\sigma}} + \frac{\sigma\sqrt{\pi}}{2+\sigma}\right) \qquad \text{(I.7.24)}$$

where τ_p is given by Eq. (I.7.9).

Now we have to address the conditions under which the decoupling approximation applied to the evaluation of the rate constants in the case of the Gaussian sink function, Eq. (I.7.15) is valid. In Ch. V the condition of a narrow reaction sink was obtained for a high barrier reaction through a narrow plateau. This condition reformulated for the Gaussian sink would call for

$$\sigma = \frac{\lambda_q}{\lambda_x} << \frac{1}{2\beta E_A} << 1, \qquad \text{(I.7.25)}$$

which is identical to the requirement $\mu<<1$ used in Eq. (I.7.23) in order to obtain Eq. (I.7.24). This looks like a reasonable extension from the problem presented in Ch. V to the reaction we are regarding here. Nevertheless, in order to obtain the precise condition we shell use Eq. (I.6.20) for the dispersion of the effective MFPT .

For the sake of convenience we rewrite Eq. (I.6.20) in the following form:

$$\frac{\int dx \frac{\psi_0(x)}{\varphi(x)} g^2(x) - \left[\int dx \psi_0(x) g(x)\right]^2}{\left[\int dx \psi_0(x) g(x)\right]^2} << 1 \qquad \text{(I.7.26)}$$

where g(x) is defined in Eq. (I.7.18). The above expression can be presented more usefully:

$$\frac{1}{(\tau_p^{eff})^2}\int dx \psi_0(x) g(x) Q(x) << 1, \text{ where} \qquad Q(x) = \frac{g(x)}{\varphi(x)} - \int dx \psi_0(x) g(x).$$

As one can see, the desired requirement would be fulfilled if Q(x) was a weak function of x and $Q(x)/\tau_p^{eff} << 1$. Having all necessary functions at hand, we can evaluate Q(x) easily:

$$Q(x) = \tau_x \int_0^1 \frac{dy}{y}\left[\frac{\exp\left(-\frac{\beta(x-\varepsilon y x_p)^2}{2(1-\varepsilon y^2)}\right)}{\sqrt{1-\varepsilon y^2}} - \frac{\exp\left(\frac{\varepsilon^2 x_p^2 y}{1+\varepsilon y}\right)}{\sqrt{1-\varepsilon^2 y^2}}\right].$$

First of all, it should be mentioned that the general sketchy analysis of the three above equations let us make the conclusion that whatever the requirement for the one-dimensional

reactions is, it should not contain restrictions on the relaxation time along the reaction coordinate, τ_x. So, only the geometrical and energetic requirements should emerge from the restriction on the dispersion in Eq. (I.7.26). To proceed further we can use the upper estimate for the above function, $Q(x) \approx Q(x_p)$ and the assumption that the first derivative of function $Q(x_p)$ in respect of the small parameter σ ($\varepsilon = 1/(1+\sigma)$) would be small compared with the effective MFPT, τ_p^{eff}. After some algebraic transformations one can find that this presumption is satisfied when

$$2\sigma E_A < 1, \tag{I.7.27}$$

which is exactly the same requirement as the one in Eq. (I.7.25) which was obtained by comparison of the reactions on harmonic oscillator potentials with the general high activation barrier reaction case described in Ch. V.

However, Eq. (I.7.27) does not give us a satisfactory answer when the reaction is activationless. We have to consider this special case separately and estimate when $Q(x) \approx Q(x_p) = Q(0)$ is much less then $\tau_p^{eff}(\beta E_A = 0)$ given in Eq. (I.7.22). After some straightforward calculations we obtained

$$\sigma < \frac{1}{8}, \tag{I.7.28}$$

which is the applicability condition for the decoupling approximation to the activationless reactions. Fig. 6 depicts how the pre-exponential factor of the effective MFPT varies for different width of the sink, σ depending on the height of the absorbing origin, x_p.

Summing up, in this Subsection we presented a complete analysis of the reaction kinetics taking place in the reaction proceeding along a one-dimensional harmonic oscillator potential surface through a pinhole or narrow Gaussian sink. The effective MFPT for the reactions on the narrow Gaussian sink was evaluated by means of the decoupling approximation using the steady-state Green's function formalism. To substantiate the decoupling approximation calculations we also evaluated the conditions of its applicability for activated as well as activationless reactions.

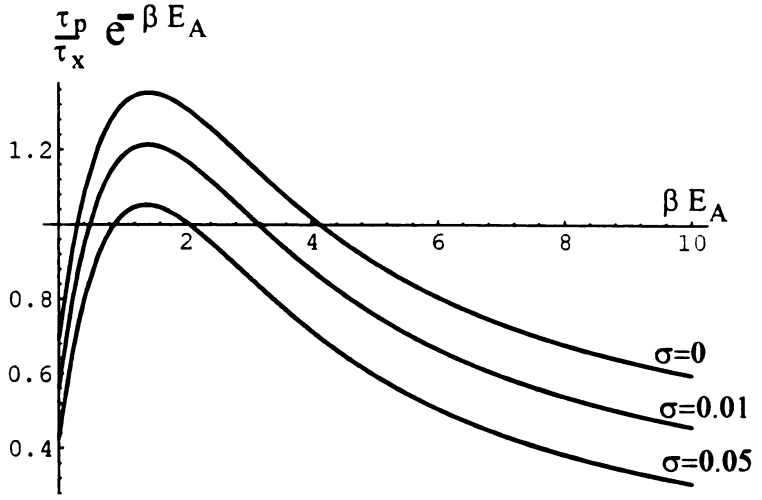

Figure 6. The dependence of the dimensionless pre-exponential factor for the effective MFPT given in Eq. (I.7.21) on the activation energy for the reaction on Gaussian sink (I.7.15). The dependence is presented for three different widths of the reaction sink, $\sigma = \lambda_q / \lambda_x$ (σ=0 corresponds to the pinhole sink $W(x)=K_0\,\delta(x-x_p)$).

2.2. Two-dimensional harmonic oscillator $V(x,y)=x^2/2 + y^2/2$

Here we consider the overdamped decay on a two-dimensional diabatic surface. Previously some numerical investigations were performed in order to obtain the rate constants for this model in reference to reactions involving electron transfer [7, 30] and in application to electronic relaxation [19]. The analytical solution seemed to be impossible to obtain. Here we demonstrate how the steady-state Green's function method enabled us to resolve this problem.

We assume that the reaction takes place on the line of intersection between the two diabatic potentials and the reactants decay irreversibly from the reaction surface. For the harmonic oscillator diabatic potentials the sink line is presented by the Dirac delta function, $\delta(x_0x+y_0y-c)$ (see Refs. [30, 52]), where $x_0 = \sqrt{2\lambda_x}$, $y_0 = \sqrt{2\lambda_y}$ and $c = \Delta G_0 - \lambda_x - \lambda_y$. Here λ_x and λ_y are the reorganization energies for the x and y coordinates for the product

diabatic surface and ΔG_0 is the exothermicity of the reaction. Thus, the sink function in Eq. (I.1.1) for the reaction is $W(x,y) = K_0\delta(x_0x + y_0y - c)$.

As one can see, the sink function for the two-dimensional potential surface is a narrow sink, but by no means it can be approximated by a point on the surface. Thus, in order to evaluate the generalized probability we have to calculate the effective MFPT given in Eq. (I.5.9).

As far as the reaction region in this case is represented by a narrow (in fact, infinitely narrow) function, the generalized probability has the form as in Eq. (I.5.4):

$$\frac{1}{æ} = \frac{1}{K_r} + \tau_p \quad \text{where} \quad K_r = \iint dxdyW(x,y)\varphi(x,y) \quad \text{and}$$

$$\tau_p = \frac{1}{K_r^2}\iint\iint dxdydx'\,dy'\,W(x,y)\overline{G}(x,x';y,y')W(x',y')\varphi(x',y'). \qquad \text{(I.7.29)}$$

Here $\overline{G}(x,x';y,y')$ is the steady-state Green's function defined in Eq. (I.4.7) when s=0, and $\varphi(x,y) = \beta / 2\pi\exp\left(-\beta(x^2+y^2)/2\right)$ is the Boltzmann distribution.

The nonadiabatic rate constant can be evaluated easily:

$$K_r = K_0\sqrt{\frac{\beta}{4\pi\lambda_0}}e^{-\beta E_A} \quad \text{where} \quad \lambda_0 = \lambda_x + \lambda_y \quad \text{and} \quad E_A = \frac{(\Delta G_0 + \lambda_0)^2}{4\lambda_0}.$$

By analogy with the previous Section, for evaluation of the mean first passage time it is convenient to introduce a new function, g(x,y) which is defined as:

$$g(x,y) = \frac{1}{K_r}\iint dx'\,dy'\,\overline{G}(x,x';y,y')W(x',y')\varphi(x',y').$$

The differential equation for the above function can be obtained directly from Eq. (I.4.7) when s=0:

$$L(x,y)g(x,y) = -\sqrt{\frac{\beta\lambda_0}{\pi}}\delta(x_0x + y_0y - c)e^{\beta E_A - \beta(x^2+y^2)/2} + \varphi(x,y). \qquad \text{(I.7.30)}$$

For the overdamped operator $L(x,y) = \frac{1}{\beta\tau_x}\frac{\partial}{\partial x}e^{-\varphi(x,y)}\frac{\partial}{\partial x}e^{\varphi(x,y)} + \frac{1}{\beta\tau_y}\frac{\partial}{\partial y}e^{-\varphi(x,y)}\frac{\partial}{\partial y}e^{\varphi(x,y)}$

the solution of Eq. (I.7.30) can be obtained in a Fourier transform form,

$\tilde{g}(\mu,\omega)=\frac{1}{2\pi}\iint dxdyg(x,y)e^{-i x\mu - i y\omega}$ so that the effective MFPT in Eq. (I.7.29) can be presented in the integral form:

$$\tau_p=\sqrt{\frac{\lambda_0}{\pi\beta x_0^2}}e^{\beta E_A}\int_{-\infty}^{\infty}d\omega\exp\left(i\frac{c}{x_0}\omega\right)\tilde{g}(\omega,q\omega). \qquad \text{(I.7.31)}$$

The final answer can be given as follows:

$$\tau_p=\tau_x\int_0^1\frac{dx}{x}\left\{\frac{\exp\left(\frac{2\beta E_A(x+q^2x^\alpha)}{1+q^2+x+q^2x^\alpha}\right)}{\sqrt{1-\left(\frac{x+q^2x^\alpha}{1+q^2}\right)^2}}-1\right\} \quad \text{where} \quad q=\frac{y_0}{x_0} \quad \text{and} \quad \alpha=\frac{\tau_x}{\tau_y} \qquad \text{(I.7.32)}$$

where τ_x and τ_y are the relaxation times along the x and y coordinates respectively. This is the average time for particles to reach the sink line, $\delta(x_0x+y_0y-c)$ on the two-dimensional harmonic oscillator potential surface if they started from the Boltzmann distribution. The effective MFPT for other types of initial distribution can also be evaluated using equations similar to Eqs. (I.7.29) - (I.7.30), but for different steady-state Green's functions which would include different initial distributions (see Eq. (I.4.12)).

As one can see, the effective MFPT is the function of two parameters - the ratio of the two relaxation times, α, and the cotangent of the sink line projection on the (x,y) plane, q. From the above formula one can conclude that when the sink line projection on the plane (x,y) is perpendicular to one of the axes, the reaction is effectively one-dimensional. So, if q=0, the projection is perpendicular to the x axis and τ_p is a function of the relaxation time along the x- axis, τ_x. When q= ∞, then the effective MFPT depends only upon the relaxation time along the y -axis, τ_y. In both these cases Eq. (I.7.32) is an analog of the one dimensional MFPT to a point given in Eq. (I.7.9). Unfortunately, one equation can not be transformed into the other directly and only numerical evaluations confirm the conclusion.

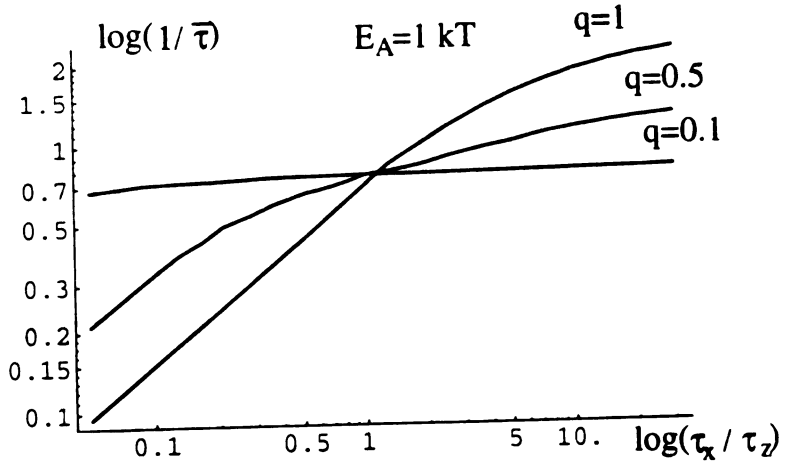

(a)

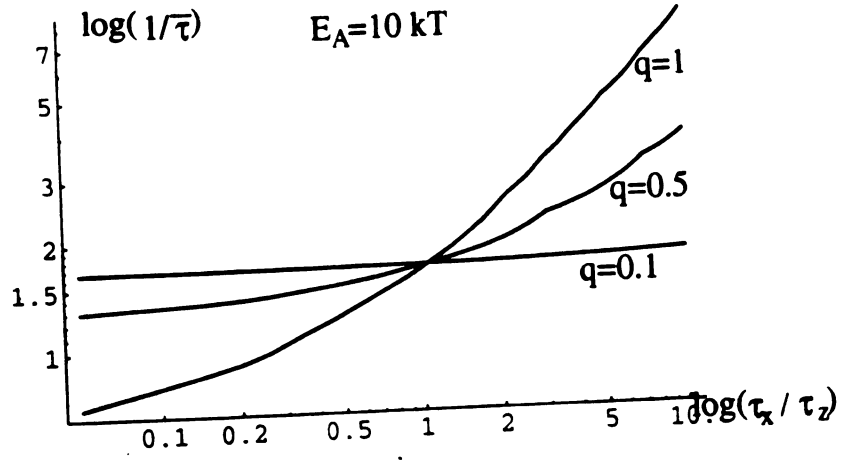

(b)

Figure 7. Dependence of the reciprocal of the dimensionless effective MFPT for the reaction on two-dimensional harmonic oscillator potential, $\bar{\tau}$ on the ratio of the relaxation times along the reactive coordinates, τ_x/τ_y is given for the two barrier heights: a) E_A=1 K_BT; b) E_A=10 K_BT. The reaction region in this case was taken as a line on the reaction surface.

The dependence of the dimensionless effective MFPT, $\bar{\tau} = \tau / \tau_x e^{-\beta E_A}$ on the parameter α is depicted in Fig. 7 for different heights of the activation barrier. Fig. 7a shows the dependence for a low barrier, $E_A=2\ K_BT$ whereas Fig 7b presents the picture for a high barrier, $E_A=10\ K_BT$ for a wide range of ratios τ_x/τ_y. If both relaxation times are approximately equal and $\alpha=1$, then the effective MFPT is quasi one-dimensional in the sense that it depends effectively only upon one relaxation time, but include two-dimensional geometric parameters. If one of the relaxation times is much faster (shorter) then the other, the analysis of the two-dimensional situation in the low barrier case is quite complicated. Both relaxation times play important roles in formation of the dynamic rate. Thus, we are unable to conclude that there exists a situation wherein one relaxation time prevails over the other. However this is not the case for high barrier reactions. As one can see from Fig. 7b, at small values of α, i.e. when $\tau_x << \tau_y$, the parameter $1/\bar{\tau}$ tends to a plateau. Thus, the effective MFPT becomes insensitive to the changes in the slower relaxation time, τ_y and the dynamic rate is fully controlled by the faster relaxation time, τ_x.

Actually, the situation in the multidimensional reactions is even more complicated when one relaxation time is faster then the other. The complete analysis of the situation with the fast/slow modes in two-dimensional reactions is considered in Ref. [52] and will be discussed here in Part II, Ch. XI.

When the activation barrier is high, it is possible to obtain a clear analytical answer for the effective MFPT. Here we carry it out for the two-dimensional reactions, but the result can be easily generalized to a higher multidimensional case.

From the results in Ch. V (see in particular Eqs. (I.5.13)-(I.5.14)), we conclude that in the case of a high activation barrier reaction, only the first derivatives of the multidimensional potential along the reactive coordinates near the activation point contribute to the dynamic rate constant. Thus, the two-dimensional potential can be represented in the form:

$$V(x,y) = V(x^*,y^*) + V_x(x - x^*) + V_y(y - y^*),$$

$$\text{where } V_x = \frac{\partial}{\partial x} V(x,y)\Big|_{x^*} \text{ and } V_y = \frac{\partial}{\partial y} V(x,y)\Big|_{y^*}. \qquad \text{(I.7.33)}$$

Therefore, if the line of intersection between the initial and final diabatic potential surfaces is high for both of the potentials, the line of intersection can be represented in the form $\delta(x_0x+y_0y-c)$ where $x_0=V_x$, $y_0=V_y$ and $c=x^* V_x+y^* V_y$. Then, applying the formalism outlined above in this Subsection to the potentials of type (I.7.33), one can obtain the following effective MFPT:

$$\tau = \tau_{2D}\sqrt{\frac{2\pi}{\beta(V_x^2+V_y^2)}}\, e^{\beta V(x^*,y^*)} \text{ where } \frac{1}{\tau_{2D}} = \frac{1}{x_0^2+y_0^2}\left(\frac{x_0^2}{\tau_x}+\frac{y_0^2}{\tau_y}\right). \qquad \text{(I.7.34)}$$

This simple result clearly demonstrates that if one relaxation time is much faster (shorter) then the other, the faster time controls the effective MFPT. So, the slower coordinate does not contribute to the delivery of the particles to the reaction region when the nonadiabatic transitions at the region of intersection are fast (in the kinetic regime when $K_r>>K_d$), for more details, see Part II, Ch. XI-XII.

3. Concluding remarks

The major portion of the present Part was to devoted a new steady-state theory for description of unimolecular irreversible reactions. The main idea behind this theory was to create a simpler method for calculation of reaction rates influenced by solvation dynamics. This method avoids use of the traditional time-dependent equations (see Eq. (I.1.1)) for evaluation of such rate constants as long-time rate constant (I.1.6) and survival probability (I.1.7). Instead, we constructed a scheme (Ch. III) based on steady-state differential and integral equations which, of course, does not include time as a variable (and thus decreases the dimension of the differential and integral equations to be solved) and provides us with a consistent technique for investigating the kinetic parameters. The theory can be applied to

both overdamped and underdamped mechanisms of stochastic motion, and diabatic as well as adiabatic irreversible reactions.

In order to prove the legitimacy of the suggested equations, the steady-state Green's functions were introduced in Ch. IV. These functions describe only the motion along the reaction potential and do not include any dependence upon the reaction decay (in the form of boundary conditions, for example, [9]). More importantly, they provide the correct transformation from the time-dependent to steady-sate equations but do not retain the property of conservation of particles inside the reaction space, Eqs. (I.4.7)-(1.4.12).

From a practical point of view, the steady-state Green's functions allowed us to simplify evaluations of the chemical rates, especially in the case of narrow reaction regions. We were able to build a complete theoretical description of such reactions, starting from the generalization of the MFPT concept and concluding a consistent introduction of the decoupling approximation in Ch. V and VI.

The MFPT defined in previous works [8] was formulated in order to evaluate the average time for particles started their stochastic motion from some point in space to reach a *point* on the surface. Its definition through the steady-state Green's functions is given by Eq. (I.5.5). The effective MPFT which we introduced in Eq. (I.5.9) is the time to reach a *region* if started from some distribution. Even though the regular MFPT is a very valuable constant in one-dimensional reactions, its use is quite restricted, especially in the case of multidimensional processes. The decoupling procedure, which is a method of solving integral equations, allows to separate the reaction motion along the surface from the mechanism of transitions. Thus, if the procedure is applicable, the rate constant consists of two parts - effective MFPT and equilibrium rate constant. The first has now been defined through the steady-state Green's functions, and calculations of the second are straightforward and can be accomplished by means of the Golden Rule ore transition state theory. One of the greatest advantages of utilization of the steady-state functions in the decoupling approximation is that it makes the procedure simple and as a consequence, its

applicability conditions become clear and could be formulated precisely, see Eqs. (I.6.20), (I.6.21).

As a conclusion, in the present Chapter we have shown some applications of the steady-state Green's function method to both adiabatic and diabatic overdamped reaction models. These models are widely used to describe a broad range of chemical reactions. For example, both the classical outer-sphere electron transfer and photochemical quenching reactions employ diabatic potentials. For this purpose we considered reactions on one- and two- dimensional harmonic oscillator surfaces. Isomerization reactions and other processes involving reorganization of chemical bonds, such as dissociation of molecules are usually described by adiabatic models. The bistable potential can be used in this case, even though the diabatic approach may be of some interest as well. In all of these cases, application of the steady-state Green's function method opens the door to simple, clear calculations of dynamical effects on the reaction rates.

So, after we have developed the steady-state theory for unimolecular reactions in Part I and have demonstrated its basic applications, our next step is to widen the level of its application and consider a more sophisticated reaction model than the one employed above. In other words, in the following Part we intend to present a theory for multidimensional processes and analyze features of the multidimensional dynamics in detail. Thus, Part II is devoted exclusively to the application of the steady-state Green's function method to description of bond-breaking electron transfer reactions in liquids which are intrinsically a two-dimensional process.

PART II APPLICATION OF THE STEADY-STATE GREEN'S FUNCTION METHOD TO BOND-BREAKING ELECTRON TRANSFER REACTIONS

CHAPTER VIII. INTRODUCTION TO PART II

The dynamical effects on the reaction rates for one-dimensional potential energy surfaces (PES) have been discussed in the previous Chapter for the bistable and harmonic oscillator potential models. As was discussed in Part I, reactions on one-dimensional potential surfaces have been the subject of the great interest for over fifty years, see Ref. [2, 6, 8, 13, 53]. However, the multidimensional nature of many reaction PES forced development of the kinetic theory towards investigation of the multidimensional surface processes. Indeed, for reactions where the intrinsic potential surfaces are multidimensional, there is no necessity to follow the lowest energy path and hence it is impossible to extract this single, reaction coordinate which could justify the existence of some effective one-dimensional reaction potential. So, we can anticipate that the investigation of the dynamics of a reacting system on its multi-dimensional surface can demonstrate a richer behavior.

In the present Part of the dissertation we demonstrate the use of the steady-state Green's function theory on reactions along two-dimensional potential surfaces, namely bond-breaking electron transfer reactions. The majority of theoretical studies of ET consider that no bonds are formed or broken during or consequent to the electron transfer event. In this case ET is a simple chemical reaction. It has been studied extensively and the one-dimensional approach in this case has shown quite satisfactory results [6, 23, 42, 54, 55]. However, there are many electron transfer reactions where bonds are broken or formed in a way that is connected with the electron transfer event [28, 29, 56, 57, 58, 59, 60, 61]. We will refer to this circumstance as bond-breaking electron transfer (BBET). For such processes, the level of the theory has lagged behind, in our view, that developed for the "standard" ET, where no bonds are broken or formed. A theory of BBET should be intrinsically more complicated than that of ET, as it must involve at least two distinct coordinates: one connected with reorganization of the solvent (outer sphere) or bond lengths (inner sphere), and the other a bond-stretch coordinate along the direction of the

chemical transformation. Only a few attempts have been made to approach the theoretical description of BBET [30, 35, 52, 62]. The purpose of this Part is to present an extended theory for BBET reactions which can include dynamical effects along both the solvent and bond-breaking coordinates.

There is great diversity in the kinds of BBET reactions that have been studied. Several examples that exemplify reactions of our interest are as follows [29, 54, 56, 63, 64]:

I) Dissociative electron transfer: e.g. reactions of aryl and alkyl halides (RX) with various nucleophiles (N^-).

$$RX + N^- \xrightarrow{BBET} R\bullet + X^- + N\bullet$$

In this mechanism, the transfer of the electron and the bond breaking are considered to be a *concerted* process. The RX bond must be stretched at the transition state, which is also a non-equilibrium state in e.g. the solvent polarization coordinate.

II) $S_{RN}1$ (consecutive) reactions : e.g. reactions of aryl and alkyl halides with various nucleophiles.

$$RX + N^- \xrightarrow{ET} R\bullet^-X + N\bullet \xrightarrow{BB} R\bullet + X^- + N\bullet$$

This is nucleophilic substitution that proceeds by first an electron transfer step, and then, decomposition of the radical anion. In this mechanism, the transfer of the electron and the bond breaking are considered to be a *consecutive* process.

III) S_N2 (concerted) reactions.

$$RX + N^- \longrightarrow (X\text{--}R\text{--}N)^- \longrightarrow RN + X^-$$

Here, the electronic charge redistribution and bond rearrangement occur in a concerted fashion. Nevertheless, these reactions may (though this is controversial

[64, 65]) be viewed as a single electron "transfer" with associated bond rearrangement.

IV) Intervalence charge transfer in the presence of a counterion.

$$AA^+ + N^- \longrightarrow A^+A + N^-$$

In this case, a self-exchange reaction ($AA^+ \longrightarrow A^+A$) is rendered asymmetric due to the presence of the counterion. The counterion forms a contact ion-pair with the electron transfer reagent and the bond breaking is in this ion-pair coordinate. Clearly, these "bonds" are much weaker than those of reactions I-III.

Reactions I and II have been extensively studied by Saveant and his coworkers[29, 56, 63, 64] where they discussed the experimental verification of both concerted and consecutive mechanisms and the conditions under which to expect one or the other. Reaction IV has been discussed by Hupp and co-workers [59]. Again, the point was made that this reaction can be viewed as either a concerted or a consecutive process. A study of a reaction with a scheme similar to IV involving counterion effects on rates of charge transfer reactions in radical anions has recently been carried out [61]. The S_N2 reaction (III) has been treated as a bond making/breaking event on an adiabatic surface under the influence of equilibrium and non-equilibrium solvation [66, 67, 68, 69]. It was shown that a two coordinate description is necessary (one coordinate corresponds to the reactive path of the chemical transformation such as isomerization or dissociation, the other is responsible for description of the solvent effects). In polar solvents with a charge-transfer reaction, this solvent coordinate is conventionally taken as a solvent polarization. In the limit of a very sluggish bath, the rate will be determined by slow polarization fluctuations, a case familiar from the solvent-controlled adiabatic limit of electron transfer theory.

Thus, the picture of BBET shows great diversity and, in order to incorporate all of the different features of the reaction, the theory has to be fairly broad. First of all, we have to distinguish between two different mechanisms which are so common in the field - the

concerted and consecutive pathways of BBET. So, the first issue to discuss is the nature of the surfaces that characterize BBET. One formulation must be found that can span the extremes of the consecutive and concerted reaction paths. By analogy to what was used to distinguish between S_N1 and S_N2 mechanisms [65], we suggest that this can be done by introducing a third, intermediate state $R^{\bullet -}X$ in addition to the initial, RX and the final, $RX^{\bullet -}$ states. Therefore, the general geometric picture for BBET should include three two-dimensional potential surfaces - one for each of the states. From the common physical sense it is clear, that if the intermediate state is sufficiently stabilized, it will lead to an intermediate of sufficiently low energy to favor the consecutive mechanism. Conversely, if it is of high energy, the concerted pathway should be favored.

After the question of the geometry of the two-dimensional potential surfaces is settle we have to consider what possible stochastic processes can be responsible for the motion of reactive particles along the chosen potentials. It is conventional to treat the electron transfer as driven by a combination of inner-sphere vibration degrees of freedom and outer-sphere solvent polarization modes. The influence of both these processes on the electron transfer have been thoroughly investigated [70, 71, 72]. The inner-sphere vibrations usually are treated as a much faster processes compared to the polarization changes [6]. By this assumption, the vibration modes only contribute to the equilibrium, not the dynamical reaction rate constant. On the other hand, polarization changes can be sufficiently slow that dynamical effects on the rate of electron transfer are associated with these fluctuations. Moreover, it is traditional to treat the polarization fluctuations as an overdamped diffusion process, though this may not always be the case [73, 74]. Thus, as far as our major concern is the dynamical influence on BBET, we will consider only the slow polarization coordinate. The general problem with the included vibrational part is analyzed in Ref. [30]

For the bond-breaking part of the whole event, in principle, both overdamped and underdamped mechanisms could be applicable. If the frequency of oscillations of the bond is much slower then the frequency of collisions with the solvent molecules, the

overdamped mechanism is appropriate. This might be the case with weak, non-covalent bonds such as the ones in intervalence charge transfer IV.

The dissociation dynamics of proper intramolecular bonds have been studied starting with Kramers' work [1]. In the absence of solvent perturbation, the bond would perform pure oscillatory motion. However, the solvent forces do affect the bond oscillations, by producing occasional transitions between the energy levels in the bond potential. This is a low friction regime in the sense that the latter forces cause only a small variation of the energy during the time of an oscillation. The effect of the solvent consists in the gradual change of the distribution over the different energy values inside the potential well for the bond-breaking coordinate, and can be modeled as a random walk on the energy levels. This is Kramers' energy diffusion regime [1]. It was proven rigorously [2] that, for the friction γ to be low, it should satisfy the following inequality $\gamma << \omega_z k_B T / D_e$ where ω_z is the frequency of oscillation inside the bond-breaking potential, and D_e is the bond dissociation energy. In other words, the force along the bond-breaking coordinate should be much larger than the thermal one. The energy-diffusion mechanism has proven to give satisfactory results for the bond-breaking process in dissociation-recombination reactions [8].

However, for the methyl halides discussed by Saveant, the bond frequency is very high, around 600 cm^{-1} [75]. This calls into question a classical treatment of the bond-breaking coordinate. It seems more reasonable to consider this coordinate as a quantum system, so the bond transformation takes place through a tunneling process. Two coordinate treatments with one quantum and the other classical are well established [76].

The plan of our work on BBET theory consists of the following sections. First of all, in Chapter IX we establish the forms of PES which are mostly suitable for BBET. Then, the choice of the surfaces naturally divides the theory into the concerted and consecutive parts. As was mentioned above, in the concerted case, the bond-breaking and electron transfer events take place simultaneously. Thus, the reactants, moving under the

influence of damping forces overcome some potential barrier and escape into the product potential well diverting from the intermediate state. For the solvent coordinate (the electron transfer mode) we shall always assume overdamped motion, so a Smoluchowskii high-friction diffusion equation will be used to describe the damping forces. For the bond-breaking mode we will consider three alternatives: overdamped, extremely underdamped (Kramers' energy-diffusion) and quantum regimes. In Chapter X we develop the theory for physically important and challenging energy diffusion mechanism along the bond-breaking coordinate. As far as we are dealing here with a two-dimensional problem, it is quite probable to observe a situation when the motion along one coordinate is much faster then the one along the other. Hence, the dynamics may change from being two-dimensional to effectively one-dimensional. Chapter XI is devoted to solution of this problem. The case where both coordinates are overdamped was accounted in Subsection 2.2 of Chapter VII. Thus in this Part, in Chapter XII we will discuss the properties of the chemical rates evaluated there and compare them with the ones evaluated for the energy-diffusion mechanism. The kinetics of BBET in the case when transformations along the bond-breaking coordinate have to obey quantum rules are evaluated in Chapter XIII. This Chapter closes the concerted part of the BBET theory.

The consecutive mechanism of BBET is discussed in Chapter XIV. In this case particles moving out of the reactant potential surface have to pass some intermediate state before they can reach the product well. Thus, at least three surfaces are involved in the reaction. Though, in principle, the total kinetic picture of the BBET is completely different then in concerted reaction, the dynamics along each of these potential surfaces are analogous to the ones that are discussed in the framework of the concerted scheme. Chapter XV contains concluding remarks concerning the steady-state Green's function theory in unimolecular reactions as well as advantages and consequences of its application to the irreversible processes.

CHAPTER IX. POTENTIAL ENERGY SURFACES

As has been discussed in the previous Chapter and exemplified in reactions I-IV, BBET involves both ET and bond-breaking. PES for the BBET reaction may be regarded simply as the addition of the surfaces for the two individual processes. This does neglect the possibility of a coupling between them, which is certainly a possibility which should be considered. But, clearly, the qualitative features we wish to explore should be evident in this simplified model. According to the scheme outlined in Ch. VIII, we intend to consider three reaction states for BBET reactions - the initial, RX, the intermediate, $R^{\bullet}X^{-}$, and the final, $RX^{\bullet -}$ state. Each of states has to be represented by a two-dimensional diabatic potential surface. The coupling between them provides transitions from one state to another and we say that the reaction has taken place when the particles from the initial state (reactants) appear into the final potential well.

For ET reactions it is well known [71, 72] that PES can be considered to be parabolic in the polarization contributions

$$V_P(x) = x^2 / 2 \qquad \text{(II.9.1.a)}$$

$$V_I(x) = (x - x_{0I})^2 / 2 + \Delta G_{0I} \qquad \text{(II.9.1.b)}$$

$$V_P(x) = (x - x_{0P})^2 / 2 + \Delta G_{0P} \qquad \text{(II.9.1.c)}$$

where ΔG_{0I} and ΔG_{0P} are the exothermicities, and x is the coordinate which characterizes the outer-sphere solvent polarization motion. The subscripts R, I and P denote the reactant (initial), intermediate and product (final) states respectively. The solvent polarization coordinate x is defined by

$$x^2 / 2 = \frac{2\pi}{c} \int \left| \mathbf{P}(\mathbf{r}) - \mathbf{P}_1^0(\mathbf{r}) \right|^2 d\mathbf{r}$$

where $\mathbf{P}(\mathbf{r})$ and $\mathbf{P}_1^0(\mathbf{r})$ are the non-equilibrium and equilibrium solvent orientational polarization and c is the Pekar factor $c=\varepsilon_\infty^{-1} - \varepsilon_0^{-1}$ with ε_∞ and ε_0 the high frequency and static dielectric constants. The outer-sphere reorganization energies are defined as:

$$\lambda_{ot} = x_{0k}^2 / 2 = \frac{2\pi}{c} \int \left| \mathbf{P}_k^0(\mathbf{r}) - \mathbf{P}_1^0(\mathbf{r}) \right|^2 d\mathbf{r}, \quad k = I, P$$

$$\lambda_{xIP} = \sqrt{2\lambda_{xP}} - \sqrt{\lambda_{xI}}\,. \qquad \text{(II.9.2)}$$

The schematic picture of the diabatic surfaces for the electron transfer coordinate is given in Fig. 8 a.

Now, the diabatic surfaces for the bond-breaking process have to be constructed in order to incorporate them into Eqs. (II.9.1)-(II.9.3). For the gas phase, Morse potentials would be appropriate for a description of the bond dissociation motion of the reactants, RX and intermediates, R•⁻X. For the dissociative state, RX•⁻, the repulsive branch of the Morse potential would be used. However, we are dealing with a liquid state problem and the requisite potentials are the potentials of mean force. The solvent environment, of course, readjust all of these potentials, especially the dissociative one. Nevertheless, with a fairly good accuracy we can state that the product and intermediate state potentials keep their shape [29]. We believe that this is not the case with the dissociative potential $V_P(z)$. The caging effect of the solvent molecules creates a shallow minimum on the repulsive surface, so that the products do not immediately separate and disappear into the bulk, but form a stable state. Thus, we choose the following form of the bond-breaking part of the reaction surfaces:

$$V_R(z) = D_e\left(\exp(-bz) - 1\right)^2 \qquad \text{(II.9.3.a)}$$

$$V_I(z) = D_e\left(\exp\left(-b(z - d_I)\right) - \sigma_I\right)^2 \qquad \text{(II.9.3.b)}$$

$$V_P(z) = D_e\left(\exp\left(-b(z - d_P)\right) - \sigma_P\right)^2 \qquad \text{(II.9.3.c)}$$

where D_e is the dissociation energy of the bond, and σ_I and σ_P are the displacements of the intermediate and final state potentials. Fig. 8 b depicts the potentials given in Eqs. (II.9.3) These Morse potentials should mimic bond-breaking reaction in the liquid.

For future calculations it is convenient to introduce the reorganization energies for the transitions from one state to another:

$$\lambda_{zRI} = D_e(1 + bd_I - \sigma_I)^2 \qquad \text{(II.9.4.a)}$$

$$\lambda_{zRP} = D_e(1 + bd_P - \sigma_P)^2 \qquad \text{(II.9.4.b)}$$

$$\lambda_{zIP} = D_e(b(d_P - d_I) + \sigma_P - \sigma_I)^2. \qquad \text{(II.9.4.c)}$$

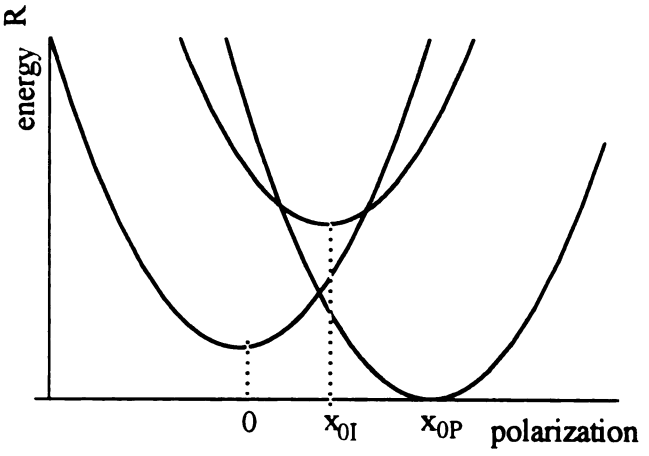

(a)

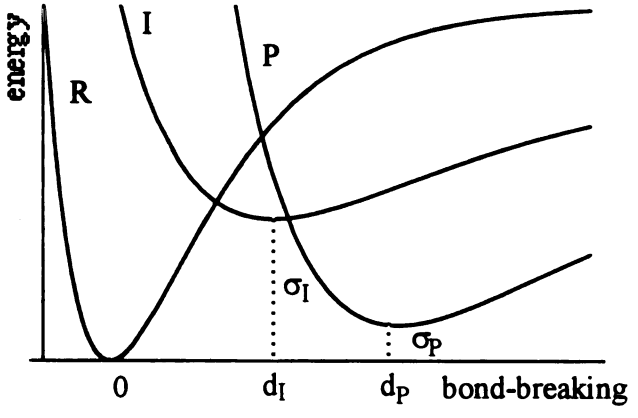

(b)

Fig. 8. Schematic picture of the potentials for each of the coordinates participating in BBET: a) the orientational polarization (or ET) coordinate; b) the bond-breaking (BB) coordinate.

If the points of intersection lie sufficiently below the dissociation energy of the Morse potentials, a harmonic approximation of them would be reasonable [30]. Expanding the Morse potentials around their equilibrium bond distances, we get:

$$V_R(z) = D_e b^2 z^2 \qquad \text{(II.9.5.a)}$$

$$V_I(z) = D_e b^2 (z - z_{0I})^2 \qquad \text{(II.9.5.b)}$$

$$V_P(z) = D_e b^2 (z - z_{0P})^2 \qquad \text{(II.9.5.c)}$$

with $z_{0K}=(1-\sigma_K)/b$. For the sake of simplicity these potentials have equal spring constants. The majority of ET reaction analyses make the same assumption. For our case the form of the product surface is not very important, because we consider irreversible reactions. The only effect it produces consists in the equation for the line of intersection between the surfaces and the harmonic approximation does not affect it dramatically. The form of the intermediate state is more important for the kinetics of consecutive BBET. For this reason in Chapter XIV we consider not only the case of approximately equal spring constants, as in Eqs. (II.9.5), but also a situation when the intermediate state is much shallower then the initial one (i.e. the bond of an intermediate is much weaker then the bond of a reactant).

Now, adding the potentials for the bond-breaking to the electron transfer term, we obtain the two-dimensional reaction surfaces

$$V_K(x,z)=V_K(x) + V_K(z), \quad \text{K=R, I, P.} \qquad \text{(II.9.6)}$$

The lines of intersection between these diabatic surfaces can be evaluated form the set of equations $V_i(x,z)=V_j(x,z)$, where i,j =R, I, P. Each of these lines has a minimum point which corresponds to the activation energy of the transitions. These minimum points can be obtained by Lagrange's method, the undetermined multiplier accounting for the constraint $V_i=V_j$. Thus, we have three sets of coordinates for the points on the surfaces which determine the activation energies of transitions: (x_{RI}^*, z_{RI}^*), (x_{RP}^*, z_{RP}^*), (x_{PI}^*, z_{PI}^*):

$$x_{RI}^* = \sqrt{2\lambda_{xI}}\,\frac{\Delta G_{01} + \lambda_I}{2\lambda_I}, \quad z_{RI}^* = \sqrt{2\lambda_{zRI}}\,\frac{\Delta G_{01} + \lambda_I}{2\lambda_I}, \quad \lambda_I = \lambda_{xI} + \lambda_{zRI} \qquad \text{(II.9.7.a)}$$

$$x_{IP}^{*} = \sqrt{2\lambda_{xIP}}\,\frac{\Delta G_{01} - \Delta G_{02} + \lambda_{IP}}{2\lambda_{IP}},\quad z_{IP}^{*} = \sqrt{2\lambda_{zIP}}\,\frac{\Delta G_{01} - \Delta G_{02} + \lambda_{IP}}{2\lambda_{IP}},$$

$$\lambda_{IP} = \lambda_{xIP} + \lambda_{zIP} \qquad \text{(II.9.7.b)}$$

$$x_{RP}^{*} = \sqrt{2\lambda_{xP}}\,\frac{\Delta G_{02} + \lambda_{P}}{2\lambda_{P}},\quad z_{RP}^{*} = \sqrt{2\lambda_{zRP}}\,\frac{\Delta G_{02} + \lambda_{P}}{2\lambda_{P}},\quad \lambda_{P} = \lambda_{xP} + \lambda_{zRP}. \qquad \text{(II.9.7.c)}$$

The relative position of these points in the reaction space determines which of the two mechanisms - concerted or consecutive - is most suitable for the reaction. Fig. 9 schematically presents the two different pictures. The concerted pathway takes place when $V_R(x_{RP}^{*}, z_{RP}^{*}) < V_R(x_{RI}^{*}, z_{RI}^{*})$ and the consecutive mechanism is preferable when this inequality is reversed.

For the sake of simplicity, in the next four chapters devoted to the concerted mechanism of BBET we will use the notation: $\lambda_x \equiv \lambda_{xP}$ and $\lambda_z \equiv \lambda_{zRP}$.

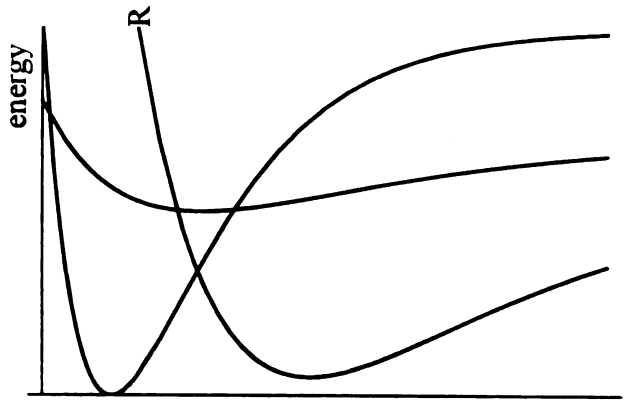

(a)

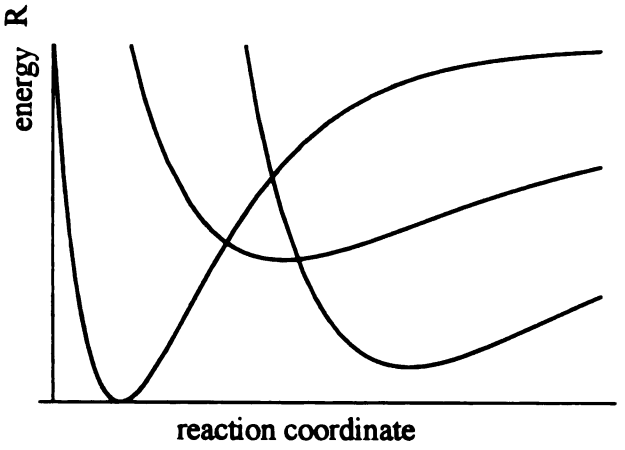

(b)

Fig. 9. Concerted pathway (a) is sketched in comparison with the consecutive (b) one.

CHAPTER X. ENERGY-DIFFUSION MECHANISM IN BOND-BREAKING ELECTRON TRANSFER REACTIONS

In this Chapter, our aim is to combine both solvent polarization dynamics (coordinate x) as described by high friction, overdamped diffusion, and bond-breaking dynamics (coordinate z) as described by low friction, energy diffusion, in one concerted process and investigate their joint influence on the BBET reaction dynamics. Hence, we assume here that the reactants undergo direct transitions into the products and essentially ignore the existence of high energy intermediate state. When the electron transfer and breaking of a bond occur in a concerted manner, we would like to understand how the relaxation times for the coordinates τ_x and τ_z, and the reorganization energies λ_x and λ_z contribute to the total kinetic rate. As in Part I, here we will consider only irreversible mechanism of the reaction, as far as the rate constants for reversible reactions can be evaluated through those ones for irreversible, see Ch. II and Eq. (I.2.2) in particular. The schematic picture of the reaction potential $V_R(x,z)$ is given on Fig. 10. This Chapter presents an integral approach which provides the overall rate constant in terms of explicitly defined equilibrium and diffusion rate constants [52] by means of the steady-state Green's function method.

1. The equation of motion and the sink function

Since we will deal with energy-diffusion along the z coordinate, it is convenient to use its energy "image" ,E, to describe the dynamics. Then the time-evolution equation for the joint probability $P(x,E,t)$.is given as (see Eq. (I.3.1))

$$\partial P(x,E,t)/\partial t = [L(x)+L(E)]P(x,E,t) - W(x,E)P(x,E,t) \qquad \text{(II.10.1)}$$

where the diffusion operator for the polarization coordinate is

$$L(x) = \frac{1}{\beta\tau_x}\frac{\partial}{\partial x}\varphi(x)\frac{\partial}{\partial x}\frac{1}{\varphi(x)}; \qquad \tau_x \equiv \tau_L \qquad \text{(II.10.2)}$$

with τ_L the longitudinal dielectric relaxation time, $\beta = 1/k_BT$, and $\varphi(x) = \sqrt{\beta/2\hbar}\, e^{-\beta V(x)}$ the Boltzmann distribution along the polarization coordinate. The dynamical operator for the bond-breaking coordinate comes from Kramers' energy diffusion problem for the harmonic oscillator potential [1]:

$$L(E) = \frac{\partial}{\partial E} D(E)\left(\frac{\partial}{\partial E} + \beta\right), \quad \text{with} \quad D(E) = \frac{E}{\beta\tau_z}, \tau_z = \frac{1}{\gamma} \tag{II.10.3}$$

where γ is the friction. The energy range is 0 to ∞, and the Boltzmann distribution for the bond breaking is $\varphi(E) = \beta e^{-\beta E}$. We will assume that reactants are initially in thermal equilibrium,

$$P(x, E, 0) = \varphi(x) \cdot \varphi(E). \tag{II.10.4}$$

The boundary conditions for Eq. (II.10.1) require that the fluxes of the particles at the boundary $x,z = \{\pm\infty\}$ are zero.

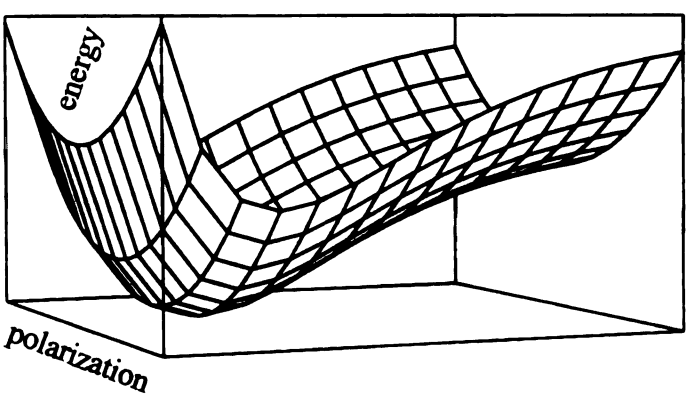

Fig. 10. Schematic plot of the potential energy surface for concerted BBET reactions.

To define the sink function $W(x,E)$, we start from the definition of the thermal equilibrium rate constant for a nonadiabatic, irreversible reaction [30]:

$$K_e = \left(\frac{2\pi V_{if}^2}{\hbar}\right) \frac{\int d\Gamma_x d\Gamma_z\, e^{-\beta H_1}\, \delta(\Delta V(x) + \Delta V(z))}{\int d\Gamma_x d\Gamma_z\, e^{-\beta H_1}} \tag{II.10.5}$$

where $\Gamma_y(\Gamma_z)$ denote the phase space coordinates $dp_x\,dx$ $(dp_z\,dz)$. H_1 is the Hamiltonian corresponding to the initial state potential $V_R(x,z)$, and ΔV is the difference in potentials for the initial and final state surfaces. Using the energy coordinate $E = p_z^2/2\mu + D_e\beta_z^2 z^2$ and introducing the identity $1 = \int dE\delta\left(E - \mu_1(\Gamma_z)\right)$ in Eq. (II.10.4) yields:

$$K_e = \int dE \int dx\, W(x,E)\varphi(E)\varphi(x) \tag{II.10.6}$$

where

$$W(x,E) = \frac{2\hbar V_{if}^2}{\hbar\sqrt{4\pi\lambda_z}} \frac{\Theta\left(E - E^*(x)\right)}{\sqrt{E - E^*(x)}}. \tag{II.10.7}$$

Here, Θ is the step function, V_{if} is the strength of coupling between the initial and final states and the activation energy is defined as

$$E^*(x) = \frac{\lambda_x}{2\lambda_z}\left[\frac{\Delta G^o + \lambda_o - \sqrt{2\lambda_x}}{\sqrt{2\lambda_x}}\right]^2 \tag{II.10.8}$$

In Eq. (II.10.8), λ_x is the reorganization energy for the polarization coordinate, $\lambda_z = D_e$ is the bond-breaking reorganization energy, which coincides with the dissociation energy, and $\lambda_o = \lambda_x + \lambda_z$.

For a high activation barrier reaction, in the sense that $\beta E^*(x) >> 1$ for all x, Eq. (II.10.6) can be approximated by

$$W(x,E) = \frac{V_{if}^2}{\hbar}\sqrt{\frac{\pi}{\beta\lambda_z}}\,\delta\left(E - E^*(x)\right), \tag{II.10.9}$$

that is a sink *line* on the potential energy surface in the x–E coordinates.

2. The reaction rate constant

Before introducing the form of the reaction rate constant, let us emphasize that, in order to derive Eq. (II.10.9), we utilized the assumption that the activation barrier of the reactions under consideration is high, $\beta E_a >> 1$, where E_a is the activation barrier energy. This is the second major assumption that we apply in our considerations – the first one is

the assumption of separability of the motions along x and z coordinates. The high activation barrier assumption permits several significant simplifications in the calculation of the reaction rate constant.

It was explicitly proved [45] (see also Appendix B or Eq. (I.7.12) and the following) that the high activation barrier kinetics are essentially mono-exponential. Thus, the rate constant can be defined simply by using the probability distribution function P:

$$K^{-1} = \int_o^\infty dt \int_o^\infty \int_{-\infty}^\infty dx dE\, P(x,E,t). \qquad \text{(II.10.10)}$$

This is the rate constant of mono-exponential unimolecular decay, traditionally represented as $P_e(t) = e^{-Kt}$ where $P_e(t)$ is the survival probability.

3. The energy diffusion operator.

For extremely low friction $\gamma \to 0$, Kramers noted that the motion of a particle inside a one-dimensional potential well is mainly oscillatory with occasional transitions between the energy levels. Thus action (or energy) is almost a constant of the motion, and is the appropriate variable with which to obtain a stochastic description. The lower the particle sits inside the well, the more difficult it is for the external fluctuations to move it on to a higher level. The energy-dependent diffusion coefficient $D(E)$ in Eq. (II.10.3) reflects this picture. As a particle reaches energy levels close to the barrier, it gains energy more readily and finally, when it has enough energy to surmount the barrier, it irreversibly escapes from the well. The reaction rate constant of this process can be expressed through the mean first passage time for a particle from the bottom of the well $E = 0$ to reach the barrier $E = E_a$ [8]

$$K = \frac{1}{\tau_p}; \qquad \tau_p = \int_o^{E_a} \frac{dE\, e^{-\beta E}}{D(E)} \int_o^E e^{-\beta E'} dE'. \qquad \text{(II.10.11)}$$

With the assumption of a high activation barrier reaction, the asymptotic value of the above integral yields the result [1]

$$K = \beta\gamma E_a e^{-\beta E_a}. \qquad \text{(II.10.12)}$$

Note that an implication of Eq. (II.10.12) is that the energy diffusion coefficient $D(E)$ appears as the constant $D(E_a) = E_a/\beta\tau_z$. This means that only the dynamics around the barrier contribute to the rate constant, and the diffusion coefficient may as well be taken as a constant for high activation barrier reactions. This conclusion permits significant simplification of the operator, Eq. (II.10.3) to

$$L(E) = \frac{E_a}{\beta\tau_z}\frac{\partial}{\partial E}\varphi(E)\frac{\partial}{\partial E}\frac{1}{\varphi(E)}. \qquad \text{(II.10.13)}$$

We will use the above form of the energy-diffusion operator, as it is consistent with our assumption of high activation barrier.

4. Integral equation formalism.

The differential equation, Eq. (II.10.1) with initial condition Eq. (II.10.4) can be written in the integral form:

$$P(x,E,t) = \varphi(x)\varphi(E) - \int_o^t d\tau \int_{-\infty}^{\infty}\int_o^{\infty} dx'dE'\, G(x,x';E,E';t-\tau)W(x',E')P(x',E',\tau) \qquad \text{(II.10.14)}$$

with the Green's function defined by the equation:

$$L(x,E)G(x,x';E,E',t) = \frac{\partial}{\partial t}G(x,x';E,E',t). \qquad \text{(II.10.15)}$$

Here, because of the global separability of the reaction potential $V(x,E) = V(x) + V(E)$ and, hence, $L(x,E) = L(x) + L(E)$, the Green's function $G(x,x';E,E',t)$ is a product of Green's functions for the independent operators along the x and E coordinates:

$$G(x,x';E,E',t) = G(x,x',t)\cdot G(E,E',t) \qquad \text{(II.10.16)}$$

where

$$L(x)G(x,x',t) = \partial G(x,x',t)/\partial t \quad G(x,x',0) = \delta(x-x') \qquad \text{(II.10.17a)}$$

and

$$L(E)G(E,E',t) = \partial G(E,E',t)/\partial t \quad G(E,E',0) = \delta(E-E'). \qquad \text{(II.10.17b)}$$

It is convenient to represent Eq. (II.10.14) in a different form, introducing a new variable, $\xi(x,E,s)=\tilde{P}(x,E,s)/P_e(s)$, where $\tilde{P}(x,E,s)$ and $P_e(s)$ are the Laplace transforms of the population probability distribution function and survival probability, respectively. Then for the high barrier case, Eq. (II.10.14) transforms to the following expression, (see Eq.I.4.13):

$$\xi(x,E,s)=\varphi(x)\varphi(E)-\int_{-\infty}^{\infty}\int_{o}^{\infty}dx'dE'\,G(x,x';E,E',s)W(x',E')\xi(x',E',s) \qquad \text{(II.10.18)}$$

with the very convenient redefinition of the reaction rate constant, as given in Eq. (I.3.12):

$$K=\lim_{s\to o}\int_{-\infty}^{\infty}\int_{o}^{\infty}dxdEW(x,E)\xi(x,E,s). \qquad \text{(II.10.19)}$$

In principle, the Green's function used in Eq. (II.10.18) should differ from the Green's function used in Eq. (II.10.14). However, because we are dealing with the high activation barrier case, this difference is of the order of the small parameter $(\beta E_a)^{-1}$, which should be neglected for the sake of consistency.

As far as the sink function *W(x,E)* is a line on the potential surface (formed from the intersection of the initial and final state surfaces), with an infinitely small width, as in Eq. (II.10.8), the decoupling approximation, described in Ch. VI can be applied to the integral equation, Eq. (II.10.18). Taking into account definition of the rate constant in Eq. (II.10.19), the result of the decoupling can be represented in the form

$$K=K_r/(1+K_r/K_d) \qquad \text{(II.10.20)}$$

with the equilibrium (non-adiabatic) rate constant

$$K_r=\int_{-\infty}^{\infty}\int_{o}^{\infty}dxdEW(x,E)\varphi(x)\varphi(E) \qquad \text{(II.10.21)}$$

and the diffusion rate constant, $K_d = 1/\tau_p$, where τ_p is the effective MFPT, originally presented in Eq. (I.5.9):

$$\tau_p=\frac{1}{K_r^2}\int_o^{\infty}dt\iiint\int dxdx'\,dEdE'\,K(x,E)G(x,x';E,E',t)K(x',E')\varphi(x',E') \qquad \text{(II.10.22)}$$

with the Green's function is defined in Eq. (II.10.16).

The Eqs. (II.10.20)-(II.10.22) give the expressions for the BBET rate constant in a general form. The important issue here is that, with the given delta function form of the reaction sink (Eq. (II.10.8)), the rate constant can be divided into separately calculable parts — a diffusive part K_d and an equilibrium rate constant part K_r.

The analytical solution for the Green's functions, with the assumption of a high activation barrier, is presented in the Appendix C. Now, we will discuss the results of their utilization.

5. General form of the non-adiabatic and diffusional rate constants

When relaxation along both coordinates is fast, the reaction is controlled by the equilibrium rate constant, Eq. (II.10.21). This regime, often called the kinetic control limit, corresponds to the physical situation where the rate constant is given by the Golden Rule expression for a nonadiabatic transition or by transition state theory for an adiabatic reaction. It assumes thermal equilibrium prevails in the initial state. Thus, the motion inside the well is so fast that it re-establishes the Boltzmann distribution inside it after each escape event. In terms of the reaction constants given by Eqs. (II.10.21) and (II.10.22), this means that $K_r << K_d$ and $K = K_r$. Calculation of the equilibrium rate constant is straightforward, taking into account the form of Eq. (II.10.8):

$$K_r = \left(\frac{2\hbar V_{if}^2}{\hbar}\right)\sqrt{\frac{\beta}{4\pi\lambda_o}}e^{-\frac{\beta(\Delta G_o+\lambda_o)^2}{4\lambda_o}} \qquad \text{(II.10.23)}$$

The other extreme regime possible in this situation corresponds to the inequality $K_r >> K_d$ and is called the diffusion-control limit. In this case, the intensity of the sink is so large that the motion inside the potential well determines the reaction rate. In principle, this regime coincides with Kramers' one-dimensional problem, which can be formulated as the mean first passage time from the bottom of a one-dimensional potential well to the point E_a [8, 53]. For multidimensional processes we have to consider the mean first passage time to a line on the multidimensional surface. For a correctly chosen (adiabatic) potential surface,

this time gives the rate constant that corresponds to the multidimensional Kramers rate constant, and is given by Eq. (II.10.22). Eq. (II.10.22) is a general recipe for calculation of the mean first passage time to a line on the multidimensional surface. We note that the Green's function in Eq. (II.10.22), in the case of high activation barrier, can be considered as the one given by Eq. (II.10.15) for any two-dimensional potential $V(x,y)$, i.e. not necessarily separated into two independent ones, as assumed in this article.

Returning to the calculation of the mean first passage time for the BBET reaction given by Eq. (II.10.22) with Green's function (II.10.16), we require the Green's functions in Eq. (II.10.17), for the case of high activation barrier. These are obtained in Appendix D:

$$G_E(E,E',t)=\sqrt{\frac{\beta\tau_z}{4\pi E_a t}}\,e^{-\frac{\beta\left(E-E'+E_z^* t/\tau_z\right)^2}{4E_a t/\tau_z}} \tag{II.10.24}$$

$$G_x(x,x',t)=\sqrt{\frac{\beta\tau_x}{4\pi t}}\,e^{-\frac{\beta\left(x-x'+x^* t/\tau_x\right)^2}{4t/\tau_x}} \tag{II.10.25}$$

where x^* and E_z^* define the minimum of the sink function given by Eq. (II.10.8). E_a is the activation energy along the z (or E) coordinate, and the activation energy along the x coordinate is $E_x^* = x^{*2}/2$. E_z^* and x^* are [30]:

$$E_z^* = \frac{\lambda_z\left(\Delta G_o+\lambda_o\right)^2}{4\lambda_o{}^2} \tag{II.10.26a}$$

$$x^* = \sqrt{\frac{\lambda_x}{2}}\,\frac{\left(\Delta G_o+\lambda_o\right)}{\lambda_o}. \tag{II.10.26b}$$

By utilizing the form of the Green's functions, Eq. (II.10.24) and Eq. (II.10.25), in Eq. (II.10.16) and then in Eq. (II.10.22), we can represent the effective MFPT as:

$$\tau_p = \frac{\lambda_o}{\lambda_z}e^{\frac{\beta\left(\Delta G_o+\lambda_o\right)^2}{2\lambda_o}}\sqrt{\frac{\tau_x\tau_z}{8\pi^2 E_a}}\int_o^\infty\frac{d\tau}{\sqrt{\tau}}\int_{-\infty}^{\infty}dz\,\mathrm{Int}(z,t)\exp\left[-\frac{\beta\left(z+x^*\tau\tau_z/\left(\tau_x E_a\right)\right)^2}{4\tau\tau_z/\left(\tau_x E_a\right)}\right] \tag{II.10.27a}$$

where

$$\mathrm{Int}(z,t) = \sqrt{\frac{\lambda_z^2}{\lambda_x^2 z + 2\lambda_x\lambda_z t + 2\lambda_z^2 t}}$$

$$\exp\left[-\frac{\beta(\lambda_x z^2 + 2\lambda_z t)}{8\lambda_z}\frac{(2\lambda_z(\Delta G_0 + \lambda_0)^2 + \lambda_0(\lambda_x z^2 + 2\lambda_z t) - 2z\lambda_z\sqrt{\lambda_x}(\Delta G_0 + \lambda_0))}{\lambda_x^2 z + 2\lambda_x\lambda_z t + 2\lambda_z^2 t}\right]$$

(II.10.27b)

Unfortunately, we were not able to calculate the mean first passage time for BBET analytically from this expression for arbitrary parameter values. Thus, the following discussion will be devoted to an analysis of the possible limiting cases, and accompanied by a numerical analysis of Eq. (II.10.27).

CHAPTER XI. FAST AND SLOW MODES IN MULTIDIMENSIONAL KINETIC PROCESSES

1. General Aspects

When one of the modes in a 2D problem is much slower than the other, it is possible to reduce the problem to an effective 1D one. As was noticed in Ref. [21], this reduction is an "adiabatic elimination procedure," which has the Born-Oppenheimer approximation as its analog in quantum mechanics. Let us take, for example, x as the slow mode. Thus, diffusion along the x coordinate is much slower than along E (or z), which, in terms of the relaxation times, can be expressed as $\tau_z << \tau_x$. In this case, the contribution of the operator $L(x)$ in Eq. (II.10.1) is small compared to that of $L(E)$, so that we can neglect it, resulting in the following expression:

$$\partial P(E,x,t)/\partial t = L(E)P(E,x,t) - W(E,x)P(E,x,t). \qquad \text{(II.11.1)}$$

In this differential equation, x is a parameter, entering the solution $P(E,x,t)$ only from the sink function. The separation performed in Eq. (II.11.1) indicates that the dynamics along the x coordinate sees only the equilibrated picture from the coordinate E created by its fast motion.

Now, let us introduce a time τ_e, as the time by which exponential (equilibrium) kinetics with some long-time rate constant has been established along the fast E coordinate (this time was introduced in Appendix A, Eq. (A17)). It was proved that this time should be of the same order as the relaxation time τ_z. Therefore, by the time τ_e, an equilibrium profile (not necessarily Boltzmann) has been established along the E coordinate. To utilize this conclusion, let us make a statement that, as we will see later, is correct: for all $t > \tau_e$ (and $\tau_z << \tau_x$), namely, that the population probability distribution function can be given as follows:

$$P(E,x,t) = R(E,x) \cdot Q(x,t). \qquad \text{(II.11.2)}$$

The equilibrium profile is represented by the steady-state function *R(E,x)* and all the time dependence is due to the dynamics along the slow coordinate x.

We can obtain *R(E,x)* and the long-time rate constant corresponding to this process from the steady-state differential equation

$$L(E)R(E,x) - W(x,E)R(E,x) = -\tilde{K}(x)R(E,x) \qquad \text{(II.11.3)}$$

with the boundary conditions for the E coordinate as in Eq. (II.10.1) and an additional condition for *R(E,x)*, which lets us define the long-time rate constant $\tilde{K}(x)$:

$$\int dE\, R(E,x) = 1. \qquad \text{(II.11.4)}$$

This method was discussed in detail in Ref. [45], see also Chapter III. It should be emphasized that Eq. (II.11.3) is *not* an eigenvalue problem, but an ordinary differential equation with some boundary conditions supported by Eq. (II.11.4) as an additional condition necessary for the definition of the long-time rate constant.

Assuming that we know the forms of *R(E,x)* and $\tilde{K}(x)$ by solving Eqs. (II.11.3) and (II.11.4), we can use the representation of Eq. (II.11.2) directly in Eq. (II.10.1), to obtain

$$R(E,x)\frac{\partial}{\partial t}Q(x,t) = Q(x,t)\left[L(E)R(E,x) - W(x,E)R(E,x)\right] + L(x)R(E,x)Q(x,t). \qquad \text{(II.11.5)}$$

Then, taking into account that the expression in square brackets is the left part of Eq. (II.11.3), integrating Eq. (II.11.4) over all E space, and using Eq. (II.11.4), we obtain a 1D differential equation for the slow coordinate with the effective sink function from Eq. (II.11.3):

$$\frac{\partial}{\partial t}Q(x,t) = L(x)Q(x,t) - \tilde{K}(x)Q(x,t). \qquad \text{(II.11.6)}$$

To sum up, we note that the above is a general scheme to reduce any 2D problem with fast and slow modes to a 1D one that contains dynamics only along the slow mode. The most difficult part of this scheme is the solution of differential equation, Eq. (II.11.3),

in order to get the effective sink function $\tilde{K}(x)$. However, the fact that we are dealing with the high-activation barrier case permits some significant simplifications of this problem. The key point is that, for high-activation barrier reactions, the long-time rate constant K is approximately equal to the generalized probability $æ = \int_o^\infty dt\, P_e(t)$, which is much easier to calculate. The reason for this is that the time interval for the non-exponential stage in the high-activation barrier reactions is so small, compared to the time scale of the reaction, that the exponential kinetics can be considered to take place at all times. Then, the long-time rate constant and generalized probability are identical. The proof can be given easily. If the kinetics is exponential, i. e., $P_e(t) = e^{-Kt}$ where K is the long-time rate constant, then the generalized probability, æ, is equal to K.

The equation for the definition of the generalized probability is usually much easier to solve than the one for the long-time rate constant (Eq. (II.11.3)):

$$L(E)R(E,x) - W(x,E)R(E,x) = -\tilde{æ}(x)f(E) \qquad \text{(II.11.7)}$$

or, in integral form:

$$R(E,x) = f(E) - \int dE'\, \overline{G}(E,E')W(E',x)R(E',x) \qquad \text{(II.11.8)}$$

with the rate constant (see Eqs. 3.5) and (II.10.20)):

$$\tilde{æ}(x) = \int_0^\infty dE\, W(E,x)R(E,x).$$

Here, $f(E) = \varphi(E)$ is the initial distribution and $\overline{G}(E,E')$ is the steady-state Green's function that satisfies the equation (for high barrier)

$$L(E)\overline{G}(E,E') = -\delta(E-E'). \qquad \text{(II.11.9)}$$

This Green's function can be defined easily (see Appendix A). If the sink function $W(x,E)$ has the form

$$W(x,E) = K_o\delta(E - E^*(x)), \qquad \text{(II.11.10)}$$

that is the case in Eq. (II.10.8), then solution of Eq. (II.11.8) is very straightforward:

$$\tilde{æ}(x) = \frac{K_{rE}(x)}{1 + K_{rE}(x)/K_{dE}(x)} \qquad \text{(II.11.11)}$$

where

$$K_{rE}(x) = \int dE W(x,E)\varphi(E) = K_o \varphi(E^*(x)) \qquad \text{(II.11.12a)}$$

$$K_{dE}(x) = \frac{\varphi(E^*(x))}{\overline{G}(E^*(x), E^*(x))}. \qquad \text{(II.11.12b)}$$

The probability-distribution function also can be found easily from Eq. (II.11.8):

$$R(E,x) = \varphi(E)\left[1 - K_o \frac{\varphi(E^*)}{\varphi(E)} \frac{\overline{G}(E^*,E^*)}{1 + K_o \overline{G}(E^*,E^*)}\right]. \qquad \text{(II.11.13)}$$

In the case of the regular diffusion-type operator $L(E) = D_E \frac{\partial}{\partial E}\varphi(E)\frac{\partial}{\partial E}\frac{1}{\varphi(E)}$, the Green's function $\overline{G}(E,E')$ for high activation barrier has the form, see Eq. (I.5.10):

$$\overline{G}(E,E') = \begin{cases} \dfrac{1}{\beta D_E V'(E^*)} \dfrac{\varphi(E)}{\varphi(E^*)} & E > E' \\ \dfrac{1}{\beta D_E V'(E^*)} & E < E' \end{cases} \qquad \text{(II.11.14)}$$

where $V'(E^*) = \partial V(E)/\partial E\big|_{E^*}$ and $E^*$is the energy at the activation barrier. Then Eq. (II.11.12b) can be rewritten as

$$K_{dE} = \beta D_E V'(E^*(x))\varphi(E^*(x)). \qquad \text{(II.11.15)}$$

Thus, for high activation barrier reactions, the sink function in Eq. (II.11.6) for the slow mode can be calculated as

$$\tilde{K}(x) = \tilde{æ}(x) = \frac{K_{rE}(x)}{1 + K_{rE}(x)/K_{dE}(x)} \qquad \text{(II.11.16)}$$

with $K_{rE}(x)$ and $K_{dE}(x)$ defined in Eqs. (II.11.12a) and (II.11.15).

As we can see from Eq. (II.11.16), the general form of the sink function $\tilde{K}(x)$ as a function of the slow coordinate is very complicated, so that an analytical solution of Eq. (II.11.6) is hard to achieve. However, if the dynamics along the fast coordinate E is so fast that we can talk about the kinetic control limit for this coordinate ($K_{rE} << K_{dE}$), then the sink function $\tilde{K}(x)$ expression simplifies dramatically:

$$\tilde{K}(x) = K_{rE}(x) = K_0 \varphi(E^*(x)). \qquad \text{(II.11.17)}$$

Moreover, the probability distribution function $R(E,x)$ from Eq. (II.11.13) simplifies to $R(E,x) \approx \varphi(E)$, and therefore it coincides with the Boltzmann distribution along the fast coordinate.

This analysis demonstrates that the separation of a multidimensional reaction into fast and slow processes can reduce the problem to consideration of a one dimensional process only. However, the case can still be very complicated if the dynamics along the fast coordinate is not fast enough to compete with the equilibrium rate constant, in other words, $K_{rE} \approx K_{dE}$ or $K_{rE} > K_{dE}$. In this case the sink function given by Eq. (II.11.6) has the form in Eq. (II.11.16) or $\tilde{K}(x) \approx K_{dE}$ respectively. We will come back to this situation in the next Chapter when we will discuss the total picture of 2D reactions. However, when $K_{rE} \approx K_{dE}$, Eq. (II.11.6) is very unlikely to be solved analytically.

When $K_{rE} << K_{dE}$ and $\tilde{K}(x) \approx K_0 \varphi(E^*(x))$, then the situation becomes similar to the one originally described in Ref. [6] for the fast and slow modes, for the case of harmonic oscillator potentials. If we assume, in accordance with Ref.[6], that $V(x) = x^2/2$ and $V(E) = E^2/2$, then the sink function of Eq. (II.11.10) transforms into (see Ref. [30] for details):

$$W(x,E) = \frac{K_0}{\sqrt{2\lambda_E}} \delta(E - E^*(x)), \qquad E^*(x) = \frac{\left[\Delta G_0 + \lambda_0 - x\sqrt{2\lambda_x}\right]^2}{4\lambda_E} \qquad \text{(II.11.18)}$$

where λ_E and λ_x are the reorganization energies for the E and x coordinates, and $\lambda_0 = \lambda_E + \lambda_x$ .The effective sink function $\tilde{K}(x)$ given by Eq. (II.11.17) has the Gaussian form:

$$\tilde{K}(x) = K_0\sqrt{\frac{\beta}{4\pi\lambda_E}}\exp\left[-\frac{\beta(\Delta G_0 + \lambda_0 - x\sqrt{2\lambda_x})^2}{4\lambda_E}\right] \qquad \text{(II.11.19)}$$

that coincides with the form of the sink function in Ref. [6] obtained by using transition state theory. Furthermore, if $\beta\lambda_E \to 0$, then $\tilde{K}(x)$ in Eq. (II.11.16) transforms into a δ-functional sink function $\tilde{K}(x)\sim\delta(x-x^*)$ with $x^*=(\Delta G_0+\lambda_x)^2/\sqrt{2}\lambda_x$ and we encounter the problem of 1D harmonic oscillator which was considered in detail in Section 2.1 of Chapter VII. However, one should remember that application of this simple sink function $\tilde{K}(x)$ for the slow mode is legitimate only if the condition $K_{rE} << K_{dE}$ is satisfied.

2. Fast bond breaking.

This situation corresponds to the case when the relaxation time for the bond-breaking coordinate is much faster then the polarization relaxation time, i.e. $\tau_z << \tau_x$. Hence, the scheme, described in the previous Section can be applied to analyze the reaction kinetics.

Here, the fast bond-breaking dynamics creates the effective sink $\tilde{K}(x)$ for the polarization to transfer the electron. Then, for the effective sink function given by Eq. (II.11.16), we can calculate K_{rE} and K_{dE} from Eqs. (II.11.12a) and (II.11.15):

$$K_{rE}(x) = K_0\sqrt{\frac{\beta}{4\pi\lambda_z}}\exp\left[-\frac{\beta\lambda_x(x-\bar{x}_0)^2}{2\lambda_z}\right]; \qquad \bar{x}_0 = \frac{\Delta G_0 + \lambda_0}{\sqrt{2\lambda_x}} \qquad \text{(II.11.20)}$$

$$K_{dE}(x) = \frac{\beta E_a}{\tau_z}\exp\left[-\frac{\beta\lambda_x(x-\bar{x}_0)^2}{2\lambda_z}\right]. \qquad \text{(II.11.21)}$$

As one can see, both of these "constants" have a Gaussian form. However, the limit $\beta\lambda_z \to 0$ in order to get a δ-function sink is not allowed in this situation, because originally, in order to get a constant diffusion coefficient $D(E)=D(E_a)=E_a/\beta\tau_z$, we required that the reorganization energy for the bond-breaking mode be much higher than the thermal energy,

$\lambda_z >> 1/\beta$ .Thus, the above rate "constants" have to be Gaussian, and the effective sink function $\tilde{K}(x)$ has the form

$$\tilde{K}(x) = \frac{K_0\sqrt{\frac{\beta}{4\pi\lambda_z}}}{1 + K_0\tau_z/(E_a\sqrt{4\pi\beta\lambda_z})}\exp\left[-\frac{\beta\lambda_x(x-\bar{x}_0)^2}{2\lambda_z}\right]. \qquad \text{(II.11.22)}$$

It can not be reduced to a delta function but can be treated as a narrow function that permits the decoupling approximation solution, when $\lambda_z/\lambda_x << 1$. Finally, for fast bond-breaking, the reaction rate constant K can be represented as

$$K = K_r^x / (1 + K_r^x / K_d^x) \qquad \text{(II.11.23)}$$

where the equilibrium and diffusion rate constants are calculated for the "narrow" sink function $\tilde{K}(x)$ in Eq. (II.11.22):

$$K_r^x = \int dx\tilde{K}(x)\varphi(x) = \frac{K_0\sqrt{\frac{\beta}{4\pi\lambda_z}}}{1 + K_0\tau_z/(E_a\sqrt{4\pi\beta\lambda_z})}\exp\left[-\frac{\beta(\Delta G_0 + \lambda_0)^2}{4\lambda_0}\right] \qquad \text{(II.11.24a)}$$

$$\frac{1}{K_d^x} = \tau_p^x = \frac{1}{(K_r^x)^2}\int_0^\infty dt\iint dxdx'\tilde{K}(x)G_x(x,x',t)\tilde{K}(x')\varphi(x'). \qquad \text{(II.11.24b)}$$

As one can see from Eq. (II.11.23), the equilibrium rate constant now depends on the fast relaxation time, so it has gained some dynamic features and cannot be obtained from the classic transition state theory.

The diffusion rate constant is given through the effective MFPT to the narrow zone $\tilde{K}(x)$ when the dynamics along the x coordinate start from the Boltzmann distribution. Here, we give the final result for the diffusion rate constant using the Green's functions for high activation barrier given in Eq. (II.10.25):

$$\frac{1}{K_d^x} = \tau_p^x = \tau_x\frac{\lambda_0}{\lambda_x}\sqrt{\frac{4\pi\lambda_0}{\beta(\Delta G_0 + \lambda_0)^2}}\left(1 - \frac{\beta\lambda_z^2}{2\lambda_0}\frac{\Delta G_0 + \lambda_0)^2}{4\lambda_0^2}\right) * \exp\left[\frac{\beta(\Delta G_0 + \lambda_0)^2}{4\lambda_0}(1 + \frac{\lambda_z}{2\lambda_x}\frac{\lambda_z^2 + (\lambda_0 + \lambda_x)2}{4\lambda_0^2})\right] \qquad \text{(II.11.25)}$$

To sum up, for the case of a narrow reaction sink function, i.e. when $\lambda_z/\lambda_x<<1$, and for the reaction controlled by the bond-breaking process ($\tau_x<<\tau_z$), the total rate constant has the form $K = K_r^x K_d^x \Big/ \left(K_r^x + K_d^x\right)$ where K_r and K_d are given in Eqs. (II.11.23) and (II.11.25).

3. Fast polarization.

Above we considered the situation when the energy-diffusion coordinate was characterized by a faster relaxation time than the polarization one. In this Section we consider the reverse situation — the polarization fluctuations are faster then the bond-breaking dynamics. In this case the scheme developed in Section 1 has to be applied when x refers to the energy-diffusion coordinate E, and E refers to the polarization coordinate x. Then, the separation in Eq. (II.11.2) has the form $P(x,E,t)=R(x,E)\,Q(E,t)$, and the effective sink function defined by Eq. (II.11.11) becomes

$$\tilde{K}(E) = \tilde{æ}(E) = \frac{K_{rx}(E)}{1 + K_{rx}(E)/K_{dx}(E)}. \qquad \text{(II.11.26)}$$

For further analysis we assume that the τ_x is so fast, that kinetic control, $K_{rx}<<K_{dx}$, along the fast polarization coordinate takes place. Then, according to Eqs. (II.11.12a) and (II.11.17)

$$\tilde{K}(E) = K_{rx}(E) = \frac{K_0}{4\pi\sqrt{\lambda_x E}}\left[e^{-\frac{\beta\lambda_z}{\lambda_x}(\sqrt{E}+\sqrt{\lambda_x/2\lambda_z}\bar{x}_0)^2} + e^{-\frac{\beta\lambda_z}{\lambda_x}(\sqrt{E}-\sqrt{\lambda_x/2\lambda_z}\bar{x}_0)^2} \right].$$

The effective sink function is the sum of two Gaussians with different shifts. The situation simplifies considerably when the polarization reorganization energy is small, $\lambda_x/\lambda_z<<1$.:

$$\tilde{K}(E) = \frac{K_0}{\sqrt{2\pi\beta\lambda_z}}\delta(E - E_a) \qquad \text{(II.11.27)}$$

with

$$E_a = \frac{x_a^2}{2} = \frac{(\Delta G_0 + \lambda_z)^2}{4\lambda_z}.$$

The analog of Eq. (II.11.6) for the energy-diffusion coordinate has the form

$$\partial Q(E,t)/\partial t = L(E)Q(E,t) - \tilde{K}(E)Q(E,t). \qquad \text{(II.11.28)}$$

For the sink function of Eq. (II.11.27) the reaction rate constant can be obtained immediately

$$K = K_r^E K_d^E/(K_r^E + K_d^E), \qquad K_r^E = K_0\sqrt{\frac{\beta}{4\pi\lambda_z}}\exp[-\beta E_a]$$
$$K_d^E = \frac{\beta E_a}{\tau_z}\exp[-\beta E_a] \qquad \text{(II.11.29)}$$

where $E_a = (\Delta G_0 + \lambda_z)^2 / 4\lambda_z$. The above diffusion rate constant precisely corresponds to the Kramers result for energy diffusion.

At this point it is interesting to compare two possible mechanisms for the bond-breaking, energy diffusion and overdamped diffusion. All the difference in the rate constants describing these two different mechanisms is due to the pre-exponential factor in the dynamic rate constant. For overdamped motion, the analog of K_d presented in Eq. (II.11.29) is (see Eq. (I.5.17)):

$$K_d = \frac{V'(z^*)}{\tau_z^{OD}}\sqrt{\frac{\beta}{4\pi}}\exp[-\beta V(z^*)]$$

for a general potential $V(z)$, where z^* is the point of transition and τ_z^{OD} is the overdamped relaxation time. For the harmonic oscillator potential with the transition taking place at the point corresponding to energy E_a, the above rate constant is given by Eq. (I.7.12)

$$K_d = \frac{1}{\tau_z^{OD}}\sqrt{\frac{\beta E_a}{2\pi}}\exp[-\beta E_a] \qquad \text{(II.11.30)}$$

Of course, the relaxation time τ_z^{OD} now has a completely different physical meaning, in that it is now proportional to the friction γ, but its value still could be comparable with $\tau_z = 1/\gamma$ for the energy-diffusion mechanism. As one can see from Eq. (II.11.30), the dependence of the pre-exponential factor upon the activation energy changes from the linear for the energy-diffusion mechanism to a slower square-root one for the overdamped motion.

To summarize, the scheme elaborated here presumes that the relaxation times for the x and E coordinates are on very different scales. According to this scheme, after the reaction has started, the faster motion along one of the coordinates (with shorter relaxation time) shapes the "conditions" of the ensuing reaction. So, by some short time, the fast relaxation equilibrates the distribution along its own coordinate in such a way that it forms a sink through which the population of the slow coordinate decays and yields the product. The rate of this reaction is controlled exclusively by the slower relaxation time.

CHAPTER XII. GENERAL ANALYSIS OF THE CONCERTED BBET THEORY

1. Energy diffusion mechanism and comparison with other BBET theories

In this Chapter we analyze the rate constant for the BBET concerted reaction taking place on a 2D potential surface, with polarization fluctuations as one coordinate and the bond-breaking process as the other. We have assumed that the reaction is irreversible and occurs through a high activation barrier. As we discussed in Chapter VIII two mechanisms are possible for motion of the reactive particles along the bond-breaking coordinate. The first one is the overdamped diffusion motion (OD mechanism) that was discussed previously, see Ch. VII, Sec.2.2 and Ref. [30]. The other, energy-diffusion mechanism (ED), was the subject of preliminary discussion in the same paper and now is considered in detail here. We now discuss the general results for the ED mechanism in the 2D BBET problem, and compare them to the results previously obtained for the ED and OD mechanisms [30].

The general result for the rate constant for the OD 2D irreversible reaction in the case of high activation barrier can be represented as $K = K_r K_d^{OD} \Big/ \left(K_r + K_d^{OD}\right)$ where K_r is the same as in Eq. (II.10.23) and

$$K_d^{OD} = \frac{1}{\tau_{OD}} \sqrt{\frac{(\Delta G_0 + \lambda_0)^2}{8\pi\lambda_0}} \exp[-\frac{\beta(\Delta G_0 + \lambda_0)^2}{4\lambda_0}] \qquad \text{(II.12.1)}$$

with the 2D relaxation time given as (see also Eq. (I.7.34))

$$\frac{1}{\tau_{OD}} = \frac{\lambda_x}{\lambda_0 \tau_x} + \frac{\lambda_z}{\lambda_0 \tau_z^{OD}}. \qquad \text{(II.12.2)}$$

Here, τ_z^{OD} is the relaxation time for overdamped diffusion motion along the bond-breaking coordinate, $\tau_z^{OD} = 1/(\beta D_z) \sim \gamma$.

As one can see, the form of the total rate constant K for the OD case is exactly the same as for the ED 2D one given in Eq. (II.10.20). Naturally, because we are dealing with two different dynamic mechanisms, the only difference we can observe lies in the dynamic

(diffusion) rate constants. Therefore, in our following discussion, we will not take into account the equilibrium rate constant K_r because it is well defined, and is not affected by changes in the BBET dynamics. All our attention in the this Chapter will be devoted to the dynamic rate constant that exhibits a very complex behavior.

The results obtained before [30] for the ED mechanism for a 2D ED BBET reaction were based on the transformation of energy-diffusion operator in Eq. (II.10.3) using the substitution $E=e^2/2$ along with some further simplifications:

$$L(E)=\frac{1}{\beta\tau_z}\frac{\partial}{\partial E}E(\frac{\partial}{\partial E}+\beta)\rightarrow L(e)=\frac{1}{\beta\tau_z}\frac{1}{e}\frac{\partial}{\partial e}e(\frac{\partial}{\partial e}+\beta)\approx\frac{1}{\beta\tau_z^E}\frac{\partial}{\partial e}(\frac{\partial}{\partial e}+\beta) \quad \text{(II.12.3)}$$

where $\tau_z^E=\tau_z/\sqrt{2\pi\beta E_a}$, $\tau_z=1/\gamma$ and $E_a=\frac{\lambda_z}{4}\left(\frac{\Delta G_0+\lambda_0}{\lambda_0}\right)^2$.

This "harmonic-like" transformation gave a result for K_d^{ED} very similar to the one given by Eq. (II.12.1):

$$K_d^{ED}=\frac{1}{\tau_{ED}}\sqrt{\frac{(\Delta G_0+\lambda_0)^2}{8\pi\lambda_0}}\exp\left[-\frac{\beta(\Delta G_0+\lambda_0)^2}{4\lambda_0}\right] \quad \text{(II.12.4)}$$

with the only difference, that τ_{ED} now is defined through a different bond-breaking relaxation time $\tau_z^E=\tau_z/\sqrt{2\pi\beta E_a}\sim 1/\gamma$.

$$\frac{1}{\tau_{ED}}=\frac{\lambda_x}{\lambda_0\tau_x}+\frac{\lambda_z}{\lambda_0\tau_z^E}. \quad \text{(II.12.5)}$$

There are of course dangers in changing the differential operator $L(e)$ into the harmonic form as in Eq. (II.12.3). However, the final operator $L(e)=\left(1/\beta\tau_z^E\right)\partial/\partial e(\partial/\partial e+\beta))$ reproduces Kramers' result (II.11.21) for the one dimensional energy diffusion process. Nevertheless, the legitimacy of using it in the 2D problem is not clear. Therefore, we will also compare the result given in Eq. (II.12.4) with the one obtained in the theory of concerted BBET and with that given by Eq. (II.10.27).

We will also compare the results obtained by numerical solution of Eq. (II.10.27) with those of the previous Chapter obtained for widely different values of the two

relaxation times, and where we also required that the faster part of the reaction was under kinetic control. As the result, the final rate constant K_d was determined through the slow coordinate, so that the long relaxation time controlled the dynamic rate (see Eq. (II.11.25) for $\tau_z << \tau_x$ and Eq. (II.11.29) for $\tau_x << \tau_z$). The discussion presented in this Chapter acts as a compliment to that of Ch. XI , and completes the description of the concerted 2D ED BBET reactions. The total, combined picture of the BBET reaction as a two dimensional process will be given later in Section 2 of this Chapter.

As we were not able to calculate dynamic rate constant of Eq. (II.10.27) analytically, we used a numerical integration procedure to compare it with K_d^{OD} and K_d^{ED}. First of all, let us consider a situation when no heat is emitted or absorbed by the system during the reaction, i.e. $\Delta G_0=0$. Then, in terms of different ratios for the reorganization energies λ_x and λ_z, we can investigate how the change in relaxation times affects the dynamic rate constants (see Fig. 11a,b,c). Fig.11 presents the logarithmic dependence of the pre exponential factors $\chi\tau_x$ (in units of the polarization relaxation time τ_x) for the dynamic rate constants $K_d = \chi \exp\left[-\beta(\Delta G_0 + \lambda_0)^2 /(4\lambda_0)\right]$ (or K_d^{OD}, or K_d^{ED}), on the ratio of the relaxation times, $\log(\tau_z/\tau_x)$ (or $\log(\tau_z/\tau_x^{OD})$, or $\log(\tau_z/\tau_x^{ED})$ respectively).

It is easy to see from the analytical expressions for K_d^{ED} and K_d^{OD} (see Eqs. (II.12.1) and (II.12.4)), that the 2D relaxation time is controlled by the shorter of the times, τ_x. and τ_z. So, in Figs. 11a,b,c we can call the area where $\log(\tau_x/\tau_z)<0$ the polarization control region and the area where $\log(\tau_x/\tau_z) >0$ the energy-diffusion control region.

It is important to note that this behavior of the 2D rate constant K_d for separation of the fast and slow modes is just opposite to the one presented in Chapter XI. Here, the shorter (faster) relaxation time controls the dynamic 2D rate (as we will see further in this Section), whereas in Chapter XI the slower relaxation time determined the rate. This is not a contradiction but the revealment of different features of the complicated 2D process at

different circumstances. The complete picture given in the next Section will clarify the situation.

Here we analyze the behavior of the rate constant K_d for three sets of the reorganization energies: i) $\lambda_x<\lambda_z$ (λ_x=1 k_BT, λ_z=20 k_BT, see Fig.11a); ii) $\lambda_x\sim\lambda_z$ ($\lambda_x=\lambda_z$=20 k_BT, see Fig.11b) and iii) $\lambda_x>\lambda_z$ (λ_x=50 k_BT, λ_z=10 k_BT, see Fig.11c). In the last case we satisfy the assumption $\lambda_z>>k_BT$, made in Chapter X.

As one can see from Fig. 11a, in the case of small polarization reorganization energies, λ_x, the region of the energy-diffusion control is very wide. In fact, the energy-diffusion rate

$$K_d = \frac{1}{\tau_z}\beta E_a e^{-\beta E_a} \qquad \text{(II.12.6)}$$

describes the BBET process not only when $\tau_z< \tau_x$, but even when they are comparable, $\tau_z \approx \tau_x$. That can easily be explained by the small contribution of the first member in Eq. (II.12.5) to the 2D relaxation time. In this region K_d and K_d^{ED} coincide, so that the rate K_d^{ED} is a good approximation to expression (II.10.27).

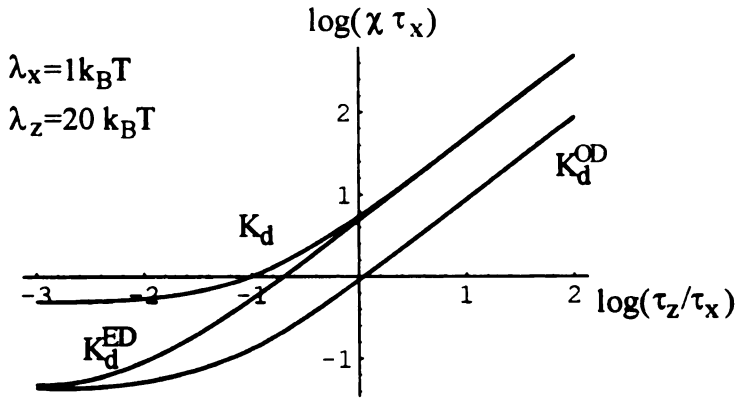

Fig. 11a

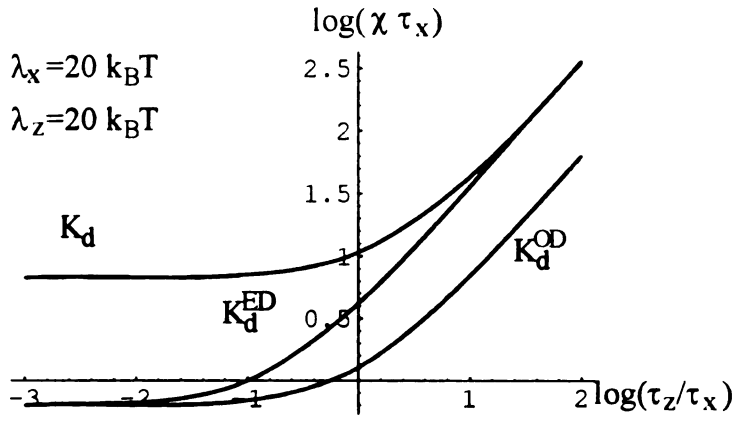

Fig.11b

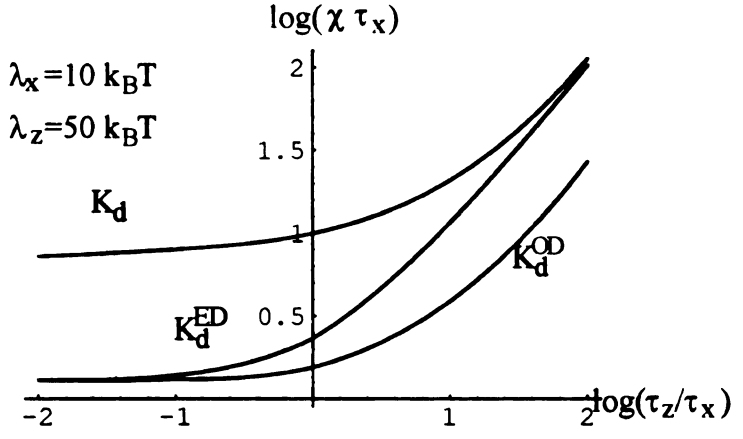

Fig. 11c

Fig. 11. The logarithmic dependence of three dimensionless pre exponential factors ($\chi\ \tau_x$) is given for three dynamic rate constants: 1) 2D BBET rate constant K_d, see Eq. (4.5); 2) BBET rate constant calculated in the "harmonic-like" approximation, see Eq. (6.4); 3) 2D overdamped rate constant given by Eq. (6.1). These dynamic constants are compared for three different sets of the reorganization energies for polarization and for bond-breaking, λ_x and λ_z respectively.

It should be noted that Eq. (II.10.27) can be significantly simplified when $\lambda_x/\lambda_z <$ 1 for an arbitrary ratio of τ_z and τ_x :

$$K_d = \chi \mathrm{e}^{-\frac{\beta(\Delta G_0+\lambda_0)^2}{4\lambda_0}} \qquad \text{(II.12.7a)}$$

with

$$\chi = \frac{\lambda_z}{\lambda_0}\frac{\beta E_a}{\tau_z}\exp\left[\frac{2\lambda_x}{\lambda_0}\left(1+2\frac{\tau_x}{\tau_z}\right)\frac{\beta(\Delta G_0+\lambda_0)}{4\lambda_0}\right]. \qquad \text{(II.12.7b)}$$

When λ_x=0 K_d and K_d^{ED} coincide completely on the whole scale of the ratio τ_z/τ_x and the reaction is controlled by the bond-breaking process with the Kramers rate constant as given in Eq. (II.11.29).

The diffusion rate constant for overdamped motion in this case differs significantly from the one for energy-diffusion:

$$K_d^{OD} = \frac{1}{\tau_z^{OD}}\sqrt{\frac{\beta E_a^K}{2\pi}}e^{-\beta E_a^K}. \qquad \text{(II.12.8)}$$

So, as one can see, the asymptotic behavior of the pre-exponential factors for K_d and K_d^{OD} are ~ λ_z and $\sqrt{\lambda_z}$ respectively.

Now, for $\lambda_x < \lambda_z$ the polarization fluctuations should control the BBET rate for smaller polarization relaxation times ($\tau_x/\tau_z <1$). As we can see from Fig.11a, in this case K_d^{OD} and K_d^{ED} are close to each other and give the same pure polarization control limit when $\tau_x << \tau_z$:

$$K_d^{OD} = K_d^{ED} = \chi(\tau_x/\tau_z \to 0)\mathrm{e}^{-\frac{\beta(\Delta G_0+\lambda_0)^2}{4\lambda_0}} \quad \text{where} \quad \chi(\tau_x/\tau_z \to 0) = \frac{\lambda_x}{\lambda_0\tau_x}\sqrt{\frac{\beta(\Delta G_0+\lambda_0)^2}{8\pi\lambda_0}}$$

(II.12.9)

However, as we can see from the figure, the real behavior in the BBET reaction at τ_x/τ_z <<1 described by K_d in Eq. (II.10.27) doesn't correspond to the pure polarization control situation, as is the case for K_d^{OD} and K_d^{ED}. The BBET rate constant K_d still exhibits some influence of the bond-breaking process on the total reaction rate. Unfortunately, the absence of the analytical solution for K_d doesn't let us analyze the reason for this behavior.

Nevertheless, we can assume, that one of possibilities is that the 2D relaxation time for the BBET dynamic constant of Eq. (II.10.27) has a different structure from the one for K_d^{OD} or K_d^{ED} (see Eqs. (II.12.2) or (II.12.5)).

The situation when $\lambda_x \sim \lambda_z$ is presented in Fig 11b. Eq. (II.10.27) doesn't permit an analytic analysis of this case. However, one can see that the region of the energy-diffusion control ($\tau_x/\tau_z > 1$, $K_d = K_d^{ED}$ as in Eq. (II.12.7)) is smaller, and valid only when τ_z is about an order of magnitude smaller then τ_x. In this case K_d^{ED} is a good approximation for K_d only on a small interval. As the ratio τ_x/τ_z decreases, the difference between K_d and K_d^{ED} decreases dramatically and tends to be more then one order, $K_d / K_d^{ED} \sim 10$ for smaller polarization relaxation times, $\tau_x < \tau_z$. So, the estimation of the total rate constant for BBET reaction by K_d^{ED} fails as we go into region of dominating polarization fluctuations.

The case corresponding to the situation when $\lambda_x > \lambda_z$ is depicted on Fig. 11c. As one can see, the energy-diffusion control of the reaction is never present for reasonable ratios τ_x/τ_z and K_d^{ED} doesn't approximate the 2D ED BBET rate K_d. When the polarization reorganization energy is much larger then the bond breaking one, $\lambda_z << \lambda_x$, and the relaxation times are comparable, in other words, when in addition to the requirement $\nu << 1$ ($\nu = \lambda_z/\lambda_x$), the inequality $\nu\,\alpha << 1$ ($\alpha = \tau_z/\tau_x$) is valid, we obtain an asymptotic behavior of the rate constant in Eq. (II.10.27):

$$K_d = \chi \exp\left[-\frac{\beta(\Delta G_0 + \lambda_0)^2}{4\lambda_0}\right]$$

$$\text{where} \quad \chi = \frac{\lambda_x}{\lambda_0 \tau_x}\sqrt{\frac{\beta\lambda_x(\Delta G_0 + \lambda_0)^2(2+\nu\alpha)}{2\pi\lambda_0^2}}F\left(\frac{1}{2},\frac{1}{2},1,\frac{2}{2+\nu\alpha}\right) * \exp\left[-\frac{\beta\nu(\Delta G_0 + \lambda_0)^2}{4\lambda_0} + \frac{\beta\nu\alpha E_a}{4}\right] \qquad \text{(II.12.10)}$$

$$\sim \frac{1}{\tau_x}\sqrt{\frac{\pi\beta(\Delta G_0 + \lambda_x)^2}{\lambda_x}}\ln\frac{32}{\nu\alpha}$$

From Fig. 12 it is clear that approximation in Eq. (II.12.10) to the constant K_d works for the ratios $\tau_z/\tau_x<1$. Also, because the picture shows the dependence of $(\chi\ \tau_x)$ on the ratio of the relaxation times, we can point out that both K_d^{OD} and K_d^{ED} tend to a constant value when τ_x is small and control the reaction (see Eq. (II.12.9)). The 2D ED BBET rate K_d for these conditions decreases logarithmically, as it is given by the asymptotic law in Eq. (II.12.10).

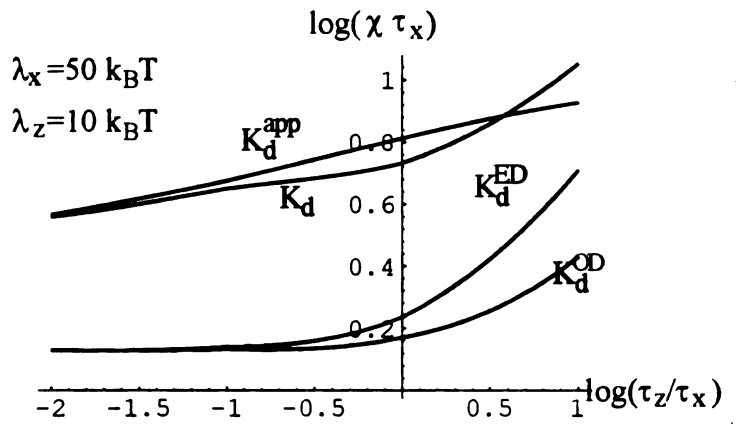

Fig. 12. The logarithmic dependence of the dimensionless pre-exponential factors $(\chi\ \tau_x)$ for the 2D BBET rate constant K_d in comparison with the approximation K_d^{app} of Eq. (II.12.10) when $\lambda_x>>\lambda_z$. The other dynamic constants, K_d^{ED} and K_d^{OD}, are also depicted.

2. Concluding remarks on the energy diffusion in BBET reactions

Thus, being intrinsically multidimensional, the BBET reactions exhibit quite complex behavior. Two relaxation times, τ_x and τ_z, provide different contributions to the dynamic part of the reaction rate constant. When both of these times are comparable, then the total rate constant has the form $K=K_r K_d/(K_r+K_d)$ where K_r and K_d are the chemical transformation and diffusion rate constants given by Eqs. (II.10.23) and (II.10.27), respectively. The behavior of the diffusion rate constant K_d is shown in Figs 11 and 12.

When one time is faster then the other, then the picture of the BBET process becomes more involved. An apparent contradiction was found between the results of Chapter XI, where the slow relaxation time controls K_d, and Section I of the present Chapter, where the fast relaxation time controls K_d. The following considerations will resolve the apparent contradiction. Let us assume that we have two coordinates, x and y. To be specific, consider the relaxation along x as fast, characterized by τ_x^{fast}, and along y as slow, characterized by τ_y^{slow}. Now, we should emphasize that in this article we have calculated the generalized probability $æ = \left[\int_0^\infty dt P_e(t)\right]^{-1}$. $P_e(t)$ is the survival probability in the reaction that, for high activation barrier reactions, coincides with the asymptotic rate constant $K = -d\ln P_e(t)/dt$. Thus, we shall focus on æ

If $\tau_x^{fast} << \tau_y^{slow}$ so these dynamics take place on very different time scales, we can roughly divide the whole 2D process into two stages. In the first stage the τ_x^{fast} dynamics is important and the y-dynamics is so slow that it can be treated as static. As discussed in Chapter XI, the fast dynamics at this stage equilibrates the distribution along its coordinate by some time τ_e, which is still short compared with τ_y^{slow}. The second stage takes place after the fast coordinate has been equilibrated and the slow relaxation time τ_y^{slow} will control the reaction rate.

Making use of this assumption suggests that we may split the total generalized probability as $æ = æ_1 + æ_2$ in order to describe these two stages separately. $æ_1$ should be calculated when the slow mode is taken as static, i.e. the Green's function for it is just a δ-function $G(y,y',t) = \delta(y-y')$ and the dynamics is described only by $G(x,x',t)$. In the second stage the fast coordinate has equilibrated, so that $G(x,x',t)=\varphi(x)$ and $G(y,y',t)$ defines the rate. It is straightforward to apply the scheme described in Chapter XI to both of these stages. We again assume that the transitions take place along the line on the surface: $K(x,y)=K_0\delta(x_0(x-x^*)-y_0(y-y^*))$ where (x^*, y^*) are the coordinates of the transition state point (see Eq. (II.9.7a) or Ref.[30]). Then,

$$æ_1 = \frac{K_0}{x_0}\left[\int dy \frac{\varphi_y(y)\left[1+\frac{K_0}{x_0}\overline{G}_x\left(\frac{x^* - y_0(y-y^*)}{x_0}, \frac{x^* - y_0(y-y^*)}{x_0}\right)\right]}{\varphi_x\left(\frac{x^* - y_0(y-y^*)}{x_0}\right)}\right]^{-1} \qquad \text{(II.12.11a)}$$

$$æ_2 = K_r \Big/ \left(1+\frac{K_r}{K_d^{slow}}\right), \qquad K_d^{slow} = \frac{\varphi_y(y^*)}{\overline{G}_y(y^*, y^*)} \qquad \text{(II.12.11b)}$$

where φ_x and φ_y are the Boltzmann distributions for the x and y coordinates, K_r is given in Eq. (II.10.23) and $\overline{G}_x$ and $\overline{G}_y$ are defined in Eq. (C1).

The analysis of the above expression for $æ_1$ and $æ_2$ reconciles the two views presented in this Chapter of the whole BBET process, when one relaxation time is much shorter then the other. In particular, if the sink strength K_0 is small compared with the diffusive rate in the first stage, as controlled by $1/\tau_x^{fast}$, then $æ_1$ is negligibly small compared to $æ_2$ and the process becomes a one-dimensional reaction diffusion process along the y coordinate. This case leads to the result given in Eq. (II.11.23):

$$1/æ = 1/æ_2 = 1/K_r + 1/K_d^y \quad \text{where} \quad 1/K_d^y \sim \tau_y^{slow} \qquad \text{(II.12.12)}$$

The dynamic part of the rate expression is controlled by the slow relaxation time τ_y^{slow}. This situation corresponds to the picture presented in Chapter XI.

However, if kinetic control does *not* apply during the first stage, as is favored by a strong reactive sink K_0 relative to $1/\tau_x^{fast}$, then $æ_1 \sim 1/\tau_x^{fast}$ and $æ_1 >> æ_2$. So the total rate constant is defined mostly during the first stage ($æ_2$ is just a small correction) and is controlled by τ_x^{fast}. The behavior of the rate constant for this case is described above in this Chapter through the 2D K_d expression.

We conclude with a few remarks regarding the assumptions made in this work. First, we considered an irreversible reaction such that after the reactive particles have left the potential well they escape out of the reaction region. This assumption is quite reasonable, taking into account that the product surface is dissociative, and that the escaping particles undergo three-dimensional motion obeying bimolecular kinetics. The

next two assumptions are more severe. In our theory we assumed that the bond-breaking and solvent polarization coordinates are independent. This idealization may be questioned. It would be natural to think that the solvation energy depends on the bond excursion, as the strength of the coupling between a solvent dipole and the charge distribution of the reacting particle are affected by the bond excursion. Lastly, we only consider high activation barrier reactions. This restriction permitted us to make important simplifications in the reaction model. The first one concerned the energy-diffusion operator that originally had an energy-dependent diffusion constant $D(E)$ (see Eq. (II.10.3)). For the high activation barrier reactions it can be taken as a constant. Secondly, high activation barrier Green's functions are very straightforward to work with. Finally, the definition of the rate constant for high activation barrier reactions coincides with the definition of the generalized probability, as in Eq. (II.10.10).

CHAPTER XIII. QUANTUM MODE IN BOND-BREAKING ELECTRON TRANSFER REACTIONS

1. General remarks and structure of the potential surfaces

In the previous two Chapters we considered the situation when the transformations along the bond-breaking coordinate were described classically, i.e. classical dynamics and interactions with solvent molecules produced the dissociation. This picture is legitimate when the bond frequency is much smaller or comparable with the thermal frequency of collisions of solvent molecules, which for room temperatures is about 200 cm^{-1}. If the bond frequency is much higher, then a classical treatment of the bond-breaking can not be applied to the process. As an example, the methyl halides discussed in Refs. [29, 63, 64] have bond frequencies around 600 cm^{-1}, which is sufficiently high that the classical dynamics for the bond-breaking coordinate may be questioned. Nevertheless, the ET part of the reaction can still be described by the overdamped changes in solvent polarization. Thus, we have to incorporate the quantum nature of one coordinate into the classical treatment of the other. This type of approach is well known and has been developed to introduce high frequency inner-sphere vibrations into the outer-sphere ET reactions. First, Jortner and Bixon [77] introduced a simple model in order to involve the quantum mode into ET dynamics. Following their work Barbara and coworkers [60, 78] used this model to interpret experimental data, in particular, to address the issue why rates could be found that are larger then possible for standard solvent- controlled ET.

In principle, the above situation corresponds to the limit of zero friction in the Kramers' energy diffusion treatment of the BB coordinate. If the quantum dissociation of the bond takes place in the concerted BBET, there is no transition from one vibrational level to another inside the initial and final Morse potential wells. In the classical regime, these transitions are initiated by collisions with solvent molecules. So, it is stated that the

collisions provide the friction which causes the system to overcome the reactive barrier and yield the products. Now the frequency of the bond vibrations, ω_b is so high, that these collisions are ineffective and can not supply enough energy to promote the population of the bond-breaking coordinate from the lower vibration levels onto the activation barrier. Thus, the dissociation of the bond takes place by means of tunneling. However, we should remember, that the low-frequency solvent polarization mode has to respond to all changes in the bond structure.

Hence, it is not difficult to find the place of BBET with a quantum BB mode in the total 2D picture of the BBET reactions which is our designation in the present Part of the dissertation. From the previous Chapter we learned that the BBET reaction can be described as a 2D process with two dynamic coordinates: the energy diffusion BB and the polarization fluctuation ET coordinates with the relaxation times τ_E and τ_x respectively. We also found out that when one relaxation time is much faster (shorter) then the other, the reaction dynamics may be reduced to a 1D process which is controlled by either the fast or the slow relaxation time. Which time controls the dynamics depends strongly on the relation between the fast time and the speed of the non-adiabatic transitions in the reaction region given by the non-adiabatic rate constant K_r.

To emerge from the energy-diffusion to the quantum mechanism of the bond-breaking we can put $\tau_E \sim \gamma \to 0$ where γ is the friction. This immediately provides $\tau_E << \tau_x$. Then, if the non-adiabatic transitions are slow compared with τ_E, then the population along the BB coordinate is always at equilibrium and all dynamical effects are provided by the slow solvent polarization relaxation, τ_x . This all have been discussed in Ch. XI, Sec. 1,2. However, there we assumed that the BB coordinate supplies only one potential surface for polarization changes for each reactants and products. This might not be the case when the friction is truly zero and instead of the classical treatment we have to use the quantum approach. In this case, the correct view on the BBET with quantum mode demands a slightly different picture, which we are going to consider here.

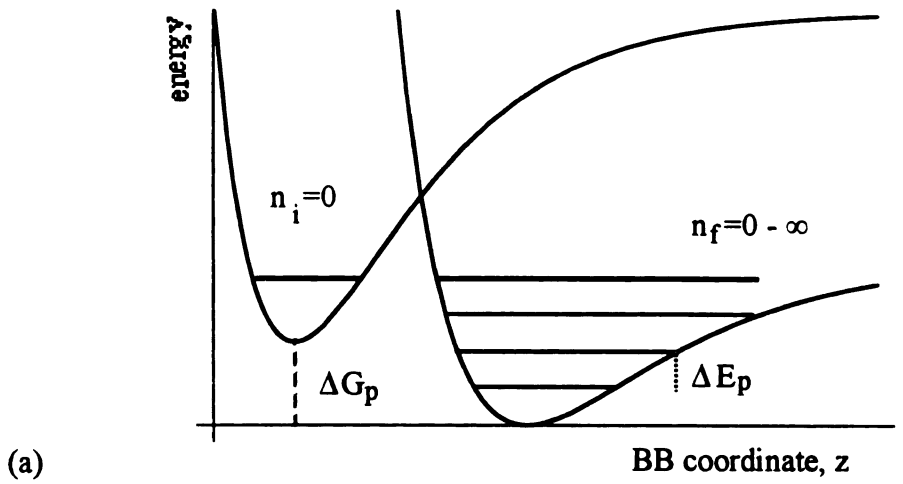

(a)

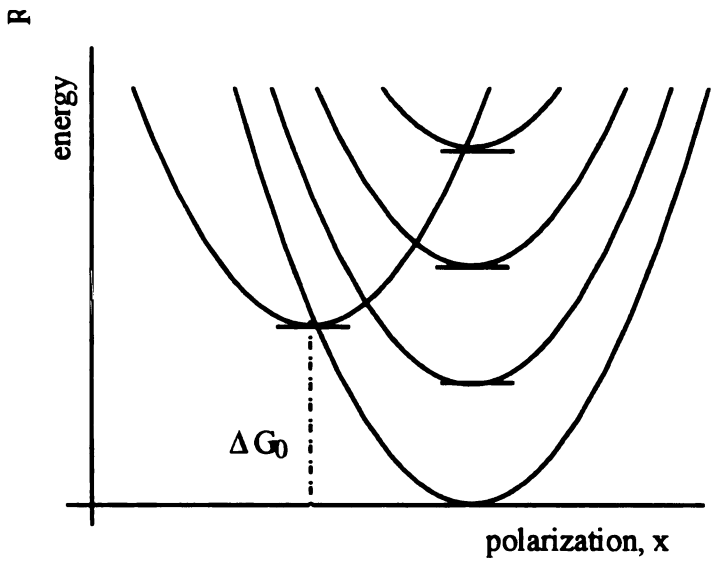

Fig. 13. Schematic potential energy surfaces for the quantum mode in BBET reactions. (a) The high frequency vibration levels in the initial and final state Morse potentials. (b) Each vibrational state of the reactant (R) and product (P) is characterized by a distinct polarization potential surface. The physical situation corresponds to an exothermic reaction ($\Delta G_0<0$).

To proceed farther, we invoke the central assumption made in Ch. IX: the coupling between the bond-breaking and electron transfer coordinates is negligible, so the coordinates are independent and the total potentials are regarded simply as an addition of the surfaces for two individual processes. Figure 13 provides a schematic view of the solvent polarization potential surfaces corresponding to the distinct vibrational states of the bond breaking coordinate. For high-frequency vibrational modes of the bond one can assume that $k_BT<<\hbar\omega_b$, so that intramolecular vibrational excitations of the reactants RX are negligible. The ET process, which now involves only overdamped polarization changes, is described now in terms of a superposition of parallel channels $RX(n_i=0)$ -> $RX^{\bullet -}(n_f)$ onto the vibrational levels n_f of the final state. Here we consider transitions only from the ground vibration level in the initial state ($n_i=0$) since it is the most populated level and the population decay from it is supposed to give the greatest contribution.. So, instead of having one initial and one final state for polarization fluctuations, we have multiple states, each corresponds to a particular vibrational level of the quantum mode, as depicted on Fig. 13.

Modification of the energetic parameters for different final states $RX^{\bullet -}(n_f)$ is straightforward. For the $n_i=0$ -> n ET process (for simplicity we will use $n=n_f$), the energy gap is

$$\Delta G_n = \Delta G_0 - n\hbar\omega_b. \qquad \text{(II.13.1)}$$

Thus, we have the following set of potentials which will be responsible for the reaction changes in the system:

$$\begin{aligned} V_R &= x^2 / 2 \\ V_{Pn} &= (x - x_0)^2 / 2 + \Delta G_n \end{aligned} \qquad \text{(II.13.2)}$$

where $\lambda_x=x_0^2/2$ is the reorganization energy of the solvent.

As we consider irreversible reaction, the reaction kinetics will be formed by the decay of the ground vibrational state population of the reactant, RX through the multiple sinks onto the set of vibrational states of the product, $RX^{\bullet -}$. These transitions are provided

by the coupling of the solvent polarization surfaces in Eqs. (II.13.2), $2\pi V_{RP}^2/\hbar$ as well as by the overlap between the bond vibrational quantum states which is described by the Franck - Condon factors [77]

$$|\langle 0|n\rangle|^2 = (S^n/n!)\exp(-S), \quad \text{where} \quad S = D_e/\hbar\omega_b \tag{II.13.3}$$

where D_e is the reorganization energy (the dissociation energy) of the quantum, bond-breaking mode.

Thus, the position-dependent sink function, *W(x)* can be expressed as a sum over all channels involving the transitions from the ground state of RX to the all exited levels of final state vibrational manifold of the quantized vibrational degree of freedom:

$$W(x) = \frac{2\pi V_{RP}^2}{\hbar}\sum_n |\langle 0|n\rangle|^2 \delta\left(V_{Pn}(x) - V_R(x)\right). \tag{II.13.4}$$

Or, we can define a partial sink $W^{0n}(x)$ located at some point x_n^* which, according to Eqs. (II.13.1)-(II.13.4), is

$$W^{0n}(x) = K_{0n}\delta(x - x_n^*), \quad \text{where} \quad K_{0n} = \frac{2\pi V_{RP}^2}{\hbar\sqrt{2\lambda_x}}|\langle 0|n\rangle|^2, \quad x_n^* = \frac{\Delta G_{0n} + \lambda_x}{\sqrt{2\lambda_x}} \tag{II.13.5}$$

and the total sink function is given as

$$W(x) = \sum_n W^{0n}(x). \tag{II.13.6}$$

Thus, we have defined all geometric parameters of the model for the quantum bond-breaking coordinate in BBET reactions. Now we will consider the dynamical influence of the solvent on the generalized probability of this process.

2. Interference of the reaction channels in BBET with the quantum bond-breaking

Our aim here is to find out the influence of the overdamped dynamics of the ET on the BBET reaction when the bond-breaking coordinate obeys the laws of quantum

mechanics. In the early works investigating the dynamic effects on reactions with multiple channels provided by a quantum mode [77, 79] it was assumed that the reaction channels are independent. This implied that each channel forms its own rate and the total survival probability is just the superposition of all independent reaction rates. Later [14], it was explicitly proved for the case of two δ-functional channels that this is not the case for reactions which are influenced by solvation dynamics. So, the picture for the reaction on a one-dimensional surface with multiple sinks is much more intricate then it was assumed at first. In order to develop this model further some numerical simulations [60, 78] were performed to fit experimental data. Here we want to proceed beyond simple numerical simulations and present application of the steady-state Green's function theory to the above mentioned model.

According to Eq. (I.3.10), the survival probability for the reaction on a single PES can be obtained by solution of the steady-state differential equation:

$$\hat{L}(x)\xi(x) - W(x)\xi(x) = -æ f(x)$$

with the operator of motion $\hat{L}(x) = \frac{1}{\beta\tau_x}\frac{\partial}{\partial x}\left(\frac{\partial}{\partial x} + \beta\frac{dV_R}{dx}\right)$ along the potential $V_R(x)$,where τ_x is the average relaxation time, and the sink function is defined in Eq. (II.13.6). For the polarization fluctuations in Debye solvents τ_x should be taken as the longitudinal relaxation time, τ_L. However, there are some other arguments in favor of different definitions of the relaxation time which are supposed to improve the description of the electronic relaxation in solvents [78].

Taking into account the δ functional form of the sink function, Eq. (II.13.5), the integral formulation (see Chapter IV) of the problem should be more profitable:

$$\xi(x) = \varphi(x) - \int \tilde{G}(x,x')W(x')\xi(x') \qquad \text{(II.13.7)}$$

where $\varphi(x) = N\exp(-\beta V_R(x))$ is the Boltzmann distribution inside the potential $V_R(x)$ and $\tilde{G}(x,x')$is the steady-state Green's function for an arbitrary initial distribution $f(x)$ defined by the equation

$$\hat{L}(x)\tilde{G}(x,x') = -\delta(x-x') + f(x). \qquad \text{(II.13.8)}$$

The generalized probability in the reaction is given as

$$æ = \int W(x)\xi(x)dx. \qquad \text{(II.13.9)}$$

Equations (II.13.7)-(II.13.9) are the one-dimensional analogs of Eqs. (I.4.13), (I.4.12) and (I.3.12) respectively.

For the sink function as in Eq. (II.13.6), from Eqs. (II.13.7) and (II.13.9) we derive:

$$\xi(x_l) = \varphi(x_l) - \sum_n K_{0n}\tilde{G}(x_l, x_n)\xi(x_n) \qquad \text{(II.13.10)}$$

and

$$æ = \sum_n K_{0n}\xi(x_n). \qquad \text{(II.13.11)}$$

It is more convenient to represent the system of Eqs. (II.13.10) and (II.13.11) in a matrix form and obtain the final answer for the generalized probability of BBET with a quantum mode:

$$æ = \vec{K}_0\vec{\xi}, \quad \text{where} \quad \vec{\xi} = (\hat{I} + \hat{F})^{-1}\vec{\varphi} \qquad \text{(II.13.12)}$$

where $\hat{I}$ is the identity matrix and

$$\vec{K}_0 = \begin{bmatrix} K_{01} \\ K_{02} \\ \\ K_{0n} \end{bmatrix}, \qquad \vec{\varphi} = \begin{bmatrix} \varphi(x_{01}) \\ \varphi(x_{02}) \\ \\ \varphi(x_{0n}) \end{bmatrix}, \text{ and } \hat{F} = \begin{bmatrix} K_{01}\tilde{G}_{11} & K_{02}\tilde{G}_{12} & K_{0n}\tilde{G}_{1n} \\ K_{01}\tilde{G}_{21} & K_{02}\tilde{G}_{22} & K_{0n}\tilde{G}_{2n} \\ \\ K_{01}\tilde{G}_{n1} & K_{02}\tilde{G}_{n2} & K_{0n}\tilde{G}_{nn} \end{bmatrix} \qquad \text{(II.13.13)}$$

where $\tilde{G}_{ij} = \tilde{G}(x_i, x_j)$ is the steady-state Green's function defined in Eq. (II.13.8). Note, the initial distribution is included in the steady-state function, so different Green's functions are required for different distributions. For the case of one-dimensional PES these functions are defined in Appendix A, see Eq. (A13).

As the simplest example we consider the case of two channels. Solution of Eq. (II.13.12) with the account of Eq. (II.13.13) gives us the generalized probability of the form:

$$æ = \frac{K_{r1} + K_{r2} + K_{r1}K_{r2}\left(\tilde{G}_{11}/\varphi(x_1) + \tilde{G}_{22}/\varphi(x_2) - \tilde{G}_{12}/\varphi(x_1) - \tilde{G}_{21}/\varphi(x_2)\right)}{1 + K_{r1}\tilde{G}_{11}/\varphi(x_1) + K_{r2}\tilde{G}_{22}/\varphi(x_2) + K_{r1}K_{r2}\left(\tilde{G}_{11}/\varphi(x_1)\tilde{G}_{22}/\varphi(x_2) - \tilde{G}_{12}/\varphi(x_1)\tilde{G}_{21}/\varphi(x_2)\right)}$$

where

$$K_{rn} = K_{0n}\varphi(x_n) = \frac{V_{RP}^2}{\hbar}\sqrt{\frac{\beta\pi}{\lambda_x}}e^{-S}\frac{S^n}{n!}\exp\left(-E_{An}\right), \text{ where } E_{An} = \frac{\beta(\Delta G_{0n} + \lambda_x)^2}{4\lambda_x} \quad \text{(II.13.14a)}$$

is the non-adiabatic rate constant for the n-th channel. As one can see from this example, for reactions taking place on multiple channels, it is impossible to separate the non-adiabatic part of the generalized probability from the dynamical part unless the reaction takes place at high barrier (at all sink). If we take into account the form of the steady-state Green's function for high barrier reactions (Eq. (I.5.10)), we can easily obtain

$$æ = \frac{K_{r1} + K_{r2}}{1 + \tau_p(K_{r1} + K_{r2}\varphi(x_1)/\varphi(x_2))} \approx \frac{K_{r1}}{1 + \tau_p K_{r1}}$$

where τ_p is the MFPT to the sink point of the lowest energy, $\tau_p = \tau_x\frac{\varphi(x_1)}{V'(x_1)}$. So, the final expression shows that only the first sink located at the lowest point contributes into the rate.

In order to observe different limiting cases possible in the reactions under study, let us introduce some "time" of non-adiabatic transitions, $\upsilon^{-1} = \frac{V_{RP}^2}{\hbar}\sqrt{\frac{\beta\pi}{\lambda_x}}$ which is, in fact, the average time of perturbation (non-adiabatic) transitions which take place in the absence of the diffusion influence (the transitions that are normally described by the Golden Rule constant). The stronger is the electronic coupling V_{RP} between the reactant and product surfaces, the shorter is the time of non-adiabatic transitions

It is easy to prove, that if for any i'th sink on the surface the inequality

$$\frac{\upsilon}{|\langle 0|i\rangle|^2} >> \tau_x \quad \text{(II.13.14)}$$

holds, i.e. the diffusion relaxation time is fast compares with the time of the non-adiabatic transitions, the electronic coupling V_{RP} is weak and the kinetic control limit takes place. In other words, $æ = K_r = \vec{K}_0\vec{\varphi} = \sum_n K_{rn}$ where K_{rn} is the non-adiabatic rate constant on the n-

the channel, and the generalized probability, indeed, is a sum of rates from the individual channels as was assumed in by Jortner and Bixon [77]. So the transitions do not disturb the population on the reactive surface significantly. This is the result of perturbation theory over the small parameter of the interstate interaction, υ.

The other limit occurs when inequality (II.13.14) is reversed, hence the electronic coupling V_{RP} is comparatively strong and the non-adiabatic transitions are fast. This is the diffusion control limit and the generalized probability is given as follows:

$$æ = K_d = \vec{e}^{+}\hat{\tilde{G}}^{-1}\vec{\varphi}, \text{ where } \hat{\tilde{G}} = \begin{bmatrix} \tilde{G}_{11} & \cdots & \tilde{G}_{1n} \\ & \ddots & \\ \tilde{G}_{n1} & \cdots & \tilde{G}_{nn} \end{bmatrix}, \qquad \text{(II.13.15)}$$

$\vec{e}$ is the unit vector. For only two channels, the above equation transforms into

$$K_d(n=2) = \frac{\tilde{G}_{11}/\varphi(x_1) + \tilde{G}_{22}/\varphi(x_2) - \tilde{G}_{12}/\varphi(x_1) - \tilde{G}_{21}/\varphi(x_2)}{\tilde{G}_{11}/\varphi(x_1)\cdot\tilde{G}_{22}/\varphi(x_2) - \tilde{G}_{12}/\varphi(x_1)\cdot\tilde{G}_{21}/\varphi(x_{21})}. \qquad \text{(II.13.16)}$$

It is easy to deduce that this rate constant, in general, can not be represented as a sum of diffusion rate constants on the independent channels. This would be possible, however, if all non-diagonal elements of the G-matrix were zeros, i.e. $\tilde{G}_{ij}/\varphi(x_i)$=0. As we will see later, usually this is an unreasonable assumption. It works only in the case of a high activation barrier in the normal regime. In all the other situations the non-diagonal elements differ significantly from zero.

As was obtained in Ch. V, Eq. (I.5.5), the ratio $\tilde{G}_{ii}/\varphi(x_i)$ is the MFPT to the point x_i if start occurred from some initial distribution *f(x)*. This MFPT here will be denoted as $\tau_p(x_i)$. From Eq. (I.5.6) we can conclude that $\tilde{G}_{ii}/\varphi(x_i) - \tilde{G}_{ij}/\varphi(x_i)$ is the MFPT from the point x_j to the point x_i (or $\tau_p(x_j -> x_i)$ in our notation). The other average time which will appear in the diffusion constant is the difference between two MFPTs - $\tau_e(x_i, x_j) = \tau_p(x_i) - \tau_p(x_j -> x_i)$ - which measures how much longer it takes to reach the point x_i if started from a Boltzmann distribution ($\tau_p(x_i)$) and if started from another point, x_j, ($\tau_p(x_j -> x_i)$). Thus, the structure of the diffusion rate constant for two channels given in Eq. (II.13.16) obtains a clear physical interpretation:

$$K_d(n=2)=\frac{\tau_p(x_2->x_1)+\tau_p(x_1->x_2)}{\tau_p(x_1)\cdot\tau_p(x_2)-\tau_e(x_1,x_2)\tau_e(x_2,x_1)}.$$

So, it easy to see, that the channels would be independent if there was no difference between two MFPTs participating in the problem - $\tau_p(x_i)$ and $\tau_p(x_j->x_i)$, which means that the steady-state Green's function should be insensitive to the choice of initial conditions and $\tau_e(x_i,x_j)=0$. As has been shown many times in this dissertation, this happens, indeed, when all decay takes place over a high activation barrier, or, in other words, if *all* sinks are positioned high. This is the only situation were the assumption about independence of the channels is legitimate.

Thus, the rate is controlled not only by the diffusion towards the sink points, but also by the motion between them. One can imagine that the decay on multiple channels produces some "holes" in the population at the points of the sinks. However, these holes are not highly localized, so that the decay at one point disturbs the population near the others and therefore the population at each sink gradually responds to the changes at all the others. Since the joint efficiency of the multiple channels is not a sum of the partial ones, they can not be considered separately. This is why we have to consider the interference between the multiple channels.

For evaluation of the rate constant in Eq. (II.13.12) for BBET reactions with the quantum bond-breaking we will need the steady-state Green's functions for the harmonic oscillator potential $V_R(x)$. We are interested in two different initial distributions - the Boltzmann, $\varphi(x)$ and the δ-functional one located at the bottom of the well, $\delta(x)$. The last distribution was taken since there are a few experimental studies which refer to it as to a probable distribution in photochemical reactions on excited potential surfaces[12, 13, 28]. From Eq. (A13) one can obtain:

(1) for $\varphi(x)$:

$$\tilde{G}(x_i,x_j)=\tau_x\frac{e^{-\beta x_i^2/2}}{\sqrt{2\pi\beta}}\left\{\ln 2+\sqrt{\pi}\left(\int_0^{\sqrt{\beta x_i^2/2}}e^{y^2}(1+erf(y))dy-\int_0^{\sqrt{\beta x_j^2/2}}e^{y^2}(1-erf(y))dy\right)\right.$$
$$\left.-2\sqrt{\pi}\Theta(x_i-x_j)\int_{\sqrt{\beta x_j^2/2}}^{\sqrt{\beta x_i^2/2}}e^{y^2}dy\right\} \qquad \text{(II.13.17a)}$$

(2) for $\delta(x)$:

$$\tilde{G}(x_i,x_j)=\tau_x\frac{e^{-\beta x_i^2/2}}{\sqrt{2\beta}}\left\{2\Theta(x_i)\int_0^{\sqrt{\beta x_i^2/2}}e^{y^2}dy-2\Theta(x_i)\Theta(x_i-x_j)\int_{\sqrt{\beta x_j^2/2}}^{\sqrt{\beta x_i^2/2}}e^{y^2}dy\right.$$
$$\left.-\Theta(x_i-x_j)\int_{\sqrt{\beta x_j^2/2}}^{\sqrt{\beta x_i^2/2}}e^{y^2}(1-erf(y))dy-\int_0^{\sqrt{\beta x_j^2/2}}e^{y^2}(1-erf(y))dy\right\} \qquad \text{(II.13.17b)}$$

We will be interested in three distinctive regimes of the reaction, namely, the normal, activationless and inverted, see Fig. 14 a-c. It is convenient to introduce the ratio of the relaxation time τ_x to the characteristic time of the non-adiabatic transitions υ, $\alpha=\tau_x/\upsilon$. This parameter is supposed to reflect the strength of the electronic coupling V_{RP} compared to the solvent relaxation. Even though we can not separate the non-adiabatic part of the generalized probability from the diffusional part, this parameter will help as to estimate

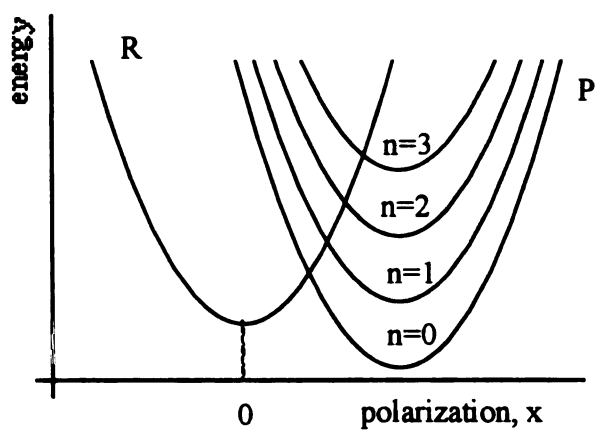

(Fig. 14a)

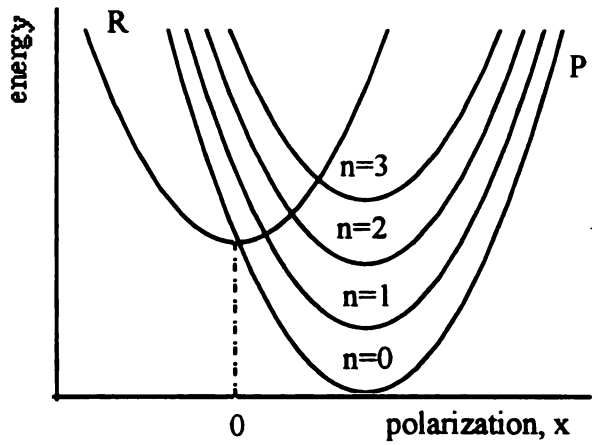

(Fig. 14b)

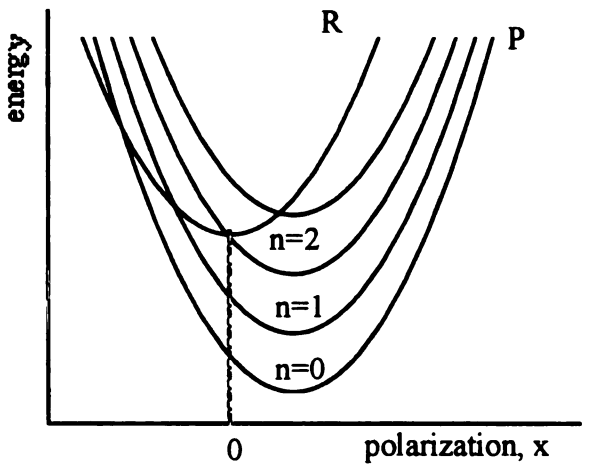

(Fig.14c)

Fig. 14. Schematic of the potential energy surfaces representing the BBET for quantum bond-breaking in three different regimes: (a) normal; (b) activationless; (c) inverted.

which part prevails at the different values of α. Moreover, the matrix $\hat{F}$ in Eqs. (II.13.12), (II.13.13) becomes function of the parameter α.

For our further investigations we will evaluate the dimensionless generalized probability $\overline{æ} = \upsilon \cdot æ$ which can be evaluated from the following expression:

$$\overline{æ} = \upsilon \cdot \vec{K}_0(\hat{I} + \hat{F})\vec{\varphi} \qquad \text{(II.13.18)}$$

If $\alpha<<1$ (or inequality (II.13.14) takes place), the generalized probability æ is supposed to tend to its kinetic control limit, K_r. Otherwise the dynamics along the potential play an important role. For $\alpha>>1$ we should expect the diffusion control limit when the generalized probability is given by Eq. (II.13.15). In this case $K_r>>K_d$. So, these two simple limits will aid us in interpreting the results of calculations of the chemical rates in BBET reactions with the quantum bond-breaking mode.

The exothermicity of the BBET reaction, ΔG_0 and the frequency of the quantum bond-breaking mode, ω_b determine the exothermicities for the set of final polarization states, ΔG_{0n} in Eq. (II.13.1). Combined with the reorganization energy for the x coordinate, λ_x, they define the activation energies E_{An} for the sink points (Eq. (II.13.14a)). Thus, these three parameters assign the energetic geometry of the reaction and hence specify the dynamical behavior. The ratio of the dissociation energy of the bond, D_e to its vibration energy $\hbar\omega_b$ determine the efficiency of tunneling and so specify the non-adiabatic rate constant, see Eqs. (II.13.3) and (II.13.5) (in all our further calculations we will take ω_b=600 $cm^{-1}\approx 3k_BT$ at room temperature, which is the approximate bond frequency in methyl and aryl halides [29]). Therefore, with the parameter α which measures relative relaxation time of the system we have five variables that influence the kinetics in BBET reactions with quantum bond-breaking.

The reaction surfaces for the normal regime are sketched on Fig.14a. We have discussed the case of high activation barrier for this regime earlier, so only low barrier reactions will concern us here. Taking λ_x=1 eV$\approx$40k_BT and ΔG_0 =-0.5 eV$\approx$-20k_BT , which are typical values for the reorganization energy for polarization and exothermicity,

we would get the desired low energy activated reaction (the activation energy of the lowest point is about $2.5k_BT$). First we investigate the behavior of the generalized probability at the two limiting cases. For kinetic control ($\alpha<<1$) depicted on Fig. 15, the rate constant is a sum of the partial non-adiabatic rate constants given by Eq. (II.13.14a). Thus, the more sinks we take into account, the larger is the rate. However as channels go up higher, the partial rates decrease proportionally to the activation factor, $exp(-\beta E_{An})$, which steadily decreases contribution from the higher channels. The other contribution to the non-adiabatic rate constant K_r comes from the Franck-Condon factor. As can be easily seen from Eq. (II.13.3), depending on the value of S the factor has a maximum at some n which means that the n-th vibrational level of the final state has the maximum overlap with the ground vibrational level of the initial state. The smaller is S, the closer this level with the maximum overlap is to the ground vibrational level of the final state.

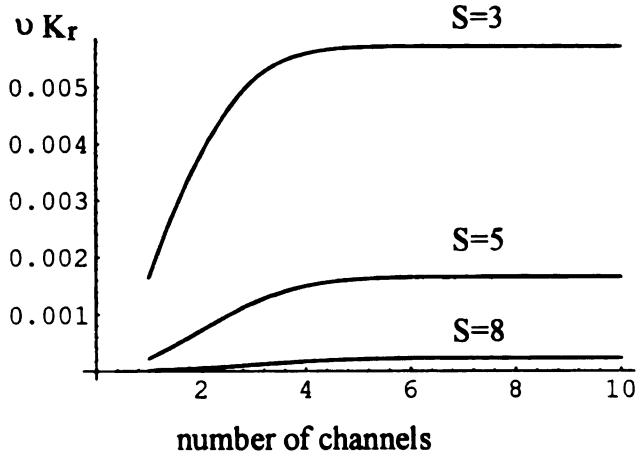

Fig. 15. The dimensionless non-adiabatic rate constant υK_r for the normal regime is evaluated for the following parameters: $\lambda_x = 1eV$ and $\Delta G_0 = -0.5eV$. Three values of the tunneling parameter $S = D_e / \hbar\omega_b$ are used: S=3 ($D_e = 9k_BT$), S=5 ($D_e = 15k_BT$) and S=8 ($D_e = 24k_BT$).

However, in the normal regime these two contributions partially counteract one another and their combination produces the simple picture presented on Fig. 15. for three different values of S. Namely, the smaller is the gap between the final state vibration levels, S, the larger is the rate constant K_r..

In contrast, the diffusion limit ($\alpha >> 1$) produces a rate constant that is not additive (see Eq. (II.13.15)). Calculations show that in the normal regime this rate does not depend upon the number of sinks and is defined, essentially, by the MFPT to the lowest sink point. For the parameters chosen above we evaluated the following: (a) for the Boltzmann initial distribution utilization of the steady-state Green's function in Eq. (II.13.17a) gives $K_d=0.066\ \tau_x$; (b) for the δ-functional initial distribution at the bottom of the potential Eq. (II.13.17b) yields $K_d=0.062\ \tau_x$. The second constant is fractionally smaller then the first one. This is very easy to understand, as the Boltzmann distribution provides some population at all point on the surface before the reaction starts, whereas the particles from the bottom for the δ(x) distribution have to spend some time spreading inside the potential, which makes the MFPT for this case longer and the rate constant smaller.

For the intermediate values of α we have to evaluate the dimensionless generalized probability given by Eq. (II.13.18). Fig. 16a shows two sets of dependencies of the constant $\overline{æ}$ for two values of S for the Boltzmann initial distribution. For the normal regime the difference between the rate constants for the two different initial distributions $\varphi(x)$ and $\delta(x)$ is negligible, so they are indistinguishable on the picture (which is not surprising because the difference between the rate constants in the diffusion control limit for the two distributions is minute). First of all it should be mentioned that in the normal regime the saturation of the rate occurs at a very small number of channels (4-5), so that accounting for a larger number of sinks does not change the chemical rate (influence of the activation factor). Another characteristic feature of the rate for multiple channels is that it increases more (compared with the rate for a single channel, n=1) for the smaller values of

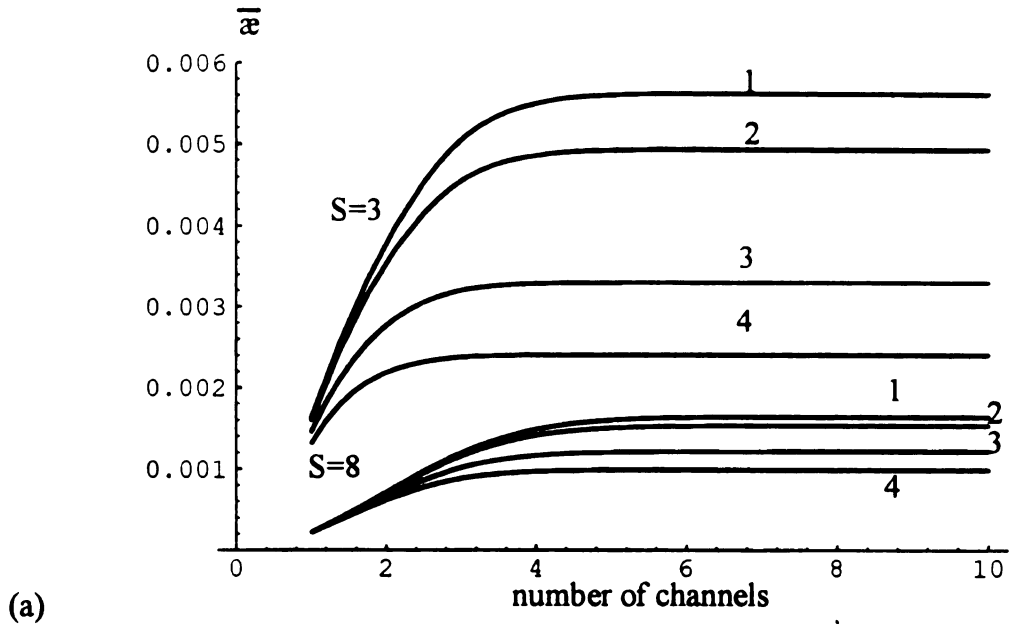

(a)

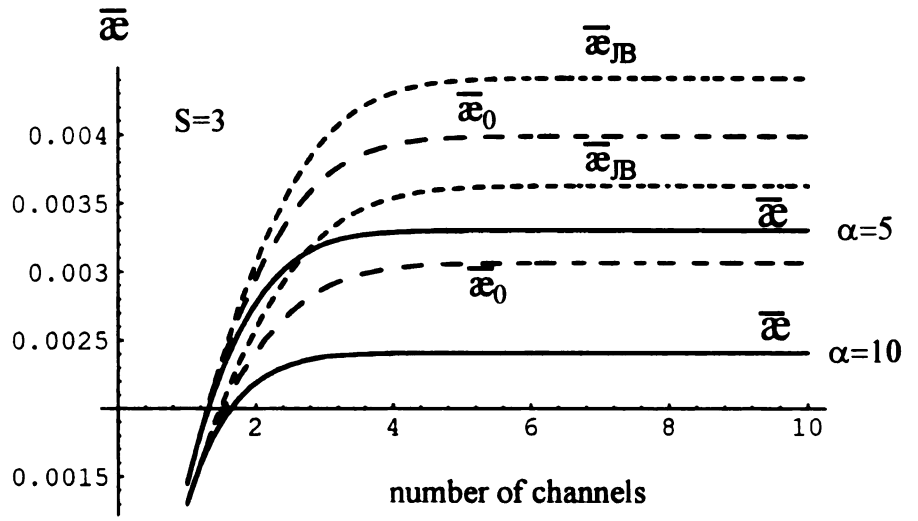

(b)

Fig. 16. Dependencies of the dimensionless rate constant $\bar{æ}$ on the number of sinks are presented for the normal regime at $\lambda_x = 1eV$ and $\Delta G_0 = -0.5eV$. Two values of the tunneling parameter $S = D_e / \hbar\omega_b$ are used: S=3 ($D_e = 9k_BT$) and S=8 ($D_e = 24k_BT$). (a) Comparison of $\bar{æ}$ for different values of α (1 – α=0.1; 2 – α=1; 3 – α=5; 4 – α=10) is made for the two values of the tunneling parameter. (b) The approximate rate constants $\bar{æ}_{JB}$ (short dashes) and $\bar{æ}_0$ (long dashes) from Eq. (II.13.20) are compared with $\bar{æ}$ for S=3 and α=5 and 10.

S and α. The reason is quite simple - we don't observe any boost in the rate for a bare diffusional case, therefore all changes are caused by the influence of the non-adiabatic part as it is the only part which is effected by aggregation of additional channels. Hence, the stronger is the dominance of the non-adiabatic part in the transition rate, the faster is the relative growth of $\bar{æ}$ with the increasing number of channels (up to the saturation limit, of course). As was discussed previously (see also Fig. 15), smaller values of S make the non-adiabatic rate constant larger which causes sharper variations in the dimensionless generalized probability $\bar{æ}$. Finally, a similar effect can be achieved by decreasing α. The smaller is α, the relatively faster is the diffusion relaxation time τ_x compared with the time of non-adiabatic transitions, υ, the closer is the situation to the kinetic control limit.

The reaction model considered here was applied to ET reaction with quantum mode in Ref. [77], where the overall rate constant was considered to be a sum of the rate constants from the independent channels. In other words, the correct generalized probability æ in Eq. (II.13.12) was approximated by the following expression:

$$\frac{1}{æ_{JB}} = \sum_n \frac{1}{æ_n} = \sum_n \left(\frac{1}{K_{rn}} + \frac{1}{K_{dn}} \right) \qquad \text{(II.13.19)}$$

where $æ_n$ is the generalized probability for decay on the n-th sink. This approximation is equivalent to the assumption that the matrix $\hat{F}$ in Eq. (II.13.13) is diagonal, i.e. $\tilde{G}(x_i, x_j) = 0$. The form of the steady-state Green's functions given by Eqs. (II.13.17) suggests that this assumption is highly debatable.

An alternative approximation of the correct generalized probability may be given by another simple formula which separates the non-adiabatic and diffusional rate constants: $æ_0 = K_r K_d / (K_r + K_d)$, where K_d is the correct rate at the diffusion control limit evaluated from Eq. (II.13.15). From Eqs. (II.13.12)-(II.13.13) and the case of two channels considered above it is clear that neither of these approximations are really applicable to the

multi-channel model. However, in order to give a qualitative picture we evaluated the dimensionless constants

$$\bar{æ}_{JB} = \upsilon æ_{JB} \qquad \text{and} \qquad \bar{æ}_0 = \upsilon æ_0 = \frac{\upsilon K_r K_d}{K_r + K_d} \qquad \text{(II.13.20)}$$

which were compared with the correct one for the normal regime (the result is shown on Fig. 16b). It is easy to see, that the difference between the correct and approximated values is quite significant (apart form the case of one sink, n=1, when Eqs. (II.13.20) are both, obviously, exact). The approximate formula for $\bar{æ}_0$ overestimates the correct rate by at least 30%, and approximation with $\bar{æ}_{JB}$ is even worse. Naturally, approximation $\bar{æ}_0$ should work better then $\bar{æ}_{JB}$, since the first one partially takes into account the interaction between individual channels in the form of the diffusion K_d constant from Eq. (II.13.15), whereas the last one neglects it completely. This neglect may resolve either in overestimation (as in Fig. 16b) or in underestimation of the correct rate depending on the contribution of the off-diagonal elements in the matrix $\hat{F}$ from Eq. (II.13.13) into the rate. One can expect that if this discrepancy is significant in the normal regime, it should only increase for the activationless and inverted reactions when the dynamic influence on the rate is stronger.

The energy scheme for the activationless regime for BBET with quantum bond-breaking is depicted on Fig. 14b. Starting with analysis of the two limited regimes, on Fig. 17 we present the behavior of the dimensionless non-adiabatic rate constant which describes the reaction when $\alpha << 1$. As one can see, the general features of its behavior are very similar to the ones for the normal regime except that now the rates are much higher as it should be for activationless processes. Again, one does not need to take very many sink into account, as long as the activation factor $exp(-\beta E_{An})$ rapidly decreases contributions from the activated channels at energies 3 k_BT and higher.

Whereas the behavior of the non-adiabatic rate constants for the normal and activationless regimes are similar, the rate constants for the diffusion control limit ($\alpha >> 1$) are very different. Unlike previously, K_d for the activationless reaction strongly depends upon the choice of the initial distribution. One should observe crucial difference between

diffusional rate constants for $\varphi(x)$ and $\delta(x)$. Because the Boltzmann distribution spreads reactive particles along the whole surface, the diffusional rate constant for K_d can not vary strongly when the sinks approach the bottom of the well (but, of course, it should not be a constant as for normal regime). This is not the case for $\delta(x)$ which provides exceptionally localized concentration of particles at the start of the reaction. So, the first two or three sinks located beside it should deliver an extremely intensive decay whose speed should be significantly higher then the one for the Boltzmann initial distribution. This difference should be somehow reflected in the generalized probability for intermediate values of α.

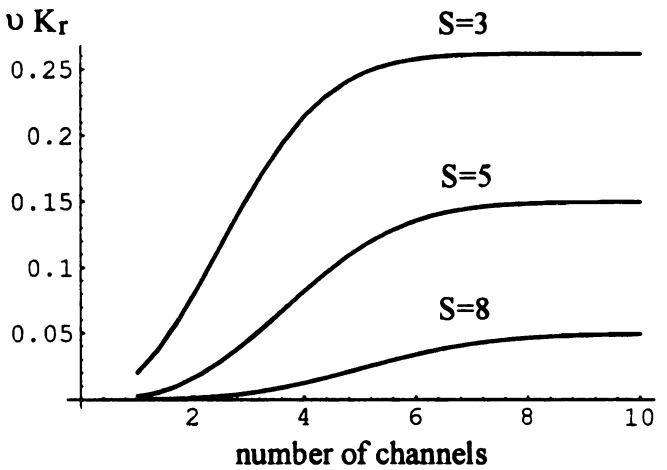

Fig. 17. The dimensionless non-adiabatic rate constant υK_r for the activationless regime is evaluated for $\lambda_x = 1eV = 40k_BT$ and $\Delta G_0 \approx -1.eV = 41k_BT$. Three values of the tunneling parameter $S = D_e / \hbar\omega_b$ are taken the same as for Fig. 15.

When the relaxation time τ_x and the average time of non-adiabatic transitions υ are comparable, evaluation of generalized probability (II.13.12) is necessary. In Fig. 18 we present the result of calculations of the dimensionless constant $\overline{æ}$ for an activationless reaction. The rate constants were evaluated for both Boltzmann and $\delta(x)$ initial distributions for λ_x=1eV=40k_BT, ΔG_0=-41k_BT, S=5 and three different values of α. For the saturation

to take place in the this regime we still only need a few sinks (6-7). So, we can conclude that as for the normal regime, as the barrier for the n-th channel reaches 3-4 k_BT, all higher sinks can be excluded from consideration.

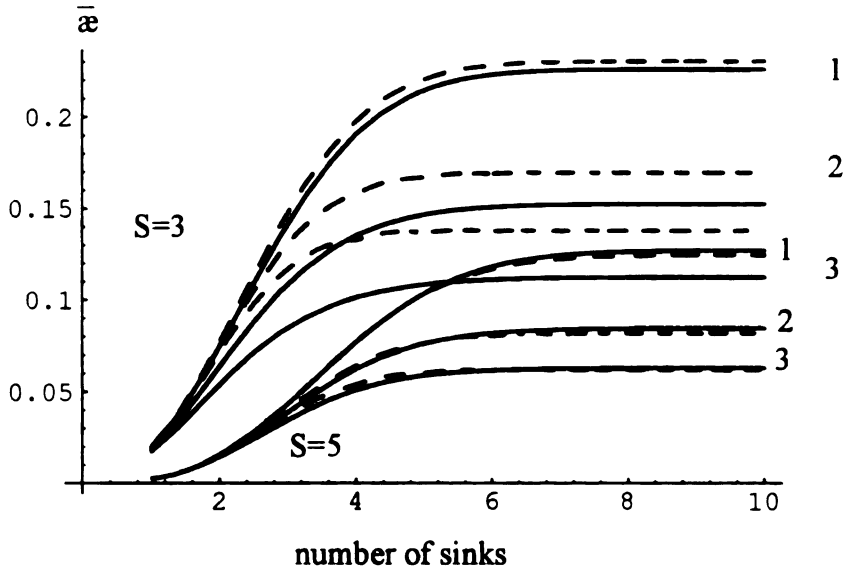

Fig. 18. Dependencies of the dimensionless rate constant $\bar{æ}$ on the number of sinks are presented for the activationless regime for $\lambda_x = 1eV$ and $\Delta G_0 \approx -1eV$. Two values of tunneling parameter $S = D_e / \hbar\omega_b$ are used: S=3 ($D_e = 9k_BT$) and S=5 ($D_e = 15k_BT$). Comparison of $\bar{æ}$ for different values of α (1 – α=1; 2 – α=5; 3 – α=10) is made for the two values of the tunneling parameter. The solid lines correspond to the Boltzmann initial distribution, and the dashed lines present *δ(x)* initial distribution.

As one can see, there is a difference between the two initial distributions. However, for S=5 this difference is insignificant. Only smaller gaps between the vibration levels (S=3) can provide a noticeable difference. The smaller is the spacing between the bond vibrational levels in the final state (the smaller is S), the bigger is the density of the sinks near the bottom of the potential where *δ(x)* is taken at the start, hence the more significant is this difference. This difference rises even more as the value of α increases and, therefore,

the diffusion influence on the rate becomes stronger. Note, that the localized distribution increases the value of the rate constant compared with that of the equilibrium one, which is in accordance with our argument concerning the diffusion control limit for this regime.

The most interesting case of the model under consideration is the inverted regime when the excited vibrational states of the products become significant and the transitions into some of them are always activationless (see Fig. 14c). So, these activationless channels should provide the maximum contribution to the rate as the activation factor for them is minimal. Let us first consider the non-adiabatic rate constant K_r. Fig. 19 shows it for $\lambda_x=40k_BT$, $\Delta G_0=-62k_BT$ and S=3, 5 and 8. As one can see, in contrast with the two previous cases, the biggest value of S provides the largest rate. As was mentioned in the discussion for the normal regime, the Franck-Condon, tunneling factor in the sink functions (see Eq. (II.13.4)) has a maximum at some values of n which depend upon S. So the ground vibration state of the reactants has the maximum overlap with a few exited vibrational levels of the products. Hence, in the inverted regime both the activation and tunneling factors may increase the efficiency of the transitions into the higher vibrational states, whereas previously they worked in the opposite directions and the higher tunneling factor used to be suppressed by the activation one.

Similar consequences of mutually supportive factors can be observed for the generalized probability of reaction in the inverted regime. A typical picture for the dependence of chemical rates on the number of sinks for this scheme is presented in Fig. 20. First of all, the overall growth of the rate for the reaction on multiple channels compared with that of on one sink is about two orders of magnitude. This is an enormous adjustment, which completely changes the total picture of the reaction. Even though the rate in the inverted regime can be slightly smaller then the one for the activationless reaction with all other parameters apart from the exothermicity ΔG_0 being equal (compare Fig. 18 and Fi. 20 for S=3), this decrease is almost insignificant compared with the changes in the exothermicity.

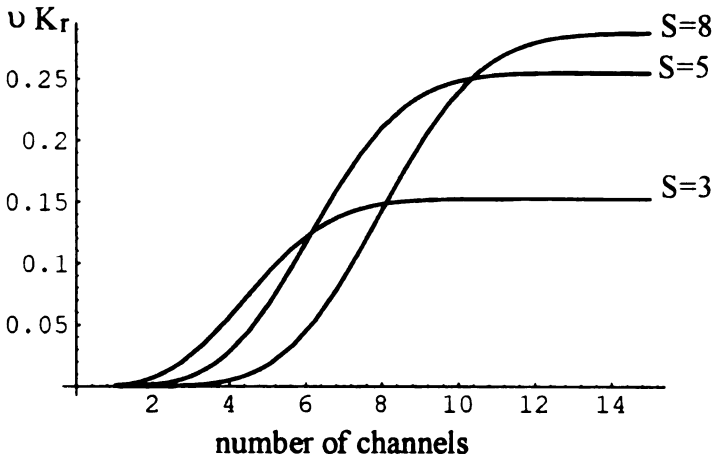

Fig. 19. The dimensionless non-adiabatic rate constant υK_r for the inverted regime is evaluated for $\lambda_x = 1eV = 40k_BT$ and $\Delta G_0 \approx -62k_BT$. Three values of the tunneling parameter $S = D_e / \hbar\omega_b$ are taken the same as for Fig. 15.

In the traditional Marcus' picture the rate constants have maximum values for activationless regime and then they should diminish with the growth of activation barrier for inverted reactions as fast as the activation factor $exp(-\beta E_A)$. This does not happen if transitions into excited vibration levels of the products are possible. The rate for multiple channel reactions should tend to almost a plateau as the exothermicity increases. Second, the largest S provides the biggest growth of the rate which is just the opposite to what we observed for the normal and activationless regimes. Thus, there should exists some Franck-Condon factors (as happened with S=8 for our choice of parameters) for which the reaction rates in the inverted regime would even increase instead of the familiar Marcus' turnover.

The reason why the larger S better stimulates growth of the generalized probability lies in the behavior of the non-adiabatic rate constants discussed above. Because both activation and tunneling factors can enhance each other for the sinks at the bottom, the relative value of K_r increases faster for the set of factors which are most mutually

supportive. As the diffusion process itself is insensitive to the intensity of the non-adiabatic transitions, the larger values of K_r always boost the total rate higher.

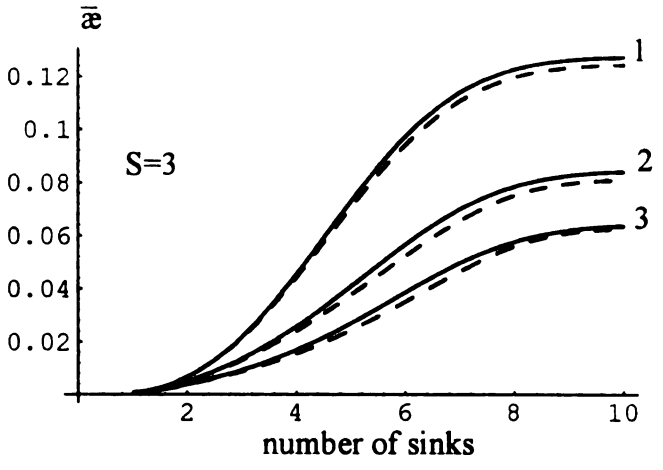

(a)

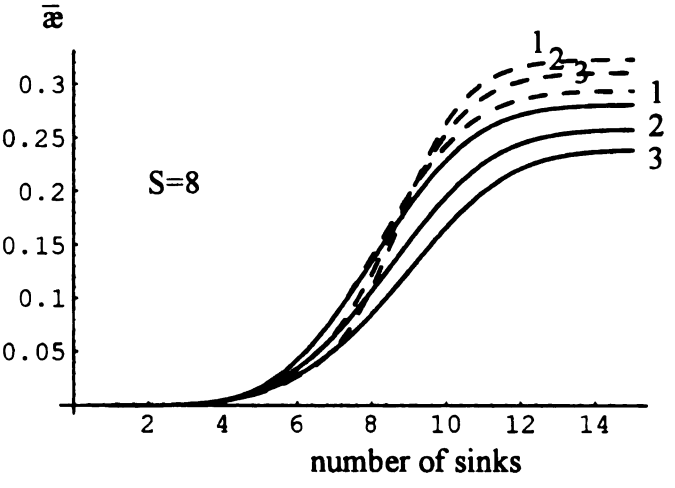

(b)

Fig. 20. The dimensionless generalized probability υK_r for the inverted regime is evaluated for $\lambda_x = 1eV = 40k_BT$ and $\Delta G_0 \approx -62k_BT$. and two values of the tunneling parameter $S = D_e / \hbar\omega_b$: (a) S=3; (b)S=8. Dashed lines are used for the $\delta(x)$ initial distribution. The other notations are: 1 - α=1; 2 - α=5; 3 - α=10.

Another feature accented on Fig. 20 is the discrepancy in the rate constants for the two different distributions we used. The saturated rates for $\delta(x)$ are somehow higher then the ones for the Boltzmann initial distribution . This can be easily explained by the argument used in the discussion of the normal regime. The reaction decay through the sinks located at the bottom of the potential well becomes significantly faster when at the start of the reaction all particles were concentrated at one point at the potential minimum. If the distribution is spread beyond the narrow area near the minimum, the particles need more time to reach the most effective sinks at the bottom which decreases the chemical rate.

3. Concluding remarks

In this chapter we explored the BBET reactions with quantum bond-breaking. We assumed that the reactive transitions occurred form the ground vibration level of the bond in the reactant state onto all vibrational levels in the product state. This mechanism is the last part of our investigation of the concerted BBET reactions. So far in Part II we have presented the theory for a broad range of mechanisms possible in the concerted BBET reactions. Predicating on the assumption of small coupling between the ET and BB modes we have considered overdamped, extremely underdamped (energy diffusion) and quantum mechanisms of the BB transformation. Which mechanism would be applicable to a real process depends upon the frequency of the breaking bond. The higher is the frequency, the weaker are collisions with the solvent, and the smaller becomes the friction until it reaches its limit $\gamma \to 0$ and the bond dissociation turns into a quantum process. The ET coordinate has been treated here as an overdamped process in accordance with the well-established technique [6].

Thus, when the friction is low, but not zero, the energy diffusion dynamics describes the BB coordinate. As the friction decreases further, the high friction ET mode takes over the dynamical changes and the BB coordinate just provides the static population for the overdamped ET. If the friction is not zero, population from the ground vibration

level of the bond decays by means of ET onto the ground vibration level of the product state. The reaction rates for this picture of BBET were evaluated in Ch. XII, Sec.2. However, if there is no friction and BB is quantum, the decay is considered to occur onto the complete set of the final vibration levels. As far as each final vibration level cuts its own sink on the reactant potential surface, we have to deal with a reaction on multiple channels.

Even if the total picture of the multiple channel reactions is very complicated, a few general conclusions could be made. As was demonstrated in the present Chapter, the rates for reactions through multiple sinks are significantly higher then their would be if we took into account only the sink leading onto the ground vibration level of the bond in the products. The deviations become high (5-10 times) for activationless reactions and increase enormously (up to a few orders of magnitude) for the inverted regime. This happens primary due to the extensive growth of the non-adiabatic part of the rate constant for multiple channels. In principle, this rise can lead to a complete change in the Marcus' turnover dependence for the rate constants on the exothermicity. So that instead of decreasing, the rate would grow as the exothermicity increases for the inverted regime. This can happen because the activationless channels in the inverted reaction can correspond to the states with the maximum overlap between the ground vibration level in reactant and some exited vibration levels of the product. At last we should note, that it is not straightforward to trace how the change of characteristic relaxation time for polarization effects the total rate, as there is no direct proportion between the changes in time and the reaction rate as it is veiled by the non-adiabatic transitions through the multiple channels.

CHAPTER XIV. CONSECUTIVE BBET

In the present Chapter we conclude the theory of BBET with a discussion of the consecutive reaction mechanism. As was outlined in Chapters VIII and IX, the structure of the PES is the characteristic that spans the differences between the consecutive and concerted pathways in the reaction. For the concerted pathway, we assume that the intermediate state is of high energy, and thus unstable. So, the reactants undergo a chemical transformation directly to the products and therefore, only two PES (for reactants and products) participate in the chemical act. We used a diabatic surface viewpoint as is standard in weakly-coupled electron transfer reactions. For the consecutive mechanism, one has to take into account the existence of a stable intermediate state and hence consider at least three potential surfaces, see Fig. 21. Thus, the reactants have to spend some time moving along the stable intermediate surface before they can reach the product well. Thus the overall reaction scheme is as follows:

$$RX + N^{-} \underbrace{\rightarrow}_{\text{first step}} RX\bullet^{-} + N\bullet \underbrace{\rightarrow}_{\text{second step}} R\bullet + X^{-} + N\bullet \qquad \text{(II.14.1)}$$

In other words, in the consecutive reaction the anion radical is formed upon the initial step and then the final transforms to the corresponding radical and the anion of the leaving group. The latter step itself can be viewed as a particular case of dissociative electron transfer where the unpaired electron located in one part of the molecule dissociatevely reduces a bond belonging to the same molecule.

This picture is analogous to what has been suggested by experimental studies of different organic halides as a method of distinguishing between the two mechanisms. It was observed that with aromatic halides the mechanism is consecutive in all investigated cases [80], whereas the bond-breaking and electron transfer are concerted with simple aliphatic halides and with perfluoroalkyl halides, at least in polar solvents [56]. It was

concluded that this pattern reveals the role of the π^* orbital where the incoming electron may be stabilized in transition. Thus, the π^* orbital can be responsible for formation of the intermediate surface. The lower the energy of this orbital (as in aromatic halides), the higher the probability of the consecutive mechanism.

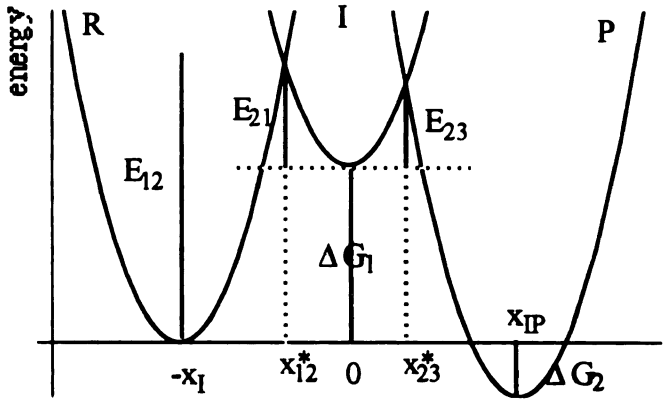

Figure 21 One-dimensional sketch of the potential surfaces used for the consecutive BBET.

Summing up, in order to discuss the consecutive mechanism we have to consider three two-dimensional PES, one for each of the reactive states - reactants, intermediates and products. The form of these surfaces was discussed in Chapter IX, see Eq. (II.9.6) and Fig. 8. Note that in our representation of the consecutive pathway we do not assume that the electron transfer (or the bond-breaking event) takes place first, as sometimes is implied [81]. In this case the BBET reaction is effectively split into two individual reactions - the ET and the dissociation of the bond. Each of these can be treated independently as a simple reaction where the rate constants can be evaluated separately from the traditional ET and bond dissociation theories (which usually involve only a single, one-dimensional PES.) Here we assume that the intermediate state involves transformation of both the electron transfer and bond-breaking coordinates, so we always have to deal with changes in both dimensions. Thus, according to scheme (II.14.1), the first step in our approach

characterizes the transitions from the state of reactants $V_R(x,z)$ to the intermediate state $V_I(x,z)$. At this point the electron is transferred from one species to the other and simultaneously the bond in the RX molecule stretches. Secondly, the R-X bond breaks and the electronic rearrangement occurs to form the leaving anion and the R• radical, i.e. the intermediates undergo the final transformation into the product state $V_P(x,z)$, see Fig. 21. We are interested in the overall rate of reaction (II.14.1) and the conditions for which the first or the second step controls the rate.

1. Reaction kinetics in the consecutive BBET

As in all of the studies presented in the dissertation, in this Chapter we assume that the BBET reaction is irreversible. For the consecutive mechanism this means that there is no significant flux of particles coming from the product state onto the intermediate surface, whereas the reverse reaction from the intermediate state into the reactants is still possible. For this reaction scheme we have to consider at least two population probability distributions which are exposed to reaction changes - $\rho_{11}(x,z,t)$ and $\rho_{22}(x,z,t)$ that correspond to populations of the reactant and intermediate potential surfaces respectively. The following system of equations should describe the reaction process if we assume the relaxation of the off-diagonal density matrix elements to be fast, as in Ref. [23, 43]:

$$\begin{aligned}\frac{\partial \rho_{11}}{\partial t} &= L_{11}\rho_{11} - iW_{12}(x,z)(\rho_{11}-\rho_{22}) \\ \frac{\partial \rho_{22}}{\partial t} &= L_{22}\rho_{22} + iW_{12}(x,z)(\rho_{11}-\rho_{22}) - iW_{23}(x,z)\rho_{22}\end{aligned} \qquad \text{(II.14.2)}$$

where $L_{11}(x,z)$ and $L_{22}(x,z)$ are the operators of motion along the reactant and intermediate state potentials respectively. W_{12} is the reaction region for the transitions from V_R to V_I surface and back and W_{23} provides only irreversible transitions from the intermediate state into the products. In the simplest case the reaction regions can be

considered as lines of the intersection between each pair of potential surfaces (so the sinks are infinitely narrow). Precisely this form of reaction regions was used when we evaluated the reaction rates for the concerted BBET, see for example Eq. (II.10.9).

The overall rate constant in the consecutive BBET reaction can be defined through the changes in the product state population:

$$æ = \left[\int_0^\infty dt \iint dx dz \rho_{11}(x,z,t)\right]^{-1} = \left[\iint dx dz \rho_{11}(x,z,s=0)\right]^{-1}. \qquad \text{(II.14.3)}$$

To proceed further we have to employ some knowledge about the form of the reaction region. If we accept that the reaction sinks are narrow (for example, they are simply lines on the potential surfaces), the integral form of differential system (II.14.2) similar to the one given by Eq. (I.4.4) becomes more profitable:

$$\rho_{11}(x,z,s) = \varphi_R(x,z)/s - \iint dx'\,dz'\, G_{11}(x,x';z,z',s) W_{12}(x',z')\left(\rho_{11}(x',z',s) - \rho_{22}(x',z',s)\right)$$

$$\rho_{22}(x,z,s) = \iint dx'\,dz'\, G_{22}(x,x';z,z',s) W_{12}(x',z')\left(\rho_{11}(x',z',s) - \rho_{22}(x',z',s)\right) - \iint dx'\,dz'\, G_{22}(x,x';z,z',s) W_{23}(x',z')\rho_{22}(x',z',s)$$

where G_{11} and G_{22} are the ordinary Green's functions defined in Eq. (I.4.1). We assumed that the reactants were initially distributed statistically, $\rho_{11}(x,z,t=0) = \varphi_R(x,z)$. The decoupling procedure analogous to the one described in Chapter VI, can be applied to the above integral equations if all sinks are narrow. As a result we can write down a very simple expression for the overall chemical rate:

$$\frac{1}{æ} = \frac{1}{K_{1r}} + \tau_1 + \frac{1}{K^{eq}}\left(\frac{1}{K_{2r}} + \tau_{21} + \tau_{12}\right), \qquad K^{eq} = \frac{K_{1r}}{K_{-1r}}. \qquad \text{(II.14.4)}$$

Here K_{1r} and K_{2r} are the non-adiabatic rate constants for the forward reactions (R)->(I) and (I)->(P) and K_{-1r} is the non-adiabatic rate constant for the reverse reaction (I)->(R):

$$K_{1r} = \iint dxdz W_{12}(x,z)\varphi_R(x,z) \qquad \text{(II.4.5a)}$$

$$K_{-1r} = \iint dxdz W_{12}(x,z)\varphi_I(x,z) \qquad \text{(II.4.5b)}$$

$$K_{2r} = \iint dxdz W_{23}(x,z)\varphi_I(x,z). \qquad \text{(II.4.5c)}$$

The first non-adiabatic rate constant determined by the shape of the reactant surface was evaluated earlier when we considered the concerted mechanism and is given by Eq. (I.7.16) or (II.10.23). Later in this Chapter we will evaluate the other two non-adiabatic rate constants which depend on the choice of the intermediate state PES (through the Boltzmann distribution $\varphi_I(x,z)$).

τ_1, τ_{12} and τ_{21} in Eq. (II.14.4) are different mean first passage times which describe the stochastic motion from one potential to another (for analogy see Eq. (I.7.29)):

$$\tau_1 = \frac{1}{K_{1r}^2}\iint\iint dxdzdx'dz' W_{12}(x,z)\overline{G}_{11}(x,x';z,z')W_{12}(x',z')\varphi_R(x',z') \qquad \text{(II.14.6)}$$

is the MFPT from the Boltzmann initial distribution inside the reactant potential, $\varphi_R(x,z)$ to the sink line onto the (I) surface, $W_{12}(x,z)$. The steady-state Green's function used in the above expression is the same as the one defined in Eq. (I.4.7) (at s=0) for the Boltzmann initial distribution. Thus, the above time deals purely with motion along the reactant state PES and does not depend upon stochastic mechanisms for any other surfaces. In fact, this is the MFPT which appeared in all rate constants for the concerted BBET; in other words, we have been evaluating this time in all previous Chapters of this Part. MFPT (II.14.6) has been evaluated for three different types of motion along the bond-breaking coordinate (we always assumed that the polarization fluctuations for the electron transfer coordinate are overdamped). For the overdamped bond-breaking dynamics MFPT (II.14.6) is evaluated in Eq. (I.7.32), for the extremely underdamped regime this time is given by Eqs. (II.10.27). Furthermore, the discussion about the reaction scheme for the case when one of the coordinate relaxation times is fast/slow (see Chapter XI) in the concerted mechanism is applicable to the MFPT in Eq. (II.14.6). In Chapter XIII we also considered the case

wherein the bond-breaking event was a quantum process. Even though the total picture of the reaction for this case would be more complicated than the one presented by the kinetic scheme in Eq. (II.14.4), MFPT τ_1 can still be approximated by the Eq. (II.13.15).

The other two MFPTs in rate constant (II.14.4) describe motion along the intermediate state potential. Again, both of these constants can be evaluated separately and independently from the type of motion inside the (R) potential. τ_{12} and τ_{21} depend only on the motion inside the intermediate state potential and the geometry of the two lines of intersection - one with the reactant state and the other one with the product state potentials.

$$\tau_{12} = \frac{1}{K_{2r}^2} \iint\iint dx dz dx' dz' \, W_{23}(x,z) \tilde{G}_{22}^{12}(x,x';z,z') W_{23}(x',z') \varphi_1(x',z'). \quad \text{(II.14.7)}$$

This MFPT is the average time to reach the reaction region W_{23} having started from the distribution along the line W_{12}. Thus, this is the time for particles escaping from the reactant state through the cut W_{12} spent on the (I) surface moving along the potential before they approach the region W_{23} and decay irreversibly into the product well. The steady-state Green's function $\tilde{G}_{22}^{12}$ can be defined using Eq. (I.4.12) for φ being a statistical distribution along the line W_{12}. The other MFPT is the average time of the reverse movement:

$$\tau_{21} = \frac{1}{K_{-1r}^2} \iint\iint dx dz dx' dz' \, W_{12}(x,z) \tilde{G}_{22}^{23}(x,x';z,z') W_{12}(x',z') \varphi_1(x',z'). \quad \text{(II.14.8)}$$

This time describes the motion of particles reflected from the region W_{23} and moving towards the line W_{12}. The steady-state function $\tilde{G}_{22}^{23}$ should be evaluated using Eq. (I.4.12) for the initial distribution spread along the line W_{23}.

Now, coming back to the form of rate constant (II.14.4) we would like to say a few words about its structure and the physical picture it represents. The constants in expression (II.14.4) are deliberately rearranged to emphasize a simple combination of reaction rates for the two steps in consecutive BBET reaction. The first step, which describes the escape of

the reactants from the (R) surface, is a combination of the first two constants in the right part of Eq. (II.14.4), $1/æ_{R\to I} = 1/K_{1r} + \tau_1$. By analogy, the superposition of the first two constants in the round brackets forms the escape rate from the (I) surface into the products, $1/æ_{I\to P} = 1/K_{2r} + \tau_{21}$. This is the rate for the second step. Finally, the reverse reaction from the intermediates onto the (R) potential is governed by the time τ_{12}. Thus, in total we have three fluxes which equilibrate the reaction - the flux of the reactants moving onto the intermediate surface and creating some population on it. The new-born population of intermediates then can either disappear into the (P) well or create a flux back to the (R) surface. Particles from the (R) well are delivered to the sink onto the (I) surface with the speed $æ_{R\to I}$. The equilibrium between the (R)->(I) and (I)->(R) fluxes maintains some population in the W_{12} transition region which is proportional to K^{eq}. Thus, the $1/K^{eq}$ serves as a population weighting factor for the rest of the rate constants which are formed by the transformations on the (I) surface. Thus, the overall rate for the consecutive BBET reaction can be expressed as follows:

$$\frac{1}{æ} = \frac{1}{æ_{R\to I}} + \frac{1}{K^{eq}}\left(\frac{1}{æ_{I\to P}} + \tau_{12}\right) \qquad \text{(II.14.9)}$$

where all rate constants can be evaluated independently. Now, from the above expression it is easy to reconstruct the traditional picture for consecutive reactions. As we have two steps, it is often asked which of them controls the reaction. First, let us assume that there is no reverse reaction (I)->(R), i.e. the MFPT τ_{12} is not regarded in the above constant. Then, we have two competing processes - formation of the intermediates from reactants and decomposition of the intermediates. From basic kinetic theory we know that the controlling step should be the one which occurs slower, i.e. with the smaller rate. This is exactly what follows from the above expression. The smaller of the constants $æ_{R\to I}$ and $æ_{I\to P}$ makes the largest contribution into the total rate. The only restriction is that the constant for (I)->(P) transitions must be weighted with the Boltzmann factor K^{eq}. Addition of the dynamical part for the reverse process (I)->(R), τ_{12}, makes the overall picture

slightly more complex in the sense that now one has to compare not two rate constants but three. If the time of return from the intermediates into the reactant state is slower than the rate of escape into the products, then the third rate constant, τ_{12} may have a chance to dominate the overall reaction rate.

Later in this Chapter we will investigate the chances for each of the three rates to be in control. Note, that from all of the constants determining kinetics (II.14.4) we have to concentrate on evaluation of only two parameters - τ_{12} and τ_{21} as the non-equilibrium constants K_{ir} are easy to determine and τ_1 has been evaluated previously.

2. Potential surfaces for the intermediate state and non-adiabatic rate constants

In this Section we establish the from of the intermediate PES and evaluate the non-adiabatic rate constants K_{-1r}, and K_{2r}, in Eq. (II.14.4). The two MFPT which describe the dynamics along the (I) surface, τ_{12} and τ_{21} will be calculated separately in the next Section of this Chapter.

Assuming that harmonic approximation (II.9.5) of the Morse potentials is acceptable, we can construct the following two-dimensional potential surfaces centered at the bottom of the intermediate PES (see Eq. (II.9.1) and (II.9.6)):

$$V_P(x,z) = (x + x_{0I})^2 / 2 + (z + z_{0I})^2 / 2 - \Delta G_1 \qquad \text{(II.14.10a)}$$

$$V_I(x,z) = x^2 / 2 + z^2 / 2 \qquad \text{(II.14.10b)}$$

$$V_P(x,z) = (x - x_{0P})^2 / 2 + (z - z_{0P})^2 / 2 + \Delta G_2 . \qquad \text{(II.14.10c)}$$

For the above choice of the PES in the consecutive BBET we have in total three lines of intersection. The minimum of each line is identified with an activation energy point, so we have three barriers to compare E_{A21}, E_{A23} and E_{A13}. The first two points correspond to the minimum points for the intersection lines of the (I) state with the (R) and (P) potentials, and the last one is the minimum point on the line between the (R) and (P) states:

$$E_{A21} = \frac{(\Delta G_1 - \lambda_I)^2}{4\lambda_I}, \quad E_{A23} = \frac{(\Delta G_1 - \Delta G_2 - \lambda_{IP})^2}{4\lambda_{IP}} \quad \text{and} \quad E_{A13} = \frac{(\Delta G_2 + \lambda_P)^2}{4\lambda_P} - \Delta G_1.$$

For the consecutive mechanism to take place the line of intersection between the (R) and (P) surfaces has to lie higher then the lines ((R),(I)) and ((I),(P)). In other words we have to require $E_{A13} > E_{A21}, E_{A23}$. If this condition fails and E_{A13} lies lower then either E_{A21} or E_{A23}, we shell say that the concerted BBET takes place and the reaction scheme behaves in accordance with the theory presented in Chapters IX - XIII of this Part.

The lines of intersection for the intermediate PES can be defined from the equalities $V_R = V_I$ and $V_P = V_I$. These lines contour the reaction sinks from the (I) surface. The first cut is formed by the (R) and (I) surfaces and provides the flux of particles from the reactant state onto the intermediate surface and back:

$$W_{12}(x,z) = K_{01}\delta(x_1 x + z_1 z - c_1), \qquad \text{(II.14.11)}$$

where $x_1 = \sqrt{2\lambda_{xI}}$, $z_1 = \sqrt{2\lambda_{zI}}$ and $c_1 = \Delta G_1 - \lambda_I$ $(\lambda_I = \lambda_{xI} + \lambda_{zI})$. Here λ_{xK} are the reorganization energies for the polarization coordinate, Eq. (II.9.2). The reorganization energies for the bond-breaking coordinate, λ_{zI} and λ_{zP} correspond to λ_{zRI} and λ_{zIP} which are given by Eqs. (II.9.4). The other line, obviously, is the intersection between the (I) and (P) surfaces:

$$W_{23}(x,z) = K_{02}\delta(x_2 x + z_2 z - c_2) \qquad \text{(II.14.12)}$$

with $x_2 = \sqrt{2\lambda_{xI}} - \sqrt{2\lambda_{xP}}$, $z_2 = \sqrt{2\lambda_{zI}} - \sqrt{2\lambda_{zP}}$ and $c_2 = \Delta G_1 - \Delta G_2 - \lambda_{IP}$ where $\lambda_{IP} = \lambda_{xI} + \lambda_{zI} + \lambda_{xP} + \lambda_{zP} - 2\sqrt{\lambda_{xI}\lambda_{xP}} - 2\sqrt{\lambda_{zI}\lambda_{zP}}$. Through this cut the particles escape from the reaction space.

Thus, after we have determined the three PES and the reaction sinks, it is straightforward to evaluate the non-adiabatic rate constants from Eqs. (II.14.5b) and (II.14.5c):

$$K_{-1r} = K_{01}\sqrt{\frac{\beta}{2\pi\lambda_I}}\exp(-\beta E_{A21}), \qquad E_{A21} = \frac{(\Delta G_1 - \lambda_I)^2}{4\lambda_I} \tag{II.14.13a}$$

$$K_{2r} = K_{02}\sqrt{\frac{\beta}{2\pi\lambda_{IP}}}\exp(-\beta E_{A23}), \qquad E_{A23} = \frac{(\Delta G_1 - \Delta G_2 - \lambda_{IP})^2}{4\lambda_{IP}}. \tag{II.14.13b}$$

Both of these constants have the same form as Marcus' ET rate constant, but the reorganization energies λ contain the contribution of the bond displacements in the (I) and (P) states. This is the only difference which distinguishes the non-adiabatic rate constants in BBET from those in ET theory. The frequency factors K_{01} and K_{02} are proportional to the coupling between the intermediate potential and the reactant or product PES: $K_{01} = 2\pi V_{RI}^2/\hbar$ and $K_{02} = 2\pi V_{IP}^2/\hbar$.

Now, after we have evaluated all of the non-adiabatic rate constants (K_{1r} is given by Eq. (I.7.16) or (II.10.23)) it is interesting to rewrite rate constant (II.14.4) in the form which separates the non-adiabatic and dynamical parts:

$$\frac{1}{\text{æ}} = \frac{1}{K_{1r}} + \frac{\cdot\ 1}{K^{eq}K_{2r}} + \exp(\beta E_{A12})\left[\chi_1 + \chi_{21} + \chi_{12}\exp(\beta(E_{A23} - E_{A21}))\right] \tag{II.14.14}$$

where we took $\tau_1 = \chi_1\exp(\beta E_{A12})$, $\tau_{21} = \chi_{21}\exp(\beta E_{A21})$ and $\tau_{12} = \chi_{12}\exp(\beta E_{A23})$. In Eq. (II.14.14) we separated the perturbation part from the rest of the factors. This separation should make analysis of the consecutive reactions easier in case the non-adiabatic transitions are weak or strong. In the first case only the first two constants would contribute to the rate as the stochastic motion is comparatively fast. In the case of strong non-adiabatic transitions the dynamic part (the combination of mean first passage times in parentheses) is responsible for the chemical rate. As one can see from Eq. (II.14.14), in the dynamic part it is essential to compare not the mean first passage times themselves, but their pre-exponential factors, χ_{ij}. This makes the dynamical analysis much more involved as the Boltzmann factors do not influence on the competition between the MFPTs. Thus, knowledge of the activation barrier heights would not be sufficient to predict the controlling

step (as a large barrier can make the appropriate MFPT very slow and hence dominant, this would easily make the high barrier reaction step (R)->(I) always in control as τ_1 would be dramatically longer than all other average times).

3. MFPT on the intermediate state PES

Now, the subject of our primary interest here is the evaluation of the effective MFPTs τ_{12} and τ_{21}. Note, that we have assumed that there is no distribution of particles on the intermediate state surface at the start of the reaction. All particles appear on the (I) surface as the result of transitions from the reactant state through the region W_{12}. Moving along the (I) surface these particles can either escape into the product well through the other cut, W_{23} or come back to the pumping region, W_{12} and return to the (R) state. Thus, the population of the (I) state is balanced by three processes: pumping of particles onto the surface from the (R) state and escape form both of the reaction regions formed by the lines of intersection of the (I) surface with the (R) and (P) PES, W_{12} and W_{23}. Both times τ_{12} and τ_{21} are the average times for particles to reach one line on the (I) surface if they have started from the other one. Therefore, even though the two times are quite different the routine for their evaluation is the same. Let us now evaluate the effective time τ_{12} using Eq. (II.14.7). The initial distribution for it is statistically spread along the cut W_{12} :

$$f_{12}(x,z) = \sqrt{\frac{\beta\lambda_1}{\pi z_1^2}}\delta(q_1 x + z - \theta_1)\exp\left(\beta E_{A21} - \beta(x^2+z^2)/2\right) \qquad \text{(II.14.15)}$$

where $q_1 = x_1/z_1$ and $\theta_1 = c_1/z_1$. This distribution should determine the form of the steady-state Green's function $\tilde{G}_{22}^{12}$ which then shall determine the desired effective MFPT. However, we do not intend to obtain the Green's function itself, instead, we will use a method similar to the one outlined in Sec. 2.2 of Ch. VII (see Eqs. (I.7.18)-(I.7.20)). Here we assume that fluctuations along both dimensions are overdamped. For details we refer

the reader to Appendix E where we evaluate the effective MFPT τ_{12} in greater detail. The final result for this MFPT is presented in Eq. (E9) and it can be rewritten as follows:

$$\tau_{12} = \tau_z \int_0^1 \frac{dx}{x} \left(\frac{\exp\left(-\frac{\beta\theta_2^2}{(1+q_2^2)} \frac{x+q_2^2 x^\alpha}{1+q_2^2+x+q_2^2 x^\alpha} \right)}{\sqrt{1-\frac{(x+q_2^2 x^\alpha)^2}{(1+q_2^2)^2}}} - \frac{\exp\left(-\frac{\beta\theta_2^2 F(x)}{2(1+q_2^2)} \right)}{\sqrt{1-\frac{(x+q_1 q_2 x^\alpha)^2}{(1+q_1^2)(1+q_2^2)}}} \right) \qquad \text{(II.14.16)}$$

where

$$F(x) = \frac{2(1+q_2^2)(x+q_1 q_2 x^\alpha)\theta_1/\theta_2 - (x+q_1 q_2 x^\alpha)^2 \left(1+\theta_1^2/\theta_2^2 \cdot (1+q_2^2)/(1+q_1^2)\right)}{(1+q_1^2)(1+q_2^2) - (x+q_1 q_2 x^\alpha)^2}.$$

As one can see, the final answer for the MFPT has five parameters. First, α is the ratio of the relaxation times along the reactive coordinates, $\alpha = \tau_z / \tau_x$, i.e. it reflects the relative speed of the overdamped relaxation on the (I) surface. The other four parameters are purely geometric and are determined by the form of the sink lines W_{12} and W_{23} given by Eqs. (II.14.10) and (II.14.11):

$$q_1 = x_1 / z_1 = \sqrt{\lambda_{xI} / \lambda_{zI}} \qquad q_2 = x_2 / z_2 = \left(\sqrt{\lambda_{xI}} - \sqrt{\lambda_{xP}}\right) \Big/ \left(\sqrt{\lambda_{zI}} - \sqrt{\lambda_{zP}}\right) \qquad \text{(II.14.17a)}$$

$$\theta_1 = c_1 / z_1 = \left(\Delta G_1 - \lambda_I\right) \Big/ \sqrt{2\lambda_{zI}} \qquad \theta_2 = c_2 / z_2 = \left(\Delta G_1 - \Delta G_2 - \lambda_{IP}\right) \Big/ \left(\sqrt{2\lambda_{zI}} - \sqrt{2\lambda_{zP}}\right). \qquad \text{(II.14.17b)}$$

Note, that $E_{A21} = \frac{\theta_1^2}{2(1+q_1^2)}$ and $E_{A23} = \frac{\theta_2^2}{2(1+q_2^2)}$ are the activation energies for the transition points for the sinks W_{12} and W_{23} respectively, which are defined by the phase factors θ_1 and θ_2 (the activation energy points are the lowest points on the intersection curves). The parameters q_1 and q_2 are the tangents of the projections of the sinks W_{12} and W_{23} on the (x,z) plane, see Fig.22. The Figure depicts the contour plot for all three PES

and the lines of intersection between (R),(I) and (I),(P) surfaces. The dashed circles represent energy contours for the activation energy points E_{21} and E_{23}.

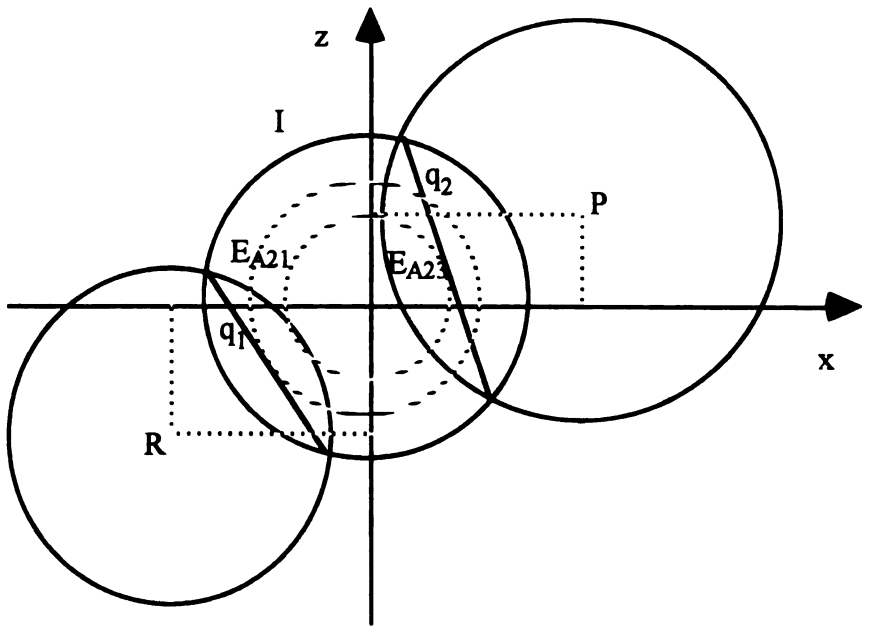

Figure 22. The projection of the PES for the consecutive BBET on the *(x,z)* plane.

If $q_1=q_2=0$, i.e. the reorganization energies for polarization fluctuations are zero (or $q_1=q_2=\infty$ and there is no bond-breaking), then Eq. (II.14.16) degenerates to the one-dimensional MFPT which is the average time to start from point x_1 and arrive at point x_2 moving along the x coordinate (or start at z_1 and reach z_2 moving along z). The expression for this time is given by Eq. (I.5.6).

Before we analyze the MFPT in Eq. (II.14.16) further, we would like to discuss the range of physical parameters participating in the process. Although we have four geometric parameters in the MFPT under study, we actually have six energies which define q_1, q_2, θ_1 and θ_2. From the form of the PES in Eq. (II.14.10) we can see that one has to think about a set of four reorganization energies - two for each of the coordinates, λ_{yI} and

λ_{yP}, y=x,z as well as about two exothermicities, ΔG_1 and ΔG_2. This allows us a substantial flexibility in the choice of parameters for τ_{12} and τ_{21}.

However, first of all, in the selection of the appropriate energies we have to remember that our choice is restricted by the requirement to deal with the concerted reaction, that is the activation energy for the direct transitions from (R) to (P), E_{A13} should be higher then the other two activation points. Of course, in every particular case this problem is somehow resolved, but here we would like to make a few general comments that should help to predict in advance what mechanism prevails in the reaction. To begin with, very high values of ΔG_1 should make the intermediate state relatively unstable and hence act in favor of a concerted reaction. Similarly, a very exothermic reaction (large negative ΔG_2) should provide a low barrier for transitions (R)->(P) and therefore may switch the reaction onto the concerted pathway.

The situation is more complicated with the selection of the reorganization energies. Let us consider the probable laws for the polarization coordinate first. From Eqs. (II.9.2) it is clear that the reference point for measuring the reorganization energies for orientational polarization is the state of reactants. The more significant is the charge redistribution in the system after it leaves the reactant state, the larger is the expected reorganization energy. Now, looking at the reaction scheme in Eq. (II.14.1) that we adopted for consecutive reactions, one may notice that it is reasonable to expect approximately similar reorganization of the charges in the intermediate and product states compared with the initial charge distribution in $RX+N^-$. Indeed, the nucleophyl radical $N^\bullet$ has lost its electron after the first stage and simply keeps moving inside the reaction cage in the course of the further transformations. Thus, its contribution to the charge redistribution is completed at the first step and therefore is the same for both λ_{xI} and λ_{xP} energies. A similar argument can be used in description of the anion radical $RX^{\bullet -}$. Even though the second step in the consecutive reaction may involve electronic rearrangement, the relative contribution to the two reorganization energies may be expected to be the same. Thus, we are allowed to

assume that the reorganization energies λ_{xI} and λ_{xP} have very similar values. If they are slightly different, we can not generally tell which one should be larger or smaller, as this matter should be subject to the molecular structure of the RX molecule.

As the polarization energies have been admitted to be similar, they do not provide a substantial contribution into the competition between the consecutive and concerted mechanisms. Hence, our last concern is the ratio between the bond-breaking reorganization energies λ_{zI} and λ_{zP}. If we think for a while about the BBET as a simple 1D bond-breaking process, we can use Fig. 21 (mentally substituting z coordinate for x) to establish some features which would be required for the consecutive mechanism to occur. From a basic geometric point of view we can state that if the transition point z_{12}^{*} lies to the left from the transition point from the (I) to (P) state, z_{23}^{*} we should encounter a consecutive reaction. This may be achieved simply by requiring $\lambda_{zI} < \lambda_{zP}$., which is quite reasonable as we take into account Eqs. (II.9.4a) and (II.9.4b) for λ_{zI} (λ_{zRI}) and λ_{zP} (λ_{zRP}). As we see from the form of the bond-breaking PES chosen in Eqs. (II.9.3), the parameters σ_K reflect how strong the structural rearrangements in the reacting species are at the bond dissociation ($\sigma_K>1$). It is normal to expect that the system in the (I) state has overcome intermediate (as the state itself is called) changes in the original bond length. At this point the bond which is about to be broken should be just stretched sufficiently to overcome the future dissociation which is awaiting the molecule at the final step. Thus, the state with the broken bond, the (P) state should present a bigger displacement for the potential surface, i.e. one may take $\sigma_P>\sigma_I>1$ which provides the desired behavior of the bond-breaking reorganization energies and gives the consecutive mechanism a good opportunity. Note, even though all of the above characteristics may be satisfied, we still have to check every time for the right order in the activation energy set.

Predicated upon the above argument, we can make a few very useful conclusions which will narrow the range of the parameter values we have to take into account. First, as all reorganization energies are positive, q_1 must be positive. Second, due to $\lambda_{xI} \approx \lambda_{xP}$ we

should have $q_2 \approx 0$ or at least quite small (however, it may be positive as well as negative). It is much more difficult to restrict the choice of the phase factors θ_1 and θ_2 as the first one is determined by three energy parameters and the other one by all six of them. The only assumption that would be reasonable and would ensure a consecutive reaction is that the phases are of a different sign (then the activation energy points for (R)->(I) and (I)->(P) transitions lie in different quarters of the *(x,z)* plane that in 1D projection corresponds to $x_{12}^{\bullet} < 0 < x_{23}^{\bullet}$,as shown on Fig. 21). Finally, the phase factors define the activation energies E_{A21} and E_{A23} which should be small enough to assure low activation barriers as the intermediate state is not supposed to be very stable.

Now we can turn to the numerical analysis of expression (II.14.16) for the MFPT on the intermediate potential surface. As we are now investigating the average time τ_{12} to travel from W_{12} to W_{23}, the particles decay on the line $\delta(q_2\, x+z-\theta_2)$. Then, if $\lambda_{xI} \approx \lambda_{xP}$ and hence $q_2=0$, the decay line is perpendicular to the z axis and the MFPT in Eq. (II.14.16) loses all dependence upon the relaxation time τ_x. In other words, the dynamics on the (I) surface become insensitive to the relaxation along the polarization coordinate, and the diffusion rate is determined only by the bond relaxation as can be seen from the following:

$$\tau_{12} = \tau_z \int_0^1 \frac{dx}{x} \left(\frac{\exp\left(\frac{\beta\varphi_2^2 x}{(1+x^2)}\right)}{\sqrt{1-x^2}} - \frac{\exp\left(\frac{\beta x}{1+q_1^2-x^2}\left(\varphi_2\varphi_1 - x\left(\varphi_2^2/2 + \varphi_{11}^2/2(1+q_1^2)\right)\right)\right)}{\sqrt{1-x^2/(1+q_1^2)}} \right)$$

Even though this average time is one-dimensional in terms of the relaxation parameters, it clearly depends upon the two-dimensional geometry layout. As now we have only three parameters to follow, the analysis of the MFPT becomes somewhat easier.

As established in Eq. (II.14.14), for comparative analysis of the diffusion rates it is adequate to investigate the behavior only of the pre-exponential factors. Fig. 23 depicts the

dependence of the dimensionless pre-exponential factor $(\tau_z \chi_{12})=\tau_z \tau_{12} \exp(\beta E_{A23})$ on the activation energies $E_{A23}=\theta_2^2$ for the absorbing line, W_{23}. We compare two sets of curves for two different values of the activation energies for the line of initial distribution, $E_{A21}=\theta_1^2/(1+q_1^2)$. In each set we considered the MFPT for $q_1=0$, 1 and 10 Fig. 23 also shows geometry of the projection of this example on the *(x,z)* plane.

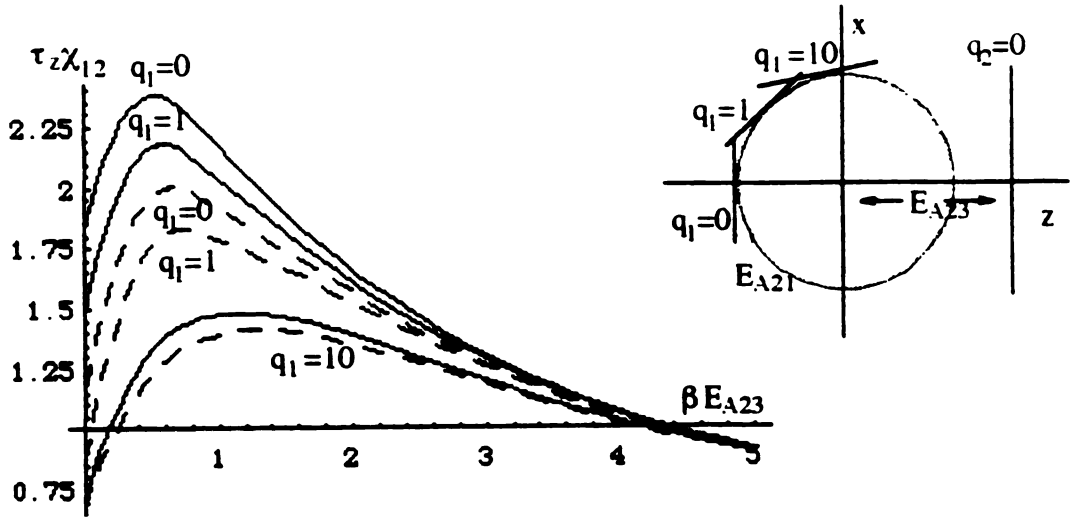

Figure 23. The dependence of the dimensionless pre-exponential factor $\tau_z\chi_{12}$ on the sink activation energy E_{A23} for three different slopes of the initial distribution line, $q_1=0$, 1 and 10. The continuous line stands for the activation energy for the initial distribution line, $E_{A21}=5k_BT$ and the dashed line represents $E_{A21}=1k_BT$.

As one can see from Fig.23, the pre-exponential factor for the MFPT, χ_{12} has a maximum at some point when the activation energy E_{A23} is very small, essentially $1k_BT$. This is, actually, typical behavior for all pre-exponential factors for the average times describing overdamped motion which transports particles over a barrier, independently from what initial distribution was involved in the dynamic process. For comparison the reader can turn to Fig. 4 for the adiabatic overdamped reactions or to Fig. 6 for reactions on the diabatic 1D

harmonic oscillator surface (in Part I). All differences in the pre-exponential factor arising from the parameters are maximized at low barriers. As should be expected, the lower energy initial distribution decreases the MFPT, since the lower the start of the particles occurs, the less time it takes for them to reach the bottom of the well, spread statistically inside the potential and then move towards the sink line. A similar argument may by used to explain why the higher slope of the q_1 projection decreases the MPFT (and hence increases the rate constant). Since in the case under consideration (q_2=0) only the motion along the z axis counts, then the shorter is the relative distance between the initial distribution and the sink in z direction, the shorter is the MFPT. From Fig. 23 it is clear that, as the parameter q_1 increases, the activation energy point moves along the circle E_{A21} which brings the initial distribution line somewhat closer to the sink line q_2. This shortens the average distance $|q_1q_2|$ (clearly, the area near the minimum of the potential is the most influenceable) and decreases the average time τ_{12}.

However, as the activation energy of the absorbing sink increases, the dependence upon all of the parameters in the initial distribution disappears (as both the activation energy E_{A21} and the slope of the initial distribution line, q_1 are parameters for the initial distribution). As the barrier for this harmonic oscillator potential increases, the pre-exponential factor for all of these parameters decreases as $1/\sqrt{E_{A23}}$, see Eq. (I.7.12).

If $q_1 \neq 0$ and the sink line W_{23} is not parallel to the x axis, then we have to consider the overdamped motion along the polarization coordinate. As we already know, the largest effect on the rate operates through a set of parameters which provide the lowest activation energy points E_{A21} and E_{A23} possible. Taking this into account, Fig. 24 presents the dependence of the pre-exponential factor $\tau_z \chi_{12}$ on the ratio of the relaxation times $\alpha=\tau_z/\tau_x$ for $E_{A21}=E_{A23}=1k_BT$. We study here behavior of the diffusion process only for moderately small values of q_2, q_2=0.1 and 0.2. As one can see, the pre-exponential factor in this case is very sensitive to the acceleration of the diffusion along the z-coordinate (when $\alpha < 1$, the relaxation time τ_z is shorter then τ_x and the relative diffusion along the bond-breaking

coordinate is faster). There are, obviously, some influences of the reaction parameters on the rates when the polarization relaxation is faster ($\alpha>1$), but the differences for various slopes q_1 are small and the deviations for $q_2=0.1$ and $q_2=0.2$ are barely noticeable. This occurs because the MFPT for the motion from one line to another is much more sensitive towards changes in the sink parameters than to variations in the initial conditions. Since in this example we considered the sink lines to be almost parallel to the x axis, then the relaxation time along z coordinate is still the most dominant of the two times τ_z and τ_x. This is why even if the motion along x ($\alpha>1$) is fast, it does not affect the pre-exponential factor as much as the fast z-motion ($\alpha<1$).

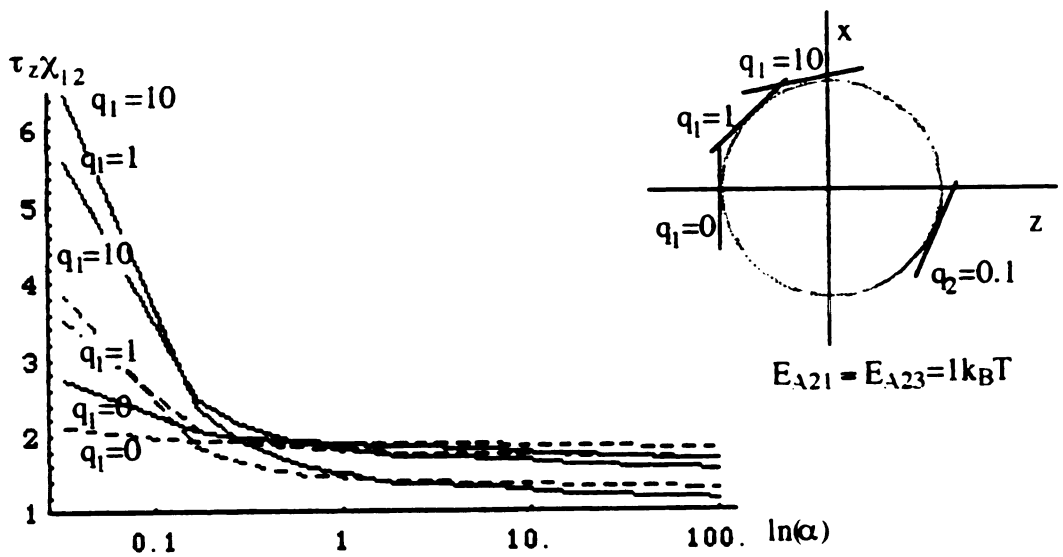

Figure 24. The dependence of the dimensionless pre-exponential factor $\tau_z\chi_{12}$ on the ratio of the relaxation times $\alpha=\tau_z/\tau_x$ for three different slopes of the initial distribution line, $q_1=0$, 1 and 10. The activation energy points for the initial distribution and the sink lines are taken the same, $E_{A23}=E_{A21}=1k_BT$. The continuous line represents the dependencies for $q_2=0.2$ and the dashed one shows a similar behavior for $q_2=0.1$.

Finally, Fig. 25 presents the example where both lines on the surface have significant slopes and thus are not parallel to any of the two axes. Similarly to Fig. 23, we considered the dependence of the pre-exponential factor on the activation energy of the sink. We took $q_1=1$ and two different values of q_2: 1) $q_2=0.5$, which makes the sink line run along the initial distribution line and so they intersect somewhere at a high energy point; 2) at $q_2=-0.5$ the two lines are pointed towards each other (see Fig.25) and intersect near the potential minimum. Hence, as the both relaxation times contribute to the MFPT we considered three different values of the ratio τ_z/τ_x: $\alpha=0.1$, 1, 10.

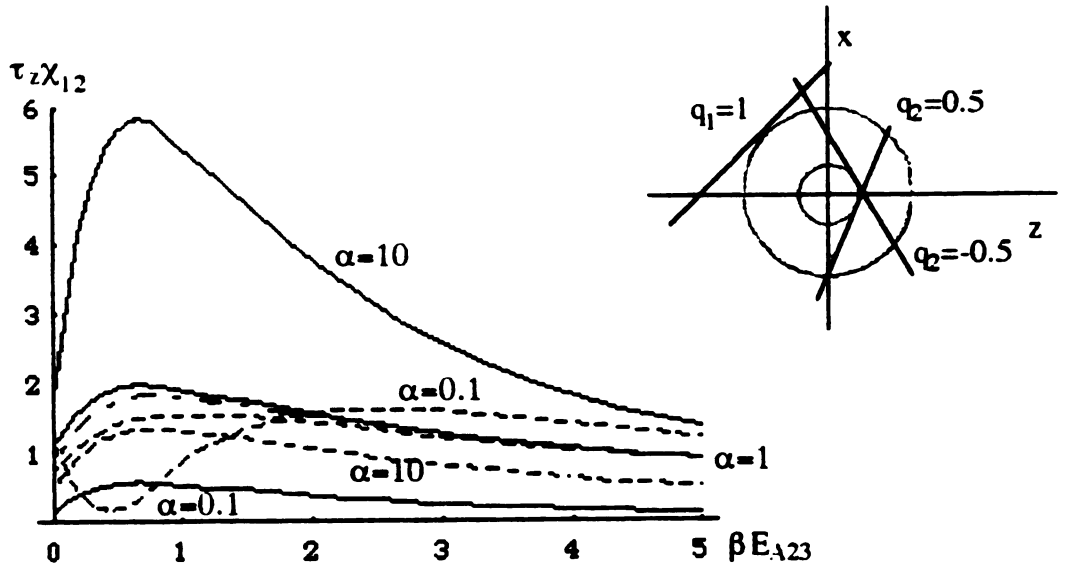

Figure 25. The dependence of the dimensionless pre-exponential factor $\tau_z\chi_{12}$ on the sink activation energy E_{A23} for three different ratios of the relaxation times $\alpha=\tau_z/\tau_x=0.1$, 1, 10. The initial distribution line activation energy was taken as $E_{A21}=1k_BT$. The continuous line stands for the positive slope of the initial distribution line, $q_2=0.5$ and the dashed line represents $q_2=-0.5$. For comparison, the dotted and dashed line gives $\tau_z\chi_{12}(\beta E_{A23})$ for $q_2=0$ (when there is no dependence upon α).

First of all, for this choice of parameters the MFPT depends on both relaxation times, i.e. it is a two-dimensional diffusion relaxation process. Even though typically the pre-exponential factors still exhibit a maximum at the barrier energies close to $1k_BT$, this is not necessarily the case.

To begin with, let us consider the sink line with a positive slope, $q_2=0.5$. Here we have a situation that has been expected: for all ratios of the relaxation times the pre-exponential factors have their maxima at very low barriers, $E_{A23}\approx 0.5k_BT$. Since we count the pre-exponential factor in the units of the relaxation time τ_z, then the smaller α correspond to the faster diffusion and vise versa. The faster diffusion τ_z decreases the MFPT from one line to another, which is the case for $\alpha=0.1$ on the picture. The situation for large α is more involved. As one can see, an increase in the relaxation time ratio by a factor of 10 has far greater influence on the MFPT for low barriers than a corresponding reduction. Indeed, in the range $E_{A23}=0 - 2k_BT$ the MFPT for $\alpha=10$ slows down compared to the MFPT for $\alpha=1$ more dramatically than the same MFPT speeds up at $\alpha=0.1$. This happens because we are considering the mean first passage times between two lines. Looking at the diagram in Fig. 25 for $q_2=0.5$ one can notice that at $E_{A23}\approx 0.5k_BT$ the average traveling distance from W_{12} to W_{23} in the x direction is shorter then the distance along the z axis (the domain near the potential minimum is the one that really counts). So, one can expect that the shorter distance provides the most intensive paths for the particles traveling from one line to the other. Therefore, the average time should be more sensitive to the changes in the relaxation time along this direction (in this case the x coordinate). Thus, the MFPT responds more to slowing the particles down along x then to the speeding them up along z.

Finally, at the negative value of the sink slope, $q_2=-0.5$, we observed the situation when the pre-exponential factor has a minimum at a low barrier instead of the traditional maximum. For the accepted choice of parameters this happens when $\tau_z<\tau_x$ ($\alpha=0.1$), see Fig. 25. The explanation can be given by employing similar arguments to the ones used in

the previous paragraph when we discussed geometry of the problem with q_2=0.5. The difference is that now the average distances are shorter for the z direction. Thus, the MFPT for α=0.1 has a richer behavior then the one for α=10. The reason why the first MFPT has a minimum instead of a maximum also lies in the geometry of the problem. As we drag the sink line from E_{A23}=0 higher, it intersects the initial distribution line at the minimum point. This configuration is optimal for the passage of particles from one line to the other and therefore the pre-exponential factor for this MFPR is minimal.

4. Concluding remarks

To sum up, in the present Chapter we have concluded the theory of BBET reaction with the discussion of the consecutive mechanism that may be an alternative to the concerted BBET considered in Chapters IX-XIII. The major distinction between the two mechanisms is the structure of the potential energy surfaces. Simplisticly speaking, in order for the consecutive mechanism to outweigh the concerted scheme, the intermediate state potential surface has to be of low energy. In this case, the particles escaping from the reactant state would have to travel primarily through the intermediate potential in order to reach the product well. In the concerted BBET the intermediate state is accepted to be quite high in energy and thus unstable, so that the direct route from reactants to products is more economical.

In our study we have established that there are three competing processes which may determine the overall reaction rate in consecutive reactions, see Eq. (II.14.9). These processes are: i) the transport of the reactants form the (R) well onto the (I) surface over the potential barrier E_{A12} (with the dynamical part defined by τ_1); ii) irreversible escape of the intermediates into the product well over the barrier E_{A23} inside the (I) potential (with τ_{21}); iii) reverse movement of the particles form the (I) state back into the products over the other potential barrier formed inside the intermediate state, E_{A21} (with τ_{12}). As was discussed above, in principle, any of these three transformations can control the whole reaction,

depending on which of them is the slowest (see Eq. (II.14.14) and the following discussion).

Since the most interesting behavior of the reaction rate given by Eq. (II.14.14) is based on the dynamics, for this analysis we will assume that the non-adiabatic transitions are fairly strong so that they do not control the reaction rate (so we are in the diffusion control limit). Therefore, out aim here is to estimate which of the three MFPT involved in the reaction kinetics have better chances in controlling total rate (II.14.4). As has been discussed previously, for comparison of the dynamical factors it is adequate to contrast the pre-exponential factors for the average times τ_1, τ_{21} and τ_{12}, see Eq. (II.14.14). In Section 3 of this Chapter we presented a few graphic dependencies for the pre-exponential factors for the MFPT, τ_{21} and τ_{12} on the intermediate potential surface. Since these MFPT are the average times to travel between two lines on the surface, these graphic dependencies may be refered to the behavior of τ_{12} as well as τ_{21}, as they both describe similar processes. The only detail which should be remembered in order to contrast the factors, is that the pre-exponential factor for τ_{12} has to be multiplied by the Boltzmann factor of the difference between the two activation barriers presented for particles by the (I) surface, $\exp(\beta (E_{A23} - E_{A21}))$. Thus, if for the intermediates the barrier to escape into the products is higher than the barrier to return back into the reactants (so that $E_{A23} - E_{A21}>0$), the time of the transitions (I)->(P), τ_{12}, may have a significant advantage over the time τ_{21} in controlling the overall rate, see Eq. (II.14.14). Naturally, particles have better chances to escape from a potential well over a low barrier which makes the appropriate MFPT shorter (and the rate of the reaction smaller). In the consecutive reactions the slower rate controls the process, therefore the MFPT over a higher barrier has better chances to dominate the overall reaction. Hence, if $E_{A23} - E_{A21}>0$, τ_{12} is slower than τ_{21} and the transitions (I)->(P) are dominant. If $E_{A23} - E_{A21}<0$, then the reverse reaction (I)->(P) may be the one which prevails for transformation of the intermediates.

To complete the discussion we present Fig.26 where we demonstrate how the MFPT inside the (R) well, τ_1, normally behaves depending on the height of the activation barrier for the (R)->(I) transformation. The expression for this MFPT, which is the average time to reach the sink line W_{12} on a 2D harmonic oscillator surface having started form the Boltzmann distribution, is given by Eq. (I.7.32). The average time τ_1 has only two geometric parameters - the barrier height, E_{A12} and the slope of the sink line, q_1 (in the notations for this Chapter). It would be reasonable to expect that the reaction (R)->(I) would take place over a moderately high barrier, say $E_{A12}>10\ k_BT$, which has to be somehow significantly higher than the barriers for the reactions (I)->(P) and (I)->(R), E_{A23} and E_{A21}. If the activation energy E_{A12} is high, then χ_{12} can be estimated as $1/\sqrt{E_{A12}}$.

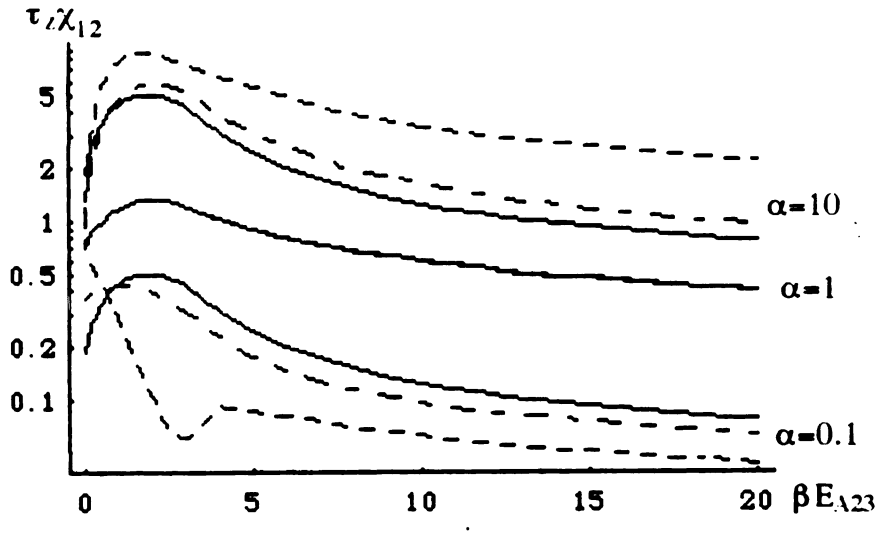

Figure 26. The dimensionless pre-exponential factor $\tau_z\chi_1$ for the MFPT on the reactant PES is presented as a function of the activation energy, E_{A12}. The continues lines present the dependencies for $q_1=1$ and the lines with the shorter dashes are for $q_1=0.1$ and the lines with the longer dashes are for $q_1=0.5$. Three ratios of the relaxation times $\alpha=\tau_z/\tau_x=0.1$, 1, 10 are considered. The curves for all three values of q_1 coincide at $\alpha=1$.

So, we have to compare the dimensionless pre-exponential factor $\tau_z\chi_1$ to the parameters $\tau_z\chi_{21}$ and $\tau_z\chi_{12}$ depicted on Figs. 23-25. From Fig. 26 (see also Sec. 3 of Ch. VII) it is straightforward to see that the factor $\tau_z\chi_1$ at $E_{A12}>10\ k_BT$ can quite easily become smaller than the other two factors, as its value at a given energy is comparable with those of for $\tau_z\chi_{21}$ and $\tau_z\chi_{12}$, but we have to compare the factors at different activation energies. In other words, the pre-exponential factor χ_1 has to be taken at much higher energy then χ_{12} or χ_{21} and hence can be much smaller than the other two (again, for the consecutive dynamics the largest pre-exponential factor should control the whole reaction). Therefore, it should not be too hard for the dynamics on the intermediate surface to control the overall reaction rate. If this is the case, then the question of which barrier on the (I) surface is higher should give a good estimate for further selection of the dominant MFPT.

Of course, the detailed picture of the consecutive reaction on a 2D potential surface is much more complicated. One has to consider not only the geometric layout of the potential surfaces including the height of the activation barriers are and so on, but also the two-dimensional dynamics. For the 2D case, in general, the answer to the question what dynamics control the overall reaction, is hard to prognosticate The difficulty is that the dynamics act in an unpredictable way, especially for the intermediate surface where the barriers are low and we can not foretell which relaxation time has the greatest effect. For the precise answer, one would have to evaluate all MFPT relevant to the discussion using Eq. (II.14.16) for the motion on the (I) surface and Eq. (I.7.32) for the dynamics inside the (R) well.

CHAPTER XV. CONCLUSION

Unimolecular reactions represent a wide range of chemical processes, their variety is enormous - everything from simple isomerization to ET in complicated biological systems. However, despite their diversity, they all take place in a closed reaction space, so that the reactants and the products co-exist in the same cage during the reaction. Exploration of all these processes is united under unimolecular reaction theory which roughly splits into two major parts - adiabatic and diabatic approaches. The influence of stochastic motion on the reaction rates for both approaches is the most intense area of interest at the present moment.

One of the traditional methods for investigation of reaction dynamics involves solution of a time-dependent Fokker-Planck equation for Brownian motion (either underdamped or overdamped). The solution generates a population probability function which decays in time in some area on the potential surface. In this theoretical scheme the reaction rate constants are determined through the time-dependent population probability function. A few one-dimensional adiabatic as well as diabatic models have been extensively developed from this method and in some cases the rate constants have been evaluated analytically. However, we require investigation of more complicated reactions, such as multidimensional surfaces processes. A few attempts have been made to obtain the rate constants analytically, but the principal difficulty is that the traditional scheme of equations is too complicated to be resolved even for two-dimensional PES reactions. Partially this is the cause of the time dependence in the intermediate calculations in the traditional evaluation scheme for the rate constants. As a consequence, numerical methods have been more and more extensively used in the theory.

In this dissertation we present a *new, steady-state* theory for evaluation of the rate constants in unimolecular reactions which at no point involves evaluation of time-dependent

functions. It is a theory based on the *steady-state* analogs of the traditional Fokker-Planck differential as well as integral equations and therefore eliminates time as a variable from all steps in the process of evaluating reaction rate constants, see Chapters III and IV. Transition from the time-dependent to steady-state formulation of the theory for unimolecular reactions was not trivial. So, in order to prove the legitimacy of the steady-state approach, in Chapter IV we introduced the *steady-state Green's functions* defined only by the motion on PES. These functions are dramatically different from all other Green's functions used in unimolecular theory previously (all the details are described in Chapter IV and Appendix A). They not only provide the correct transition from the time-dependent to steady-state equations, more importantly, they have a straightforward physical meaning. In the simplest interpretation a steady-state Green's function defines MFPT from some initial distribution (either a function or a point) on PES to a *point*. Furthermore, the specific properties of these functions allowed us to generalized the concept of MFPT and introduce a method for evaluation of the *effective MFPT*, which is the time for particles to reach a *region* on PES (in contrast to a single point) having started from a distribution. The effective MFPT is a major dynamical characteristic in multidimensional reactions and may be the only average time of interest in one-dimensional processes (such as adiabatic reaction over not extremely high barriers and diabatic reactions on sinks which are wider then a pinhole).

Among the most common reactions are the reactions taking place on narrow reaction sinks. In the frameworks of the steady-state method we introduced the *decoupling approximation* for solution of integral equations for this case, as outlined in Chapter VI. It is consistent and very simple to use, yet became possible only due to the steady-state Green's function technique. Moreover, the steady-state approach enabled us not only to design the decoupling scheme, but also formulate the *criterion of its applicability*. It was proved explicitly that for narrow sink reactions the general evaluation of the rate constant can be significantly simplified as it is possible to separate the dynamical effects from the

reaction itself. As a result, the rate constant for this case consists of two parts which can be evaluated separately: equilibrium (non-adiabatic) rate constant and effective MFPT (the average time for particles to reach the narrow sink). The procedure for evaluation of the effective MFPT requires utilization of the steady-state Green's functions.

Furthermore, as a logical extension for Part I, the steady-state Green's function theory was applied to a few reaction models. First, we considered one-dimensional systems in order to test our theory on well developed examples. In Chapter V we resolved the problem of high activation barrier reactions for narrow and moderately wide reaction regions for a broad range of potentials. In Chapter VII overdamped reactions on one- and two-dimensional harmonic oscillator potential surfaces as well as the transitions in a bistable potential were analyzed carefully using our method

For the bistable potential we evaluated the reaction rate of escape from the reactant well under the influence of the position-dependent friction, $\gamma_{eff}(x)$ over all range of barriers. The barriers did not have to be high and the evaluations did not involve the harmonic approximation on the top and in the bottom of the potential. If the barrier is not very high, the reverse movement of the particles from the product well into the reactant well significantly decreases the reaction rate.

As an example of irreversible decay on diabatic surfaces we considered reactions on one- and two-dimensional harmonic oscillator surfaces. We assumed that the one-dimensional reaction takes place on a pinhole sink, which is located at the point of intersection with the final state diabatic surface, so that the reaction rate constants were evaluated by using the MFPT to the point. For the more sophisticated case of a two-dimensional harmonic oscillator we were also able to obtain an analytical expression for the rate constant. For the two-dimensional surface the reaction sink was taken to be the line of intersection between the two diabatic surfaces. In this case the rate constant was determined through the effective MFPT, which was found to be a complicated function of the relaxation times along each of the reaction coordinates. For low barriers both relaxation

times seem to contribute to the reaction, even if one is considerably faster then the other. However, for high barrier reactions the dynamic influence is more straightforward, so that the faster relaxation time controls the reaction rate.

In order to extend application of the steady-state Green's function theory to more complicated systems, in Part II we developed a theory for *bond-breaking electron transfer reactions*, or BBET. The reaction scheme for these processes in outlined in Chapter VIII. These reactions are intrinsically *two-dimensional* as they require transformation of the reaction system along both electron transfer and bond- breaking coordinates. To our knowledge, this theory is the first consistent theory aimed at description of such reactions.

As was established, it is necessary to introduce some intermediate state in order to distinguish between two possible mechanisms observed in experiments - the consecutive and concerted. The difference between the mechanisms is provided by the structure of the two-dimensional diabatic potential surfaces for reactants, intermediates and products, as discussed in Chapter IX. Treating these two mechanisms separately, our BBET theory is based on the diabatic formalism and is aimed at understanding the dynamical effects on the overall reaction rates.

The *concerted* mechanism takes place if the intermediate state is of high energy and thus unstable. In this case, one has only two diabatic PES to take into account as the reactants overcome direct transformation into the products. The theory presented in Chapters X-XIII concentrates on the complex multidimensional dynamics in the concerted BBET. Assuming that the polarization fluctuations are always overdamped with the relaxation time τ_x, we viewed two classical and one quantum characters of the dynamics along the bond-breaking coordinate. The classical overdamped and energy diffusion dynamics are appropriate for description of extremely low or moderate frequencies of the breaking bond, whereas the quantum nature of the coordinate should be considered for the bond frequencies of 600 cm^{-1} and higher.

The *energy diffusion* regime appeared for us to be of a special importance, as the bond period is usually short with respect to the solvent collision time. We explored this energy diffusion mechanism (characterized by the relaxation time τ_z) in Chapters X and XI, by means of the steady-state Green's function method, and succeeded in obtaining the techniques required to consider overdamped diffusion along one coordinate (ET) and energy diffusion along the other (BB). We found that for our choice of the two-dimensional PES, the overall rate constant in the concerted BBET can still be separated in two parts, $1/K=1/K_r + \tau_p$ - where one is responsible for the chemical transformation (non-adiabatic) and the other describes the dynamics along the two coordinates (the effective MFPT). The effective MFPT, τ_p was found to have a *very complex* dependence upon the two relaxation times τ_x and τ_z. As the dynamic scales become different a rich variety of behavior becomes possible as to which time controls the overall reaction rate, see Chapter XII. A special method of analysis was developed for the situation where one dynamics is fast/slow compared with the other one. As a result we obtained that even though the overall rate consists of the two independent parts, the purely dynamical question which time controls τ_p can be answered only through comparison of the fastest relaxation time with K_r. Despite the fact that the overdamped regime along the BB coordinate has many features which are similar to those of the energy diffusion dynamics, the comparative analysis of the two mechanisms was also performed in Chapters XI and XII.

The steady-state Green's function method transpired to be extremely useful for developing the theory for the *quantum bond-breaking* coordinate in the concerted BBET as discussed in Chapter XIII. For frequencies that are high enough to call into question the classical treatment of the BB coordinate we incorporated the quantum effects in the dynamical picture on the BBET reactions. In this case the original two-dimensional structure was reduced to the set of one-dimensional diabatic potentials for the polarization fluctuations (ET coordinate) which provided population decay from the reactant diabatic

surface through multiple channels into the products. In this picture the overall rate constant can *never* be separated into non-adiabatic and diffusion parts.

We found that, generally, one can expect an increase in the reaction rate when going from the classical (energy diffusion) to the quantum treatment for high bond frequencies. This occurs because the multiple channels created by quantum vibration levels of the products usually depopulate the state of reactants much faster than the single sink between the two diabatic surfaces in the classical treatment. For a broad set of examples we demonstrated that there is a strong interference between the channels in quantum BBET so that they can not be treated independently. In other words, the overall reaction rate in quantum BBET *is not additive* with respect to the partial rates on each cannel. We found that one can increase the reaction rate dramatically by taking into account presence of the multiple channels, especially if the ET happens to take place in the inverted Marcus' regime. This increase (in some cases up to a few order of magnitude) happens primarily due to extensive growth of the non-adiabatic part of the rate constant for multiple channels. The interference between the non-adiabatic and diffusion parts in this case is so strong that it can cause changes in the Marcus' turnover dependence of the rate constant on the exothermicity. So, the reaction rate, in principle, does not decrease for high exothermicities in the inverted regime, instead, it can even grow with increase of ΔG_0.

Consecutive BBET occurs if the intermediate state is sufficiently stabilized, which leads to participation of an additional (intermediate) PES, which for this mechanism has to depend upon both the ET and BB coordinates. First, as in the concerted BBET the overall reaction rate in the consecutive mechanism can be under complete dynamical control. Moreover, all of the features of the dynamical effects obtained for the concerted reactions are exhibited in the consecutive BBET. Only now two-dimensional dynamics along each of the two surfaces (for reactants and intermediates) have to be considered as these dynamics compete with each other for control over the total rate. Thus the overall picture of consecutive BBET is extremely complicated, especially if some of the relaxation times are

faster/slower than others. The steady-state analysis of this situation is presented in Chapter XIV. Three effective MFPT were found to be in competition. One effective MFPT is responsible for transitions from reactants to the intermediates and two others are formed by the motion on the intermediate surface (one towards the products and the other one back to the reactants). Using the decoupling approximation from Chapter VI we evaluated all three effective MFPT and predicted the conditions at which each average time may control the overall reaction rate. In particular, we found that if the overall rate in the consecutive BBET is strongly influenced by dynamics, the motion on the intermediate surface generally has better chances to control the dynamical rate of the consecutive reaction.

This dissertation is devoted to the creation and development of a new, steady-state theory for the investigation of dynamical effects in unimolecular reactions. The greatest advantage of this theory is that it suggests an alternative technique for evaluation of the rate constants in closed reaction space processes. The technique is based on *steady state differential and integral equations.* Removal of time as a variable decreases the dimension of the base equations and opens up new possibilities in analytical solution of multiple problems, especially for multi-dimensional reactions. As a demonstration we developed a theory for description of bond-breaking electron transfer reactions that are intrinsically two-dimensional. The theory may be applied to underdamped as well as overdamped dynamics, and both adiabatic and diabatic potential surfaces. We believe that our introduction of the steady-state equations is the first theoretical study which allows calculation of the unimolecular rate constants directly through the time-independent equations. It is expected that our approach, because of its specific technique and relative mathematical simplicity will prove fruitful for many further applications.

APPENDIX A. PSEUDOSTATIONARY GREEN'S FUNCTION. CALCULATION OF $G_0(x,x')$ and τ_p

APPENDIX A: PSEUDOSTATIONARY GREEN'S FUNCTION. CALCULATION OF $G_0(x,x')$ AND τ_p.

As we mentioned in Ch. IV, there is a problem concerned with solution of steady-state equations (I.3.9) and (I.3.10) using the formal Green's function defined through the equation:

$$\hat{L}(\vec{x},\vec{v})G_0(\vec{x},\vec{v},\vec{x}',\vec{v}') = -\delta(\vec{x}-\vec{x}')\delta(\vec{v}-\vec{v}'). \qquad \text{(A1)}$$

It is obvious, that this function can be applied to the solution of this steady-state problem. As one can see, the above equation can not be considered as a limiting case of Eq. (I.4.1) at s->0, as far as the formal Green's function G_0 (we will call it pseudostationary function) has no links with the Green's function $G(\vec{x},\vec{v},\vec{x}',\vec{v}';s)$. Moreover, the latter function diverges at s->0 and satisfies the boundary conditions which differ from the ones for the formal function $G_0(\vec{x},\vec{v},\vec{x}',\vec{v}')$. Indeed, G_0 does not retain the property of concervation of particles, but according to (A1) satisfies the following condition:

$$-\iint \hat{L}(\vec{x},\vec{v})G_0(\vec{x},\vec{v},\vec{x}',\vec{v}')d\vec{x}d\vec{v} = 1. \qquad \text{(A2)}$$

It means that the number of particles in the reaction system is not conserved anymore, because Eq. (A2) implies the appearance of a constant flux of particles into the reaction space. So, it is possible to set the kinematic flux to zero at only one boundary. The additional condition for the solution of Eq. (A1) should be taken as:

$$\iint G_0(\vec{x},\vec{v},\vec{x}',\vec{v}')d\vec{x}d\vec{v} = const. \qquad \text{(A3)}$$

Thus, it is obvious, that $G_0(\vec{x},\vec{v},\vec{x}',\vec{v}')$ differs dramatically from the steady-state Green's functions $\tilde{G}$ or $\overline{G}$ defined in Ch. IV. From the other hand, G_0 is obviously appropriate for solution of the steady-state differential equations (I.3.9) and (I.3.10) as well. The integral form of Eq. (I.4.6) may be represented as:

$$\xi(\vec{x},\vec{v}) = \varphi(\vec{x},\vec{v}) + æ\iint G_0(\vec{x},\vec{v},\vec{x}',\vec{v}')f(\vec{x}',\vec{v}')d\vec{x}'d\vec{v}' -$$
$$-\iint G_0(\vec{x},\vec{v},\vec{x}',\vec{v}')W(\vec{x}')\xi(\vec{x}',\vec{v}')d\vec{x}'d\vec{v}' \qquad \text{(A4)}$$

which is exactly the same as the one in Eq. (I.4.9).

At the first glance, it seems strange that such completely different functions as G_0 and $\overline{G}$ end up with the same differential equation for $\xi(\vec{x},\vec{v})$. However, if we analyze the boundary conditions and the properties of both functions, e can conclude that equation (A4) is built in such a way that all differences cancel and both solutions for $\xi(\vec{x},\vec{v})$ are identical. Preference to one or another method can be dictated only by convenience in calculation of the different Green's functions.

It is easy to find out the connection between Green's functions $\tilde{G}$ and G_0, which may be represented as:

$$\tilde{G}(\vec{x},\vec{v},\vec{x}',\vec{v}') = G_0(\vec{x},\vec{v},\vec{x}',\vec{v}') - \iint G_0(\vec{x},\vec{v},\vec{x}',\vec{v}')f(\vec{x}',\vec{v}')d\vec{x}'d\vec{v}'. \qquad \text{(A5)}$$

Thus, the desired Green's function $\tilde{G}$ can be obtained through the pseudostationary Green's function G_0 , as far as G_0 can be defined more easily than $\tilde{G}$. However, as we will show further in Appendix A, calculations involving G_0 produce some restrictions to the form of the Boltzmann distribution $\varphi(\vec{x},\vec{v})$.

Let us calculate the Green's function $G_0(x,x')$ from Eq. (A1) for one-dimensional motion using overdamped operator (I.1.2) . Direct integration under condition (A3) (for the case when const=0) and assuming that flux at the boundary $x=-\infty$ is zero yields

$$G_0(x,x') = \varphi(x)\{\int_{x'}^{\infty}\frac{dy}{D(y)\varphi(y)}\int_{y}^{\infty}\varphi(z)dz - \Theta(x-x')\int_{x'}^{x}\frac{dy}{\varphi(y)}\}. \qquad \text{(A6)}$$

Notice, that at the integration by parts we used the condition:

$$\lim_{y->\infty}\int_{y}^{\infty}\varphi(x)dx\int_{x'}^{y}\frac{dx}{\varphi(x)}dz = 0. \qquad \text{(A7)}$$

For the further transformations we used the Boltzmann distribution φ(x) in the form:

$$\varphi(x) = \frac{1}{Z_0}\exp(-\beta V(x)) \qquad (V(x)\text{->}\infty \text{ at } x\text{->}\pm\infty). \tag{A8}$$

Carrying out the transformation:

$$\int_y^\infty \varphi(x)dx = \frac{1}{Z_0}\int_y^\infty \exp(-\beta V(x))dx = \frac{1}{Z_0}\exp(-\beta V(x))\int_y^\infty \exp[\beta(V(y)-V(x))]dx,$$

substitution of variable z=x-y and using the Taylor's series expansion over the small parameter z in the integrand, we obtain:

$$\frac{1}{Z_0}\exp(-\beta V(y))\int_0^\infty \exp[\beta(V(y)-V(y+z))]dz \sim \frac{1}{Z_0}\exp(-\beta V(y))\int_0^\infty \exp(-\beta V'(y)z)dz.$$

Or, finally, we have the estimate:

$$\int_y^\infty \varphi(x)dx \underset{y\to\infty}{\sim} \frac{K_B T}{Z_o V'(y)}\exp(-\beta V(y)). \tag{A9}$$

By analogy with the above procedure, we can analyze another integral:

$$\int_{x'}^{y}\frac{dx}{\varphi(x)} = Z_0\exp(-\beta V(y))\int_0^{y-x'} e^{-\beta(V(y-z)-V(y))}dz \underset{y\to\infty}{\sim} Z_0\exp(-\beta V(y))\int_0^\infty e^{-\beta V'(y)z}dz$$

or, shorter:

$$\int_{x'}^{y}\frac{dx}{\varphi(x)} \underset{y\to\infty}{\sim} \frac{Z_0}{\beta V'(y)}e^{\beta V(y)} = \frac{1}{\varphi'(y)} \tag{A10}$$

Therefore, condition (A7) is fulfilled when:

$$V'(y)^{-2} \to 0 \text{ as } y\to\infty,\ V(y) \underset{y\to\infty}{\sim} y^{1+\varepsilon}\ (\varepsilon > 0). \tag{A11}$$

The most rigid condition turns out to be the requirement of convergence of the first integral in Eq. (A6), because we have:

$$\int V'(y)^{-1}dy \to const \text{ as } y \to \infty,\ V(y) \underset{y\to\infty}{\sim} y^{2-\varepsilon}\ (\varepsilon > 0) \tag{A12}$$

which means, that it diverges even for the harmonic potential. Meanwhile, abstracting from that problem i. e. assuming that the function V(y) increases sufficiently at y->±∞ ($V(y)\sim y^n$, n>2), we obtain the steady-state Green's function using Eq. (A5) and integrating by parts:

$$\tilde{G}(x,x') = \varphi(x)\left\{\int_{-\infty}^{x}\frac{dy}{D(y)\varphi(y)}\int_{-\infty}^{y}f(z)dz + \int_{x'}^{\infty}\frac{dy}{D(y)\varphi(y)}\int_{y}^{\infty}\varphi(z)dz - \Theta(x-x')\int_{x'}^{x}\frac{dy}{D(y)\varphi(y)} - A\right\} \tag{A13}$$

where:

$$A = \int_{-\infty}^{\infty}\frac{dy}{D(y)\varphi(y)}\int_{y}^{\infty}\varphi(z)dz\int_{-\infty}^{y}f(z)dz$$

Clearly, the above formulas require the above mentioned restriction for the form of the reaction potential V(x). However, carrying out the transformation of identity, both of them may be rewritten in the form:

$$\tilde{G}(x,x') = \varphi(x)\{\int_{-\infty}^{x}\frac{dy}{D(y)\varphi(y)}\int_{-\infty}^{y}\varphi(z)dz\int_{-\infty}^{y}f(z)dz + \int_{x}^{\infty}\frac{dy}{D(y)\varphi(y)}\int_{y}^{\infty}\varphi(z)dz\int_{y}^{\infty}f(z)dz +$$

$$+\int_{x'}^{x}\frac{dy}{D(y)\varphi(y)}(\int_{y}^{\infty}\varphi(z)dz - \Theta(x-x'))\} =$$

$$= \varphi(x)\left\{\int_{0}^{x}\frac{dy}{D(y)\varphi(y)}\int_{-\infty}^{y}f(z)dz - \int_{0}^{x'}\frac{dy}{D(y)\varphi(y)}\int_{y}^{\infty}\varphi(z)dz - \Theta(x-x')\int_{x'}^{x}\frac{dy}{D(y)\varphi(y)} + B\right\} \tag{A14}$$

where:

$$B = \int_{0}^{\infty}\frac{dy}{D(y)\varphi(y)}\int_{y}^{\infty}\varphi(z)dz\int_{y}^{\infty}f(z)dz + \int_{-\infty}^{0}\frac{dy}{D(y)\varphi(y)}\int_{-\infty}^{y}\varphi(z)dz\int_{-\infty}^{y}f(z)dz. \tag{A15}$$

Now expressions (A14) and (A15) require sufficiently weak behavior of reaction potential V(y) as y->±∞ For example, at f(z)=φ(z) it is sufficient, that:

$$V(y) \underset{y\to\pm\infty}{\sim} K_B T \ln|y|^{3+\varepsilon} \quad (\varepsilon > 0). \tag{A16}$$

Thus, for all potentials which grow up not very sharply at y->±∞ the calculation of the function $\tilde{G}(x,x')$ should be carried out by direct solution of Eq. (I.4.12) without usage of function $G_0(x,x')$, because it does not require such a rigid restriction as the one presented by Eq. (A12). MFPT to the point x_p is given by Eq. (I.5.5). For the averaged relaxation time τ_e we have:

$$\tau_e = -\frac{\overline{G}(x_p,0)}{\varphi(x_p)} = -\frac{\overline{G}(0,x_p)}{\varphi(0)} = \frac{1}{D}\left\{\int_0^{x_p}\frac{dy}{\varphi(y)}\int_y^{\infty}\varphi(z)dz - B_0\right\} \quad (x_p>0) \tag{A17}$$

where B_0 is the value of B at $f(x)=\varphi(x)$.

The most simple expression for $\tilde{G}(x,x')$ and τ_p can be obtained for the case $f(x)=\delta(x-x_0)$ immediate from Eqs. (A13) and (I.5.5):

$$\tilde{G}(x,x') = \frac{\varphi(x)}{D}\left\{\Theta(x-x_0)\int_{x_0}^{x}\frac{dy}{\varphi(y)} + \int_{x'}^{x_0}\frac{dy}{\varphi(y)}\int_y^{\infty}\varphi(z)dz - \Theta(x-x')\int_{x'}^{x}\frac{dy}{\varphi(y)}\right\}. \tag{A18}$$

APPENDIX B. CALCULATION OF τ_p AND $\tilde{G}(x, x', s)$ FOR HIGH ACTIVATION POTENTIAL BARRIER.

APPENDIX B CALCULATION OF τ_p AND $\tilde{G}(x,x';s)$ FOR HIGH ACTIVATION BARRIER

Let us assume, that f(x)=δ(x), then from the first equation in Eq. (I.5.6) at x_0=0 we get:

$$\tau_p = \int_0^{x_p} \frac{dy}{D(y)\varphi(y)} - \int_0^{x_p} \frac{dy}{D(y)\varphi(y)} \int_y^{\infty} \varphi(z)dz \,. \tag{B1}$$

According to asymptotic estimate (A10) we should keep only the first member which grows exponentially when βV(x)>>1. The second integral changes like $\int V'(x_p)^{-1}dx_p$ and can not compete with the first one. Then, τ_e in (A17) is:

$$\tau_e \approx \int_0^{x_p} \frac{dy}{D(y)\varphi(y)} \int_y^{\infty} \varphi(z)dz \,. \tag{B2}$$

So, at high activation potential barrier we have $\tau_p >> \tau_e$ and using the next order at the asymptotic expansion in Eq. (A10) we can write:

$$\tau_p \approx \frac{Z_0}{D} e^{\beta V(x_p)} \int_0^{\infty} (1 + \beta V''(x_p)x^2/2) e^{-\beta V'(x_p)x} dx$$
$$= \frac{Z_0}{D\beta V'(x_p)} \left(1 + \frac{V''(x_p)}{\beta V'(x_p)^2}\right) e^{\beta V(x_p)}. \tag{B3}$$

It should be mentioned that the correction term in the pre-exponential part $V''(x_p)/(\beta V'(x_p)^2)$ is of the same order of magnitude as $(\beta V(x_p))^{-1} << 1$.

Let us now assume that f(x)=φ(x). Taking into account Eq. (I.5.5) for τ_p has the form:

$$\tau_p \approx \frac{1}{D} \int_0^{x_p} \frac{dy}{\varphi(y)} - \frac{1}{D} \left(2 \int_0^{x_p} \frac{dy}{\varphi(y)} \int_y^{\infty} \varphi(z)dz - B_0 \right). \tag{B4}$$

This expression makes clear that the estimation of MFPT given in Eq. (B3) is still valid for φ(x). Moreover, we can conclude that the result obtained for τ_p is legitimate for any initial distribution f(x) if its width is not significantly larger than the one for φ(x).

Now we calculate the non-steady-state functions $\overline{G}(x_p,0,s)$ and $\tilde{G}(x_p,x_p,s)$ assuming that the second member on the left side of Eq. (I.4.10b) is the first order correction on the value s. Representing the steady-state Green's function as:

$$\tilde{G}(x,x';s)=\tilde{G}(x,x')+\tilde{G}^{(1)}(x,x';s) \tag{B5}$$

we can rewrite the appropriate differential equation for it as:

$$D\frac{\partial}{\partial x}\varphi(x)\frac{\partial}{\partial x}\frac{1}{\varphi(x)}\tilde{G}^{(1)}(x,x')=s\tilde{G}(x,x'). \tag{B6}$$

Moreover, the function $\tilde{G}(x,x';s)$ satisfies the same boundary conditions and condition (I.4.11) that the steady-state function $\tilde{G}(x,x')$. After integration of Eq. (B6) we arrive at

$$\frac{\tilde{G}^{(1)}(x_p,x';s)}{\varphi(x_p)}=\frac{s}{D}\int_{-\infty}^{\infty}\varphi(y)dy\int_{y}^{x_p}\frac{\tilde{g}(z,x')}{\varphi(z)}dz\equiv$$

$$\equiv\frac{s}{D}\left\{\int_{0}^{x_p}\frac{\tilde{g}(y,x')}{\varphi(y)}dy-\int_{0}^{\infty}\frac{\tilde{g}(y,x')}{\varphi(y)}dy\int_{y}^{\infty}\varphi(z)dz+\int_{-\infty}^{0}\frac{\tilde{g}(y,x')}{\varphi(y)}\int_{-\infty}^{y}\varphi(z)dz\right\} \tag{B7}$$

where

$$\tilde{g}(y,x')=\int_{-\infty}^{y}\tilde{G}(z,x')dz=-\int_{y}^{\infty}\tilde{G}(z,x')dz. \tag{B8}$$

Moreover, $\tilde{g}(y,x)\to 0$ at $y\to\pm\infty$. At the condition $\beta V(x_p)\gg 1$, the biggest contribution to Eq. (B7) is given by the first integral in the right hand side:

$$\frac{\overline{G}^{(1)}(x_p,0;s)}{\varphi(x_p)}\approx\frac{s}{D}\int_{0}^{x_p}\frac{\overline{g}(y,0)}{\varphi(y)}dy;\qquad\frac{\tilde{G}^{(1)}(x_p,x_p;s)}{\varphi(x_p)}\approx\frac{s}{D}\int_{0}^{x_p}\frac{\tilde{g}(y,x_p)}{\varphi(y)}dy \tag{B9}$$

where $\overline{g}$ is function $\tilde{g}$ at $f(x)=\varphi(x)$.

Using expression (A14) at $x\geq 0$ in the second definition in Eq. (B8), and integrating by parts Eq. (B9), we obtain:

$$\frac{\overline{G}^{(1)}(x_p,0;s)}{\varphi(x_p)} \approx \frac{s}{D^2}\left\{\frac{1}{2}\left(\int_0^{x_p}\frac{dy}{\varphi(y)}\int_y^{\infty}\varphi(z)dz\right)^2 + \int_0^{x_p}\frac{dy}{\varphi(y)}\int_y^{\infty}\frac{dz}{\varphi(z)}\left(\int_z^{\infty}\varphi(w)dw\right)^2 - B_0\int_0^{x_p}\frac{dy}{\varphi(y)}\int_y^{\infty}\varphi(z)dz\right\}$$

$$\approx \frac{1}{2}s\tau_e^2$$

(B10)

The comparison of expressions (B10) and (A17) shows that the function $\overline{G}(x_p,o;s)$ achieves its steady-state value when $s\tau_e << 1$.

To consider the function $\tilde{G}(x_p,x_p;s)$ it is sufficient to take into consideration the case f(x)=δ(x). So, using expression (A18) at x_0=0, x≥0, x'=x_p in the second definition in (B8), we can obtain the first order correction for the Green's function under consideration from the second expression in Eq. (B9) integrating by parts:

$$\frac{\tilde{G}^{(1)}(x_p,x_p;s)}{\varphi(x_p)} \approx -\frac{s}{D^2}\left\{2\int_0^{x_p}\frac{dy}{\varphi(y)}\int_y^{\infty}\varphi(z)dz\int_0^{y}\frac{dz}{\varphi(z)} - \left(\int_0^{x_p}\frac{dy}{\varphi(y)}\int_y^{\infty}\varphi(z)dz\right)^2\right\}. \qquad \text{(B11)}$$

Changing the upper integration limit y for x_p≥0 in the first term and regarding the definition of τ_p and τ_e for the case of a high activation potential barrier we have:

$$\left|\frac{\tilde{G}^{(1)}(x_p,x_p;s)}{\varphi(x_p)}\right| < 2s\tau_e\tau_p. \qquad \text{(B12)}$$

From Eq. (B10) we can conclude, that function $\tilde{G}(x_p,x_p,s)$ as well as $\overline{G}(x_p,0,s)$ reach their steady-state values at $s\tau_e$<<1.

APPENDIX C. THE TIME-DEPENDENT GREEN'S FUNCTION FOR HIGH ACTIVATION BARRIER

APPENDIX C. THE TIME-DEPENDENT GREEN'S FUNCION FOR HIGH ACTIVATION BARRIER

The case of high activation barrier reactions for 1D motion was investigated in Chaper V. There, it was shown that for any monotonically increasing potential $V(x)$ (it should grow monotonically starting from some point), the dynamical operator

$$L(x) = D_x \frac{\partial}{\partial x} e^{-\beta V(x)} \frac{\partial}{\partial x} e^{\beta V(x)} \tag{C1}$$

for high barrier transforms into

$$L_{HB}(x) = D_x \left[\partial^2 / \partial x^2 + \beta V'(x_p) \right] \tag{C2}$$

where V' denotes the derivative and x_p is the point of location of the reaction sink on the surface, $V(x_p) > V(x_0)$ and the only requirements are: i) $\beta V(x_p) >> 1$ and ii) $\beta V'(x_p) >> 1$.

Therefore, the Green's functions given in Eqs. (II.10.17) can be defined through the operator in Eq. (C2)

$$L_{HB}(x) G(x, x', t) = \frac{\partial}{\partial t} G(x, x', t), \qquad G(x, x', 0) = \delta(x - x'). \tag{C3}$$

A straightforward evaluation of the above function yields the expression

$$G(x, x', t) = \frac{1}{\sqrt{4\pi D_x t}} \exp\left[-\frac{\beta \left(x - x' + \beta V'(x_p) D_x t \right)^2}{4\beta D_x t} \right]. \tag{C4}$$

The above Green's function was used to evaluate Eqs. (II.10.27).

APPENDIX D. THE STEADY-STATE GREEN'S FUNCTION FOR HIGH ACTIVATION BARRIER

APPENDIX D. THE STEADY-STATE GREEN'S FUNCTION FOR HIGH ACTIVATION BARRIER

The steady-state differential equation given in Eq. (II.11.7) was formulated in Ref. 30. Its integral analog is given by Eq. (II.11.8). If the reaction does *not* occur at a high barrier then the Green's function in Eq. (II.11.8) should be defined through the following equation

$$L(x)G(x,x') = -\delta(x-x') + f(x) \tag{D1}$$

where $f(x)$ is the initial distribution. For the dynamical operator

$$L(x) = \frac{d}{dx}\left(D(x)\varphi(x)\frac{d}{dx}\ \frac{1}{\varphi(x)} \right) \tag{D2}$$

the above equation is easy to solve and yields

$$\tilde{G}(x,x') = \varphi(x)\left\{ \int_{-\infty}^{x} \frac{dy}{D(y)\varphi(y)} \int_{-\infty}^{y} f(z)dz + \int_{x'}^{\infty} \frac{dy}{D(y)\varphi(y)} \int_{y}^{\infty} \varphi(z)dz - \Theta(x-x') \int_{x'}^{x} \frac{dy}{D(y)\varphi(y)} - A \right\} \tag{D3}$$

with

$$A = \int_{a}^{b} \frac{dy}{D(y)\varphi(y)} \int_{y}^{b} \varphi(z)dz \int_{a}^{y} f(z)dz.$$

Here a and b are the lower and upper boundaries respectively ($\pm\infty$ are included).

For a high barrier where $\beta V(E) >> 1$, Eq. (D1) transforms into Eq. (II.11.9) and the general Green's function in Eq. (D3) transforms to Eq. (II.11.14). (Note that the dynamical operator changes to the form of Eq. (C2).)

APPENDIX E. EVALUATTION OF THE EFFECTIVE MFPT FOR THE INTERMEDIATES ON TWO-DIMENSIONAL HARMONIC OSCILLATOR POTENTIAL SURFACE

APPENDIX E. EVALUATION OF THE EFFECTIVE MFPT FOR THE INTERMEDIATES ON TWO-DIMENSIONAL HARMONIC OSCILLATOR POTENTIAL SURFACE

In order to evaluate the effective MFPT τ_{12}, first we represent Eq. (II.14.7) in the form:

$$\tau_{12} = \frac{1}{K_{-1r}} \iint dxdz W_{23}(x,z) g(x,z) \tag{E1}$$

where

$$g(x,z) = \frac{1}{K_{-1r}} \iint dx' dz' \tilde{G}_{22}^{12}(x,x';z,z') W_{23}(x',z') \varphi_I(x',z').$$

Taking into account the form of the initial distribution on the (I) surface for τ_{12}, Eq. (II.14.15), the original equation for the steady-state Green's functions, Eq. (I.4.12) can be transformed into the following one in order to evaluate the desired function *g(x,z)*:

$$\left(L_x + L_z\right) g(x,z) = f_{12}(x,z) - f_{23}(x,z), \quad L_\mu = \frac{1}{\beta \tau_\mu} \frac{\partial}{\partial \mu} \left(\frac{\partial}{\partial \mu} + \beta \mu \right), \quad \mu = x,z \tag{E2}$$

where τ_x and τ_z are the coordinate relaxation times and f_{12} is given by Eq. (II.14.15) and f_{23} is as follows:

$$f_{23}(x,z) = \sqrt{\frac{\beta \lambda_{IP}}{\pi z_2^2}} \delta\left(q_2 x + z - \theta_2\right) \exp\left(\beta E_{A23} - \beta (x^2 + z^2)/2\right) \tag{E3}$$

where $q_2 = x_1 / z_1$ and $\theta_2 = c_2 / z_2$.

Because the operators of motion in Eq. (E2) are independent, the Fourier transformation is a convenient method for solution of this equation. As the result of

applying the Fourier transformation $\tilde{f}(\eta,\nu)=\frac{1}{2\pi}\iint dxdzf(x,z)\exp(-ix\nu-iz\eta)$ to Eq. (E2) one can obtain a first order partial differential equation for the function $\tilde{g}(\eta,\nu)$:

$$\left[\frac{\eta}{\tau_z}\frac{\partial}{\partial\eta}+\frac{\nu}{\tau_x}\frac{\partial}{\partial\nu}+\left(\frac{\eta^2}{\beta\tau_z}+\frac{\nu^2}{\tau_x}\right)\right]\tilde{g}(\eta,\nu)=\tilde{f}_2(\eta,\nu)-\tilde{f}_1(\eta,\nu) \qquad \text{(E4)}$$

where

$$\tilde{f}_i(\eta,\nu)=\exp\left(-i\frac{\theta_i(\eta+q_i\nu)}{1+q_i^2}-\frac{(q_i\eta-\nu)^2}{2\beta(1+q_i^2)}\right), \qquad \text{i=1,2}$$

where $q_i = x_i/z_i$ and $\theta_i = c_i/z_i$ are defined through the parameters of the sink lines W_{ij} given by Eqs. (II.14.11) and (II.14.12) ($z_1^2 + x_1^2 = \lambda_I$, $z_2^2 + x_2^2 = \lambda_{IP}$ and $E_{A21}=\frac{\theta_1^2}{2(1+q_1^2)}$, $E_{A23}=\frac{\theta_2^2}{2(1+q_2^2)}$).

The boundary conditions for the above differential equation come from the requirement for the steady-state Green's function which originated function g, Eq. (I.4.12a). Thus we have to call for the restriction $\tilde{g}(0,0)=0$.

In order to solve Eq. (E2) one has to evaluate the principle integral of the homogeneous part $\left[\frac{\eta}{\tau_z}\frac{\partial}{\partial\eta}+\frac{\nu}{\tau_x}\frac{\partial}{\partial\nu}\right]r(\eta,\nu)=0$, which in this case is quite simple: $r=\eta^{1/\tau_z}\nu^{-1/\tau_x}$. Substitution of variables $\eta=r^{\tau_z}\nu^{\alpha}$ (where $\alpha=\tau_z/\tau_x$) in differential equation (E4) yields a first order differential equation

$$\frac{d}{d\nu}\tilde{g}(r,\nu)+\left(\frac{\nu}{\beta}+\frac{r^{2\tau_z}\nu^{2\alpha-1}}{\beta\alpha}\right)\tilde{g}(r,\nu)=\tau_z(\tilde{f}_2(r,\nu)-\tilde{f}_1(r,\nu))/\nu. \qquad \text{(E5)}$$

This ordinary differential equation is easy to solve. Substituting back the variables $r=\eta^{1/\tau_z}\nu^{-1/\tau_x}$ into the solution of Eq. (E5) we obtain:

$$\tilde{g}(\eta,\nu)=\tau_z\exp\left(-\frac{\eta^2+\nu^2}{2\beta}\right)\int_0^1\frac{dx}{x}\left(\tilde{g}_{02}(\eta,\nu,x)-\tilde{g}_{01}(\eta,\nu,x)\right) \qquad \text{(E6)}$$

where

$$\tilde{g}_{0l}(\eta, v, x) = \exp\left(-i\theta_l \frac{\left(\eta x^{\alpha} + q_l v x\right)}{1+q_l^2} + \frac{\left(\eta x^{\alpha} + q_l v x\right)^2}{2\beta(1+q_l^2)} \right), \quad l = 1,2. \tag{E7}$$

It is easy to show that function (E6) can be utilized for calculation of the effective MFPT in Eq. (E1). Thus, the final expression for evaluation of τ_{12} obtains the form:

$$\tau_{12} = \sqrt{\frac{\lambda_I}{\pi\beta z_2^2}} \exp(\beta E_{23}) \int_{-\infty}^{\infty} d\eta \tilde{g}(\eta, q_2\eta) \exp(i\theta_2\eta). \tag{E8}$$

Taking into account the form of function $\tilde{g}$ from Eq. (E6) we arrive at the final expression for the MFPT τ_{12}:

$$\tau_{12} = \tau_z e^{\beta E_{23}} \int_0^1 \frac{dx}{x} \left(\frac{\exp\left(-\frac{\beta\theta_2^2 b_2^2(x)}{2(1+q_2^2)a_2(x)} \right)}{\sqrt{a_2(x)}} - \frac{\exp\left(-\frac{\beta\theta_2^2 b_1^2(x)}{2(1+q_2^2)a_1(x)} \right)}{\sqrt{a_1(x)}} \right) \tag{E9}$$

where

$$b_1(x) = 1 - \frac{\varphi_1}{\varphi_2} \frac{x + q_1 q_2 x^{\alpha}}{1+q_1^2} \quad \text{and} \quad b_2(x) = 1 - \frac{x + q_2^2 x^{\alpha}}{1+q_2^2}$$

$$a_1(x) = 1 - \frac{\left(x + q_1 q_2 x^{\alpha}\right)^2}{(1+q_1^2)(1+q_2^2)} \quad \text{and} \quad a_2(x) = 1 - \frac{\left(x + q_2^2 x^{\alpha}\right)^2}{(1+q_2^2)^2}.$$

Thus, Eq. (E9) gives the mean time for particles to reach a line on a two-dimensional harmonic oscillator potential surface if they started moving from some other line. In the specific case of τ_{12} we had the starting line taken as $\delta(q_2x + z - \theta_2)$ and the sink line at which the particles arrive was $\delta(q_1x + z - \theta_1)$, see Eqs. (II.14.11) and (II.14.12). In order to get the other effective MFPT, τ_{21} we have to switch the direction of motion, i.e. the

particles would have to start at $\delta(q_2x+ z -\theta_2)$ line and finish on $\delta(q_1x+ z -\theta_1)$. Eq. (E9) can still be used for evaluation of τ_{23}, but the indexes 1 and 2 have to be substituted for 2 and 1 respectively and the activation energy for the reaction (I)->(P), E_{A23} should be replaced with the activation energy for the sink into the (R) well, E_{A21}.

BIBLIOGRAPHY

BIBLIOGRAPHY

1. H. A. Kramers, *Physica* 7, 284 (1940).
2. V. I. Mel'nikov, S. V. Meshkov, *J. Chem. Phys.* **85**, 1018 (1986).
3. A. M. Berezhkovskii, E. Pollak, V. Y. Zitserman, *J. Chem. Phys.* **97**, 2422 (1992).
4. A. M. Berezhkovskii, V. Y. Zitserman, *Chem. Phys.* **164**, 341 (1992).
5. Z. Wang, J. Tang, J. R. Norris, *J. Chem. Phys.* **97**, 7251 (1992).
6. H. Sumi, R. A. Marcus, *J. Chem. Phys.* **84**, 4894 (1986).
7. W. Nadler, R. A. Marcus, *J. Chem. Phys.* **86**, 3906 (1987).
8. P. Hanggi, P. Talkner, M. Berkovec, *Rev. Mod. Phys.* **62**, 251 (1990).
9. A. Szabo, K. Schulten, Z. Schulten, *J. Chem. Phys.* **72**, 4350 (1980).
10. T. Fonseca, J. A. N. F. Gomes, P. Grigolini, F.Marchesoni, in *Adv. Chem. Phys.* M. W. Evans, P. Grigolini, G. Pastori-Parravicini, Eds. (Wiley, New York, 1985), vol. 62, Ch. 9,.
11. M. Compiani, *J. Chem. Phys.* **98**, 602 (1993).
12. B. Bagchi, G. R. Fleming, D. W. Oxtoby, *J. Chem. Phys.* **78**, 7375 (1983).
13. B. Bagchi, G. R. Fleming, *J. Phys. Chem.* **94**, 9 (1990).
14. A. I. Burshtein, P. A. Frantsuzov, A. A. Zharikov, *J. Chem. Phys.* **96**, 4261 (1992).
15. A. Nitzan, in *Adv. Chem. Phys.* M. W. Evans, P.Grigolini, Eds. (Wiley, New York, 1988), vol. 70, pp. 489.
16. A. M. Berezhkovskii, A. M. Frishman, E. Pollak, *Reaction Dynamics in Clusters and Condensed Phases*. J. Jortner, Ed., (Kluwer Academic Publishers, The Netherlands, 1994).

17. K. Tominaga, G. C. Walker, W. Jarzeba, P. F. Barbara, *J. Phys. Chem.* **95**, 10485 (1991).

18. K. Tominaga, G. C. Walker, W. Jarzeba, P. F. Barbara, *J. Phys. Chem.* **95**, 10475 (1991).

19. C. S. Poornimadevi, B. Bagchi, *Chem. Phys. Lett.* **168**, 276 (1990).

20. J. L. Skinner, P. G. Wolynes, *J. Chem. Phys.* **72**, 4913 (1980).

21. N. Agmon, S. Rabinivich, *J. Chem. Phys.* **97**, 7270 (1993).

22. B. D. Aguda, H. O. Pritchard, *J. Chem. Phys.* **96**, 5908 (1992).

23. L. D. Zusman, *Chem. Phys.* **49**, 295 (1980).

24. R. I. Cukier, *J. Chem. Phys.* **88**, 5594 (1988).

25. R. I. Cukier, M. Morillo, J. M. Casado, *Phys. Rev. B* **45**, 1213 (1992).

26. E. Akesson, G. C. Walker, P. F. Barbara, *J. Phys. Chem.* **1991**, 4188 (1988).

27. T. J. Kang, et al., *J. Phys. Chem.* **92**, 6800 (1988).

28. W. Adcock, et al., *J. Am. Chem. Soc.* **116**, 4653 (1994).

29. J.-M. Saveant, *J. Am. Chem. Soc.* **109**, 6788 (1987).

30. J. Zhu, O. B. Spirina, R. I. Cukier, *J. Chem. Phys.* **100**, 8109 (1994).

31. D. Ben-Amotz, C. B. Harris, *J. Chem. Phys.* **86**, 4856 (1987).

32. D. Huppert, H. Kantey, E. M. Kosower, *Faraday Discuss. Chem. Soc.* **74**, 161 (1982).

33. J. N. Onuchic, *J. Chem. Phys.* **86**, 3925 (1987).

34. A. M. Berezhkovskii, V. Y. Zitserman, *Chem. Phys.* **157**, 157 (1991).

35. D. V. Matyshov, Y. A. Maletin, *Chem. Phys.* **127**, 325 (1988).

36. A. A. Kipriganov, A. B. Doktorov, A. I. Burshtein, *Chem. Phys.* **76**, 149 (1983).

37. D. Toussaint, F. Wilczek, *J. Chem. Phys.* **78**, 2642 (1983).

38. A. A. Kipriganov, I. V. Gopich, A. B. Doktorov, *Chem. Phys.* **187**, 241 (1994).

39. H. Mori, *Progressive Theor. Phys. (Kyoto)* **33**, 423 (1965).

40. R. Zwanzig, *Lectures Theor. Phys.* **3**, 106 (1961).

41. R. A. Marcus, *J. Phys. Chem.* **96**, 1753 (1992).

42. J. Zhu, J. C. Rasaiah, *J. Chem. Phys.* **95**, 3325 (1991).

43. A. I. Burshtein, I. S. Oseledchik, *Zn. Eksp. Teor. Fiz.* **51**, 1072 (1966).

44. D. Y. Yang, R. I. Cukier, *J. Chem. Phys.* **91**, 281 (1989).

45. O. B. Spirina, A. B. Doktorov, *Chem. Phys. in press* , (1995).

46. V. M. Berdnikov, A. B. Doktorov, *Chem. Phys.* **69**, 205 (1982).

47. H. Sumi, *J. Chem. Phys.* **100**, 8825 (1994).

48. A. B. Doktorov, E. A. Kotomin, *Phys. Stat. Sol. B* **114**, (1982).

49. K. M. Keery, G. R. Fleming, *Chem. Phys. Lett.* **93**, 332 (1982).

50. K. L. Sebastian, *Phys. Rev. A* **46**, R1732 (1992).

51. A. Erdelyi, *Asymptotic expansions.* (Dover, New York, 1956).

52. O. B. Spirina, R. I. Cukier, *J. Chem. Phys. in press* , (1995).

53. A. M. Berezhkovskii, A. N. Drozdov, V. Y. Zitserman, *Russian J. Phys. Chem.* **62**, 1353 (1988).

54. L. Eberson, *Electron Transfer Reactions In Organic Chemistry.* (Springer-Verlag, Berlin, 1987).

55. I. Rips, J. Jortner, *J. Chem. Phys.* **87**, 2090 (1987).

56. C. P. Andrieux, E.Differding, M. Robert, J.-M. Saveant, *J. Am. Chem. Soc.* **115**, 6592 (1993).

57. C. Bulliard, M. Allan, E. Haselbach, *J. Phys. Chem.* **98**, 11040 (1994).

58. Y. Huang, D. D. M. Wayner, *J. Am. Chem. Soc.* **116**, 2157 (1994).

59. J. T. Hupp, Y. Dong, R. L. Blackbourn, H. Lu, *J. Phys. Chem.* **97**, 3278 (1993).

60. G. C. Walker, E. Akesson, A. E. Johnson, N. E. Levinger, P. F. Barbara, *J. Phys. Chem.* **96**, 3728 (1992).

61. P. Piotrowiak, J. R. Miller, *J. Phys. Chem.* **97**, 13052 (1993).

62. E. D. German, A. M. Kuznetsov, *J. Phys. Chem.* **98**, 6120 (1994).

63. J.-M. Saveant, *Acc. Chem. Res.* **26**, 455 (1993).

64. J.-M. Saveant, *Adv. Phys. Org. Chem.* **26**, 1 (1990).

65. A. Pross, *Adv.Phys. Org. Chem.* **21**, 99 (1985).

66. A. M. Berezhkovskii, *Chem. Phys.* **164**, 331 (1992).

67. A. M. Berezhkovskii, V. Y. Zitserman, *Chem. Phys.* **164**, 341 (1992).

68. S. Lee, J. T. Hynes, *J. Chem. Phys.* **88**, 6863 (1988).

69. S. Lee, J. T. Hynes, *J. Chem. Phys.* **88**, 6853 (1988).

70. R. A. Marcus, N. Sutin, *Biochim. Biophys. Acta* **811**, 265 (1985).

71. R. A. Marcus, *Annu. Rev. Phys. Chem.* **15**, 155 (1964).

72. V. G. Levich, in *Physical Chemistry - An Advanced Treatise* H. Henderson, W. Yost, Eds. (Academic, New York, 1970) pp. 985.

73. J. T. Hynes, *J. Phys. Chem.* **90**, 3701 (1986).

74. D. F. Calef, P. G. Wolynes, *J. Phys. Chem.* **87**, 3387 (1983).

75. L. J. Bellamy, *The Infra-red Spectra of Complex Molecules*. (Chapman and Hall, London, 1975).

76. J. Ulstrup, *Charge Transfer Processes in Condesed Media*. (Springer-Verlag, Berlin, 1979).

77. J. Jortner, M. Bixon, *J. Chem. Phys.* **88**, 167 (1988).

78. P. J. Reid, P. F. Barbara, *J. Phys. Chem.* **99**, 3554 (1995).

79. J. Jortner, *J. Chem. Phys.* **64**, 4860 (1976).

80. C. P. Andrieux, C. Blocman, J.-M. Dumas-Bouchiat, J.-M. Saveant, *J. Am. Chem. Soc.* **101**, 3431 (1979).

81. R. Dogonadze, A. M. Kuznetsov, *Progr. Surf. Sci.* **6**, 1 (1975).